

The  
**GEOLOGICAL BULLETIN**  
of the  
**PUNJAB UNIVERSITY**

Number 23

December, 1988

**CONTENTS**

	Page
Mineralogy of the Sardhai Formation, Eastern Salt Range, Punjab, Pakistan.	
<i>By M. Ashraf Siddiqui and F.A. Shams</i>	1
The Micropalaeontology of the Maastrichtian Carbonate Environments of Libya.	
<i>By Aftab A. Butt</i>	13
Miospore Forms from the Upper Devonian Deposits of New York State and Pennsylvania U.S.A.	
<i>By Sarfraz Ahmed</i>	26
Tectonic Elements and Emplacement of Dykes and Plug Like Bodies, as demonstrated by Pegmatites of Evje-Iveland area of Southern Norway.	
<i>By Sherjil Ahmad Khan Lodhi</i>	77
Chemical quality of Water Samples from Sain Area (Angoori) Islamabad Pakistan.	
<i>By Zahid Karim Khan and Syed Alim Ahmad</i>	94
Some Dasycladacean and Gymnocodiacean Algae from the Wargal and Chhidru Formations, Sakesar Section, Salt Range, Pakistan.	
<i>By Ovidiu Dragastan Dorothee Mertmann and Sarfraz Ahmed</i>	104
Geotechnical aspects of the Dhok Pathan Formation at the Kalabagh Dam Site, Pakistan.	
<i>By M.H. Malik and Saeed Farooq</i>	117
Study of Surface features of Feldspar Grains of Pleistocene Sandstones from Potwar, Pakistan.	
<i>By M. Saleem Bajwa and F.A. Shams</i>	128



# MINERALOGY OF THE SARDHAI FORMATION, EASTERN SALT RANGE, PUNJAB, PAKISTAN

BY

M. ASHRAF SIDDIQUI and F.A. SHAMS

Institute of Geology, University of the Punjab, Lahore, Pakistan.

**Abstract :** *The Sardhai Formation of Permian age in the Eastern Salt Range, Punjab, Pakistan indicated unusual nature and abnormal mode of formation, it also carries sporadic copper ore minerals. In view of marked facies variation in Sardhai Formation from Eastern Salt Range to Khisor Range, the clayey part of the Formation was investigated in detail for its mineralogical character along with some sedimentological indicators. This is the first detailed study on this important rock formation.*

## INTRODUCTION

This paper reports research work based on old reports that copper minerals occur in the Warchha Sandstone and Sardhai Formation (Lavender clays) of Salt Range, Punjab (Fleming, 1852, Theobald, 1854; Wynne, 1878). These workers gave a short note but attached only stratigraphic significance to the host material which was never subjected to systematic investigation. This position continued till a prominent mineralized zone was located recently (White, Undated; Ahmed 1969). In order to fill this gap, detailed studies were carried out by the present authors.

The specimens for present research were taken from a measured section at specific intervals. Each specimen was investigated petrographically for coarse-grained minerals, while XRD method was used to identify the fine-grained minerals. Comparative studies were made with specimens from another section (G) towards the West.

## General Geology

The Salt Range is the most important sedimentary region in Pakistan positioned

between the Indo-Pak Shield in the South and the Himalayas in the North. It is more than 200 km long and extends East-West from river Jhelum to river Indus with a Trans-Indus extension. Structurally, it appears more or less as levelled plateau tops, ending abruptly on the south as steep escarpments and cliffs overlooking the Punjab alluvial plain. In the north, the Range inclines gently towards and underlies the rolling tableland of the Potwar Plateau. The latter represents a synclinal trough between the Salt Range and the Rawalpindi-Murree foot-hills, filled by fresh water Tertiary deposits.

Gee (In Pascoe, 1959) proposed the name "Nilawahn Series" for the Permian Formation that conformably overlies the Zaluch Group and disconformably overlies the Cambrian succession of the Salt Range. The palaeozoic lithological succession of the Salt Range indicated a major unconformity marked by the Tobra Formation of glacial origin. Above this, was laid the sandstone facies of the Dandot Formation that is succeeded conformably by the Warchha Sandstone which is transitional to the overlying Sardhai Formation. It is in the



latter two lithologies that copper mineralization has been located, particularly enriched in the Sardhai Formation.

Zaluch Group	Amb Formation
Permian	
Nilawahn Group	<div style="display: inline-block; vertical-align: middle;"> <div style="font-size: 3em; vertical-align: middle; margin-right: 5px;">{</div> <div style="display: inline-block; vertical-align: middle;"> Sardhai Formation  Warchha Sandstone  Dandot Formation  Tobra Formation </div> </div>

-----Unconformity-----

Middle Cambrian	Baghanwala Formation.
-----------------	-----------------------

### The Sardhai Formation

The name Sardhai Formation was given by Gee (1964), previously named as "Lavender clay stage" (Gee in Pascoe, 1959) and "Lavender clays" (Wynne, 1978).

Sardhai Formation is fully exposed at Sardhai in the Eastern Salt Range. It is composed of bluish and greenish-grey clays with some minor sand and siltstone beds, and carbonaceous shale. There are nodules of copper ore minerals composed of malachite and chalcopryrite, common in the Central Salt Range. The Sardhai Formation has transitional contact with the Warchha Sandstone, and conformable upper contact with the Amb Formation. It is 50 m thick in Khisor Range and 65 m in the Western Salt Range. At the type locality in the Eastern Salt Range it is about 42 m thick. It is largely unfossiliferous with occasional plant remains and fish scales and fossils in the Khisor Range. The fossils show that the Sardhai Formation is of early Permian age (Shah, 1977).

### MINERALOGY

The major mineral constituent of the Sardhai Formation are clays, quartz, Calcite, and ore minerals, while muscovite, albite, microcline, epidote, biotite, dolomite and merlinoite make the minor constituents. Table 1 and 2 summarise results of this study.

**Clay Minerals.** XRD methods were used to identify clay minerals and other minerals having grain size less than 10 micron. The clay minerals in the shale of the Sardhai Formation constituting 31.8 to 97.4% of the rock are as follows:—

1. Hectorite
2. Dickite
3. Sepeolite
4. Illite
5. Saponite

There paragenetic modes of occurrence are indicated in Table 2.

**Quartz.** Quartz (0.19-13.2%) is the most common mineral. It is light greyish in colour with medium relief and shows strain extinction in slightly deformed rocks. Fragments of vein quartz and quartzite are present. Larger grains show fractures that are sometime filled with other fine-grained minerals. It occurs as fine to coarse (.05-.90 mm) and angular ( $R = .3-.7$ ,  $S = .3-.9$ ) grains and is generally a mixture of different grain sizes.

**Calcite.** In most of the specimens, calcite (0.38-51.92%) grains are very fine with no rhombohedral cleavage. It is present in the form of detrital calcite, spherulitic carbonate and shreds of calcite, as fragment of calc-schist and as oolitic carbonate.

**Muscovite.** Muscovite (0.05-10.01%) is colourless to variegated colour and occurs in flaky form. In some thin sections, it occurs in very fine fibrous form. It is mostly present in the form of inclusion in other minerals.

**Hematite.** Hematite (0.02-6.83%) is reddish brown in crossed polars and has metallic luster in reflected light, occurring as fine to medium (.10-.35 mm) and angular to rounded ( $R = .3-.7$ ,  $S = .3-.9$ ) grains.



**Biotite.** Biotite (2.04-15.0%) is present in brown to variegated colour and shows alteration to clay like material (hydromuscovite).

**Copper Ore Minerals.** Copper ore minerals are present in nodular form in the shaly part of the Formation, consisting of native copper, cuprite, malachite and rare azurite.

#### Modal Relationship

The modal data of specimen analysed were plotted on triangular diagram : clay minerals-calcite-quartz ; ignoring minor minerals which otherwise too have no direct bearing on lithology (Fig. 4). The distribution of plotted positions shows that most of the plots are located near clay corner of the triangle, only few falling in the area extended towards the calcite corner. Quartz is never in any significant quantity. As such, the rocks appear to be claystone rather than shale in the strict sense of classification. The apparent reciprocal relationship between calcite and clay minerals may not mean a mutual genetic relation but more rooted in the mineralogy of parent rocks of the sediment.

#### DISCUSSION AND CONCLUSION

The importance of Sardhai Formation as a geological unit has been recognised since Wynne (1878) published his findings, further established by investigation of Noetling (1901). The mere name "Lavender Clays", indicated its unusual nature and abnormal mode of formation, further proved by the presence of copper minerals.

In view of marked facies variation in Sardhai Formation from Eastern Salt Range to Khisor Range, it was considered important that the clayey part of the Formation is investigated which has remained neglected over almost a century. One reason for this could be the absence of fossils in the clayey part as such a situation normally does not attract the atten-

tions of stratigraphers. Absence of detailed mineralogical and related studies did not throw any light on its lithological nature and the mode of origin, considering that the Nilawan Group initiated with a glaciogene rock material at the Tobra stage, the nature of the geological processing, the origin of the Sardhai Formation could be found by detailed mineralogical and geochemical investigation. Therefore, this aspect of the problem was given special attention. Some salient results of mineralogical studies are as follows :—

1. There are a number of clay minerals present, as mixture of more than one mineral but showing difference in combinations as well as their abundances.
2. Zeolite minerals are present which has their own significance.
3. Copper minerals showing minor occurrence as compared with facies in the Central Salt Range.

Among the clay minerals, hectorite is present in all samples taken from three sections, the dickite is the next clay mineral in abundance which is present in most of the samples except the top layers in the section A. The saponite occurs in the one specimen of section A ; however, is present in all the specimen of section B but is a minor mineral in the sections A and B. Illite is a rare mineral being present in the section B and appears in only two specimens of section A. This nature and mode of occurrence of clay minerals, therefore, shows that the Sardhai Formation is not a uniform clay bed, although it has a distinctive status.

The section B is relatively at a higher level than section A and this shows the different nature and combination of clay minerals of different kind. The presence of hectorite in all specimens is indicative of the fact that the



source material was suitable for the formation of montmorillonite group minerals, apparently this may mean that the source area was composed of volcanic ashes, of intermediate (andesitic) composition. On the other hand, the common presence of dickite shows that volcanic ash of acidic composition was also involved. It is also significant that feldspar and carbonates are not present in specimens taken from section B. which once again points towards the ashy nature of source material. Another point of reference is the most absence of merlinoite in the section B. The acidic nature of the material is, however, proved in the rocks of this section.

As far as G section is concerned, besides common presence of hectorite and other clay minerals, both alkali feldspar and plagioclase are present in almost all the rocks along with carbonate as well as common occurrences of merlinoite. This shows that at this stage, crystalline igneous rocks of acidic to intermediate composition provided the source material. This is also shown by the presence of hydromica, illite, which was absent in rocks of the section B. Therefore, variation in the source material gave rise to the variation in the mineral compositions in rocks of the two sections. Significantly, their combinations are also supported by the four specimens taken from section G near Mianwali where feldspar, merlinoite and carbonate make common combination.

The lithological nature of the Sardhai Formation shows its detrital origin so that the constituent clay minerals suffered transportation. This is also shown by the presence of nodules which are actually transported and rolled fragments from source area. The general absence of coarse detritus shows that the processes involved were related more to glacial action rather than to fluvial and aeolian actions. The presence of basic plagioclase is an

important evidence of glaciogene origin, which inhibited the alteration of plagioclase. The geological framework of this part of the Indo-Pak subcontinent shows that the Permian Period, saw rifting of the continent attended with volcanic activity. On the other hand, the presence of Kirana Hill Group in the southeast is also important where rhyolitic to andesitic lavas, ashes and glasses are known to exist. The presence of Permian rifting is not known from Salt Range area, although the presence of Permian coal is significant in Western Salt Range. However, as this coal also shows features of transportation, it appeared that the source is not within the Salt Range but lies outside. It is tempting to consider the Kirana Hills as the source area in view of nearness as well as due to presence of volcanic material. The only problem is imposed by the hypothesis of Crawford (1973), which claims that the Salt Range had NW-SE orientation, conformable with the Himalayan trend, but was rotated anticlockwise through  $70^\circ$  and pushed southward along Jhelum Fault. If this position is accepted, then the relationship goes to the Punjab volcanicity of Permian age. On the other hand, Crawford's hypothesis has been challenged on paleomagnetic basis and if this position is accepted then the source area would lie in the Kirana outliers of the Indo-Pak shield. Due to presence of alluvial in-filling of Indus basin, direct connection cannot be accepted; nevertheless, it is safe to conclude that the source area composed of volcanic material and mode of transportation was glacial action. The change of facies of Sardhai Formation from Eastern Salt Range to Khisor Range i.e. from clay materials to argillaceous carbonates, shows that the basis of deposition varies from continental margins to the continental shield. Therefore, the direction of transportation was from East to West with the carbonate facies dominating in the western direction and clayey beds forming in the eastern



direction. For understanding the specific condition of formation, and nature of facies variation, it is important that outcrops of

Sardhai Formation in the Western Salt Range and Khisor Range are also studied in similar detail.

### ACKNOWLEDGMENT

The authors wish to thank Dr. K. Hussain, Centre for Solid State Physics, Punjab University, Lahore for help in the XRD work.

**TABLE 1**  
Showing modal data in the shally part of the Sardhai Formation

No.	Rock No.	Clay Minerals	Quartz	Calcite	Muscovite	Ore Minerals	Feldspar	Epidote	Biotite
1	A-1	63.03	7.97	28.00	0.05	0.92	—	—	—
2	A-4	53.29	2.96	42.13	0.33	0.96	—	0.25	—
3	A-5	68.57	2.65	26.52	—	1.24	—	1.00	—
4	A-6	44.80	2.58	36.84	0.18	6.57	—	—	10.0
5	A-8	81.08	10.47	0.38	0.63	6.83	0.63	—	—
6	A-9	77.07	10.03	4.75	7.25	—	—	—	—
7	A-10	31.82	15.2	51.92	1.93	1.08	—	1.00	—
8	B-1	97.39	0.43	0.80	1.07	0.28	—	—	—
9	B-2	90.35	2.46	4.07	0.37	2.73	—	—	—
10	B-3	91.72	2.01	5.02	1.9	1.15	—	—	—
11	B-3-A	840.8	8.11	—	2.14	0.24	—	—	5.40
12	B-4	96.90	0.98	—	2.10	—	—	—	—
13	B-5	94.90	1.75	—	2.25	1.10	—	—	—
14	B-7	94.05	1.15	—	3.30	1.50	—	—	—
15	B-8	98.66	0.19	0.15	0.74	0.23	—	—	—
16	B-11	84.92	3.06	10.00	0.36	1.64	—	—	—
17	B-13	95.12	2.38	1.10	0.90	0.50	—	—	—
18	B-14	71.75	1.10	2.20	0.95	0.55	—	—	15.95
19	C-1	87.07	8.03	—	3.90	—	—	—	—
20	C-3	85.08	1.94	—	10.01	1.02	—	—	2.04
21	C-13	89.73	7.77	—	2.03	0.02	—	—	—
22	C-14	90.05	5.95	—	2.83	1.17	—	—	—



TABLE 2

Showing paragenetic presence of various clay minerals indicated by (✓) in the Section A.

Rock No.	Clay Minerals				Quartz	Carbonate		Merlinite	Ore Mineral	Feldspar	
	Hecto-rite	Dickite	Sep/Sap	Illite		Calcite	Dolomite		Hematite	Albite	Microcline
A-O	✓	—	—	—	✓	—	✓	✓	—	✓	✓
A-O-4	✓	—	—	✓	✓	—	✓	✓	—	✓	✓
A-1	✓	—	Saponite	—	✓	✓	✓	✓	—	✓	✓
A-2	✓	✓	—	—	✓	✓	✓	✓	—	✓	✓
A-5	✓	✓	Saponite	—	✓	—	—	—	✓	—	—
A-6	✓	—	—	—	✓	✓	✓	✓	✓	—	—
A-7	✓	✓	—	—	✓	✓	✓	✓	✓	✓	✓
A-8	✓	✓	Sepeolite	—	✓	✓	—	✓	✓	✓	✓
A-9	✓	✓	—	—	✓	✓	—	✓	✓	✓	✓
A-10	✓	✓	✓	✓	✓	✓	—	✓	✓	✓	✓

TABLE 2

Showing paragenetic presence of various clay minerals indicated by (✓) in Section B.

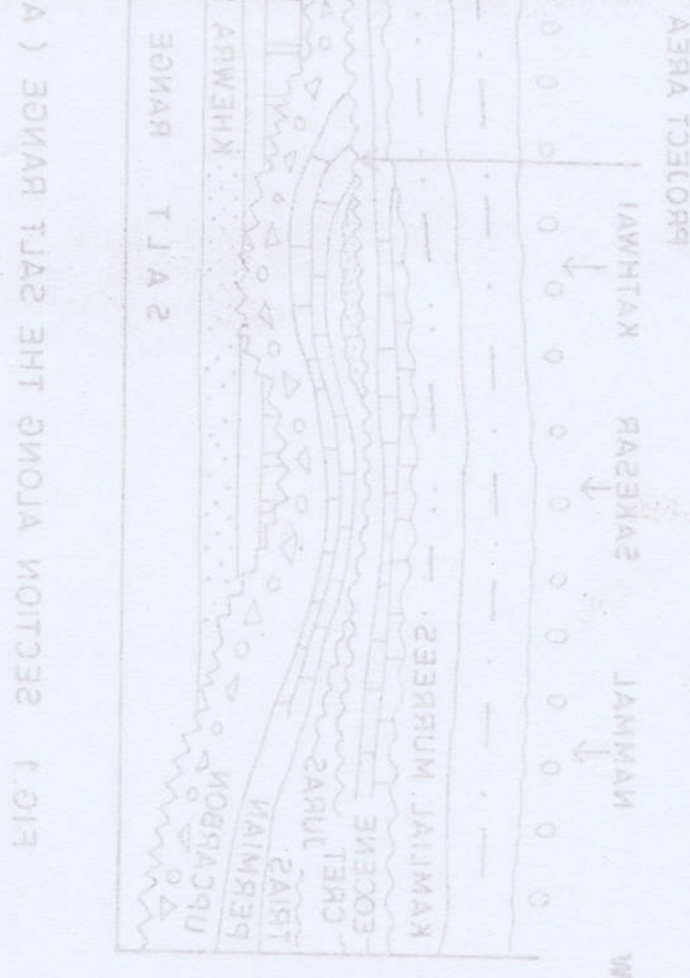
Rock No.	Clay Minerals				Quartz	Carbonate		Merlinite	Ore Mineral	Feldspar	
	Hecto-rite	Dickite	Sepeolite	Illite		Calcite	Dolomite		Hematite	Albite	Microcline
B-1	✓	✓	✓	—	✓	—	—	✓	✓	—	—
B-2	✓	✓	✓	—	✓	✓	—	—	✓	—	—
B-4	✓	✓	✓	—	✓	—	—	—	✓	—	—
B-5	✓	✓	✓	—	✓	—	—	—	—	—	—
B-11	✓	✓	✓	—	✓	✓	—	—	—	—	—
B-12	✓	✓	✓	—	✓	—	—	✓	—	—	—
B-13	✓	✓	✓	—	✓	—	—	—	✓	—	—
B-14	✓	✓	✓	—	✓	—	—	—	✓	—	—



TABLE 2

Showing paragenetic presence of various clay minerals indicated by (✓) in Section G.

Rock No.	Clay Minerals				Quartz	Carbonates		Merlinite	Ore Mineral Hematite	Feldspar	
	Hectorite	Dickite	Saponite	Illite		Calcite	Dolomite			Albite	Microcline
G-3	✓	✓	✓	✓	✓	—	✓	✓	✓	✓	✓
G-8	✓	✓	✓	✓	✓	✓	—	✓	✓	✓	✓
G-10	✓	✓	✓	✓	✓	✓	—	✓	✓	✓	✓
G-12	✓	✓	✓	✓	✓	✓	✓	✓	—	✓	✓





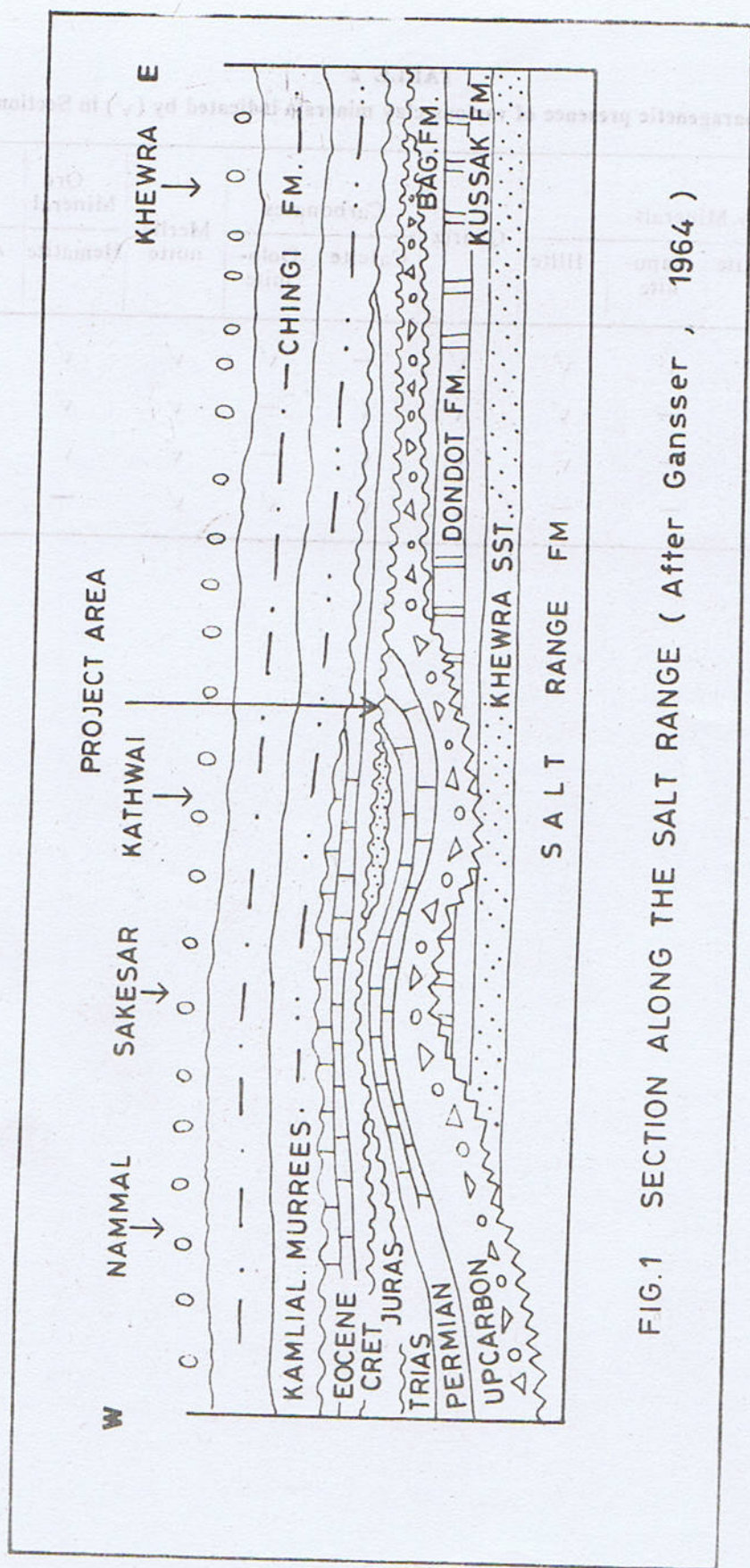
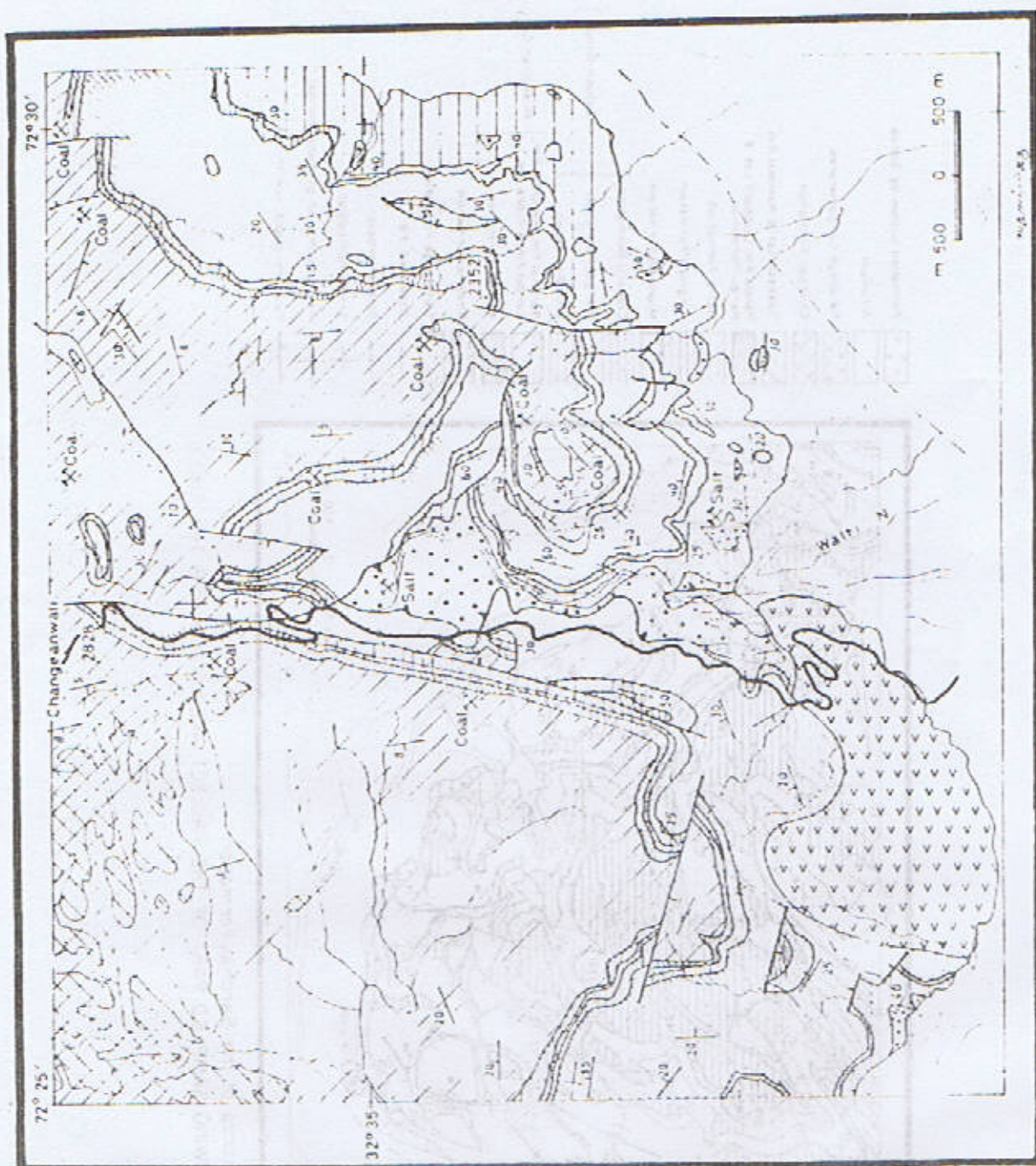


FIG.1 SECTION ALONG THE SALT RANGE ( After Gansser , 1964 )





Outcrop of the Sardhar Formation

FIG 2 SHOWING SAMPLED PART OF THE PROJECT AREA (After E R Gee, 1981)





FIG. 3. SHOWING SAMPLED PART OF THE PROJECT AREA (AFTER R 300 1990)



## REFERENCES

- Ahmad, Z. 1963. Delineation of mineral deposits of Pakistan. *Geol. Surv. Pakistan*, 15: 220.
- Balmain, M. 1967. Economic Minerals Deposits. John Wiley and Sons, Inc. New York, 696-700.
- Barrett, P. D. K., Smith, M. J., and E. G. Berry. 1960. Mineral Powder Diffraction File, Search Manual ICDD. International Centre for Diffraction data, Pennsylvania, U.S.A.
- Geol. Surv. Pakistan. 1960-61. *Geological Survey of Pakistan Series Geol. Surv. Pakistan*.
- Herring, A. 1955. Report on the Geology of the Salt Range and mineral wealth of Salt Range in Punjab. *Geol. Surv. of Pakistan*, 15: 220-229.
- Garnett, A. 1964. *Geology of Hindustan*. 2nd Edition. Butterworths.
- Huang, Walter T. 1961. Petrology. McGraw-Hill Book Company, New York, 228-267.
- Moore, W. W. 1964. The study of rocks. Harper and Row, New York.
- Pettijohn, F. J. 1975. Sedimentary rocks. Harper and Row, London, 280-282.
- Shah, S. A. 1975. Stratigraphy of the Salt Range, Punjab. *Geol. Surv. Pakistan*, 15: 230.
- Theobald, W. 1952. Notes on the Geology of the Salt Range in Punjab. *Geol. Surv. Pakistan*, 15: 230.
- Wynn, A. B. 1958. On the Geology of the Salt Range in Punjab. *Geol. Surv. Pakistan*, 15: 230.

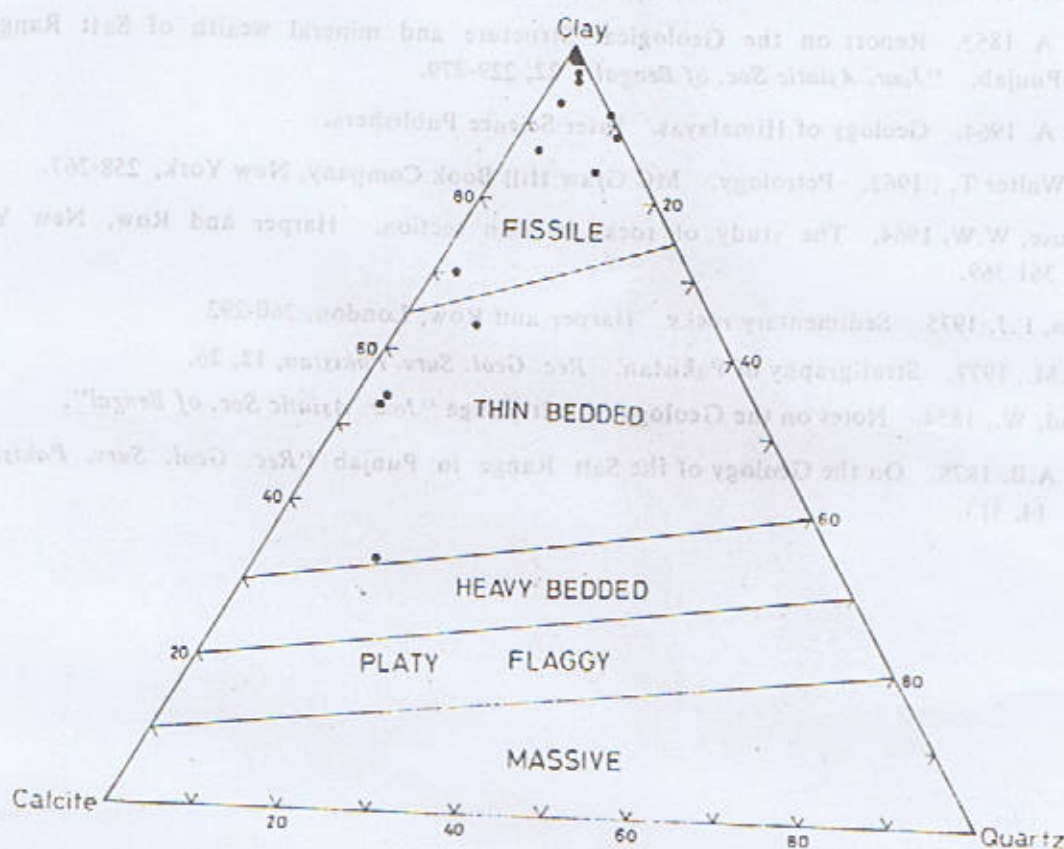


FIG. 4. SHOWING PLOTS OF NORMALIZED PERCENTAGE OF 22 CLAY SPECIMENS - SOME PLOTS OVERLAP AT THE CLAY CORNER (Classification subdivision after Pettijohn, 1975)



## REFERENCES

- Ahmad, Z., 1969. Directory Mineral deposit of Pakistan "*Rec. Geol. Surv. Pakistan*, 15" 220.
- Bateman, M. 1967. Economic Minerals Deposits. John Wiley and Sons, Inc. New York, 696-700.
- Bayliss, P., D.K. Smith Marv E. Mrose and L.G. Berry; 1980. Mineral Powder Diffraction File, Search Manual JCPDS. International Centre for Diffraction data, Pennsylvania, U.S.A.
- Gee, E.R. 1980-81. Maps Pakistan Geological Salt Range Series. *Geol. Surv. Pakistan*.
- Fleming, A. 1852. Report on the Geological Structure and mineral wealth of Salt Range in Punjab. "*Jour. Asiatic Soc. of Bengal*", 22, 229-279.
- Gansser, A. 1964. Geology of Himalayas. Inter Science Publishers.
- Huang, Walter T.; 1962. Petrology. MC Graw Hill Book Company, New York, 258-267.
- Moorhouse, W.W. 1964. The study of rocks in thin section. Harper and Row, New York, 361-369.
- Pettijohn, F.J. 1975. Sedimentary rocks. Harper and Row, London, 260-292.
- Shah, S.M., 1977. Stratigraphy of Pakistan. *Rec. Geol. Surv. Pakistan*, 12, 26.
- Theoblad, W., 1854. Notes on the Geology of Salt Range "*Jour. Asiatic Soc. of Bengal*".
- Wynne, A.B. 1878. On the Geology of the Salt Range in Punjab "*Rec. Geol. Surv. Pakistan*", 14, 313.

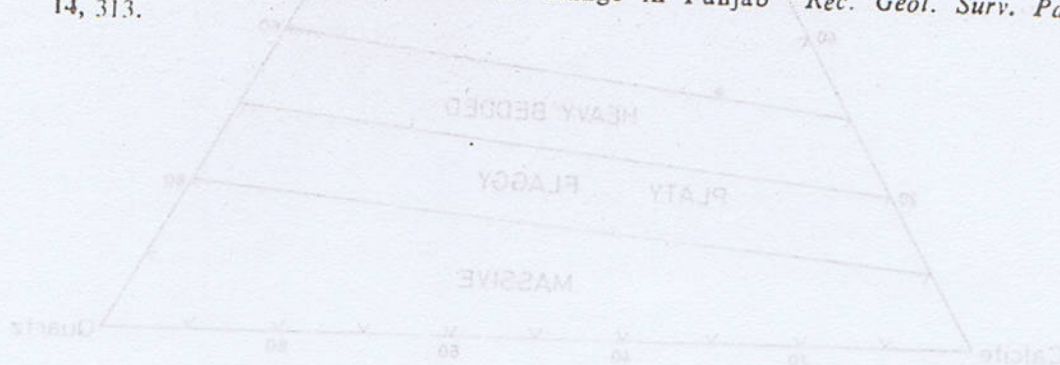


FIG. 1. SHOWING PLOTS OF NORMALIZED PERCENTAGE OF 11 CLAY SPECIMENS (207) PLOTS OVERLAP AT THE CLAY CORNER (Classification according to Pettijohn 1975)



# THE MICROPALAEONTOLOGY OF THE MAASTRICHTIAN CARBONATE ENVIRONMENTS OF LIBYA\*

BY

AFTAB A. BUTT

Institute of Geology Punjab University, New Campus, Lahore-20, Pakistan

**Abstract:** *The Maastrichtian carbonate environments occur in northern Libya among the structural units of the Ghadames Basin, the Sirte Basin, the Cyrenaica Platform and the Jabal Al Akhdar. In the offshore Pelagian Shelf, these environments are also present where the Tunisian stratigraphic terminology is in practice.*

*The Maastrichtian carbonate environments of the Sirte Basin are distinguished into shallow-water marine facies containing age-diagnostic benthonic foraminiferal species, *Orbitoides apiculatus*, *Omphalocyclus macroporus* and *Siderolites calcitrapoides* and an outer neritic facies characterised by globotruncanids, heterohelics and some benthonic smaller foraminifera. The *Globotruncana gansseri* Zone is the most prominent in planktonic biostratigraphy whereas a single benthonic foraminiferal *Bolivina incrassata gigantea* Zone is present.*

*In the Ghadames Basin, outer neritic facies is succeeded by shallow-water facies analogous to the biofacies of the Sirte Basin. Other regions demonstrate single type of environment, either shallow shelf deposition in the Cyrenaica Platform, or an outer neritic facies in the Jabal Al Akhdar and in the offshore region where planktonic biostratigraphy can be used.*

## INTRODUCTION

In northern Libya, three major structural units constitute the Maastrichtian strata. These are from west to east, the Ghadames Basin, the Sirte Basin and the Cyrenaica Shelf (Fig. 1). North of the Cyrenaica Shelf is the Jabal Al Akhdar Trough which also comprises Maastrichtian sediments of limited geographical extent.

The Upper Cretaceous depositional history of the three major structural units is very much inter-related (Fig. 2). The evolution of the structural configuration of these units during the Upper Cretaceous affords to investigate the depositional style, lithofacies variation and

the problems of stratigraphic terminology.

From the cross-section (Fig. 2), it can be visualised that active subsidence happened in the Sirte Basin throughout the Late Cretaceous bringing thickness and facies variations on the NW-SE fault block system. Meanwhile, the adjacent areas of the Ghadames Basin and the Cyrenaica Platform acted as the shallow shelf areas to the actively subsiding Sirte Basin. However, certain similarities do exist in the biofacies of these regions, for example, the *Orbitoides*, *Omphalocyclus*, *Siderolites* biofacies. Attempts to correlate stratigraphic units between the shelf or platform areas and the

\* Paper read at the Symposium "Micropalaeontology of Carbonate Environments", Devon, Plymouth, England (Sept., 1985) under the auspices of the British Micropalaeontological Society.



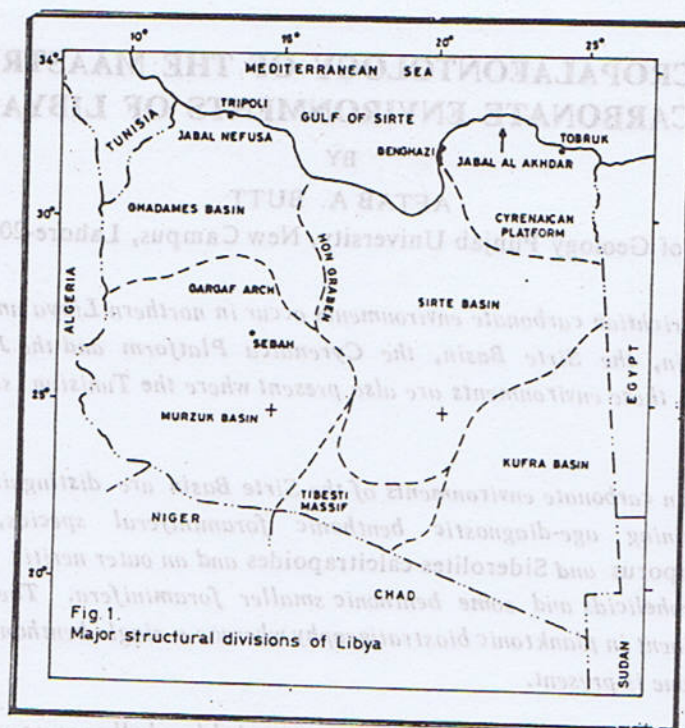
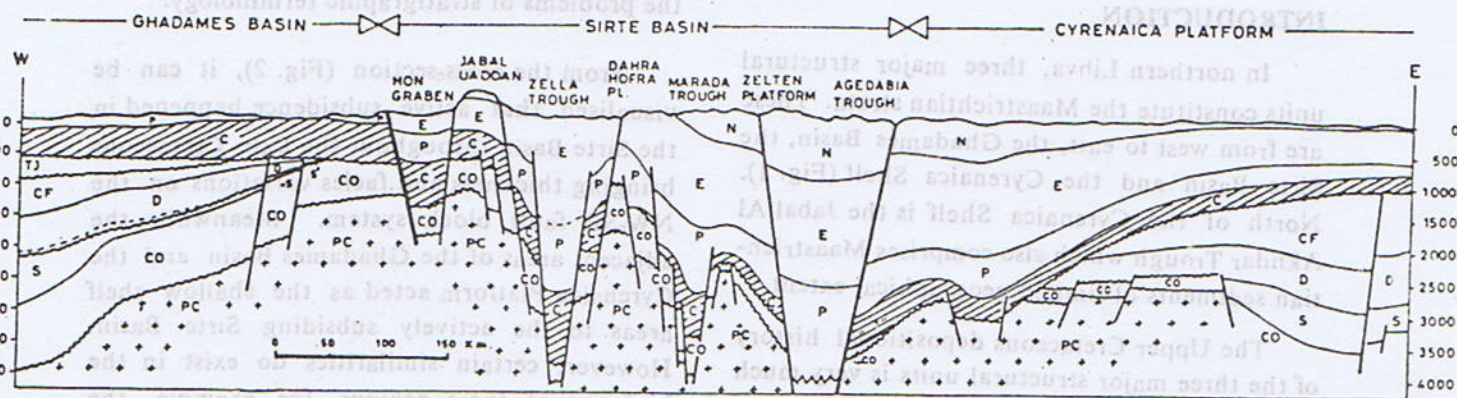


Fig. 1.  
Major structural divisions of Libya



KEY - N=Neogene, E=Eocene, Oligocene, P=Paleocene, C=Cretaceous, TJ=Triassic-Jurassic, CF=Carboniferous, D=Devonian, S=Silurian, CO=Cambrian-Ordovician, PC=PreCambrian (Basement)

Fig. 2. EAST-WEST CROSS-SECTION THROUGH THE GHADAMES BASIN, THE SIRTE BASIN AND THE CYRENAICA PLATFORM (FROM MASSA AND DELORT, 1984). HATCHED AREA DEMONSTRATES THE PALEOGEOGRAPHIC SETTING OF THE STRUCTURAL UNITS DURING THE UPPER CRETACEOUS.



basinal areas have been of fundamental importance to obtain a reliable time-stratigraphic control to aid petroleum exploration activity in terms of reserves.

The Jabal Al Akhdar Trough along the coastal area of Marsa Al Hilal is represented by an outer neritic marine facies throughout the Late Cretaceous and in this respect, certain analogy of continued subsidence during the Maastrichtian time may also be envisaged with that of the Sirte Basin.

### MAASTRICHTIAN CARBONATE ENVIRONMENTS AND BIOFACIES

#### Sirte Basin

The Sirte Basin is ranked first for its gigantic hydrocarbon yield as compared to the Ghadames Basin or the Pelagian Shelf. Therefore, its stratigraphy (lithofacies, biofacies) has been worked out in detail, even the Upper Cretaceous, say, the shallow-water Maastrichtian Waha Limestone forms a significant petroleum reservoir rock in the basin (Waha-Defa Fields).

The Maastrichtian sedimentation of the Sirte Basin is quite varied and interesting to note. It is influenced by the horst-graben tectonic style of the basin, thus causing thickness and facies variations. Because of the varied paleogeographic setting of the basin, Barr & Weegar (1972) established various formation names.

First, the Kalash Limestone, essentially an argillaceous limestone of outer neritic facies containing several age-diagnostic planktonic and benthonic foraminifera. This formation is widespread in the basin and offers good possibilities for the biostratigraphic framework. In general, it overlies and underlies the stratigraphic units which have been deposited in a continued outer neritic facies, for example, the Hagfa Shale above and the Sirte Shale below.

In the eastern part of the Sirte Basin, however, the name Kalash Limestone is being used conventionally since its distinction is made on the basis of E-Log pattern from the poorly fossiliferous continuous shallow-water carbonate sequence (i.e., Concession 31, NE Sirte Basin).

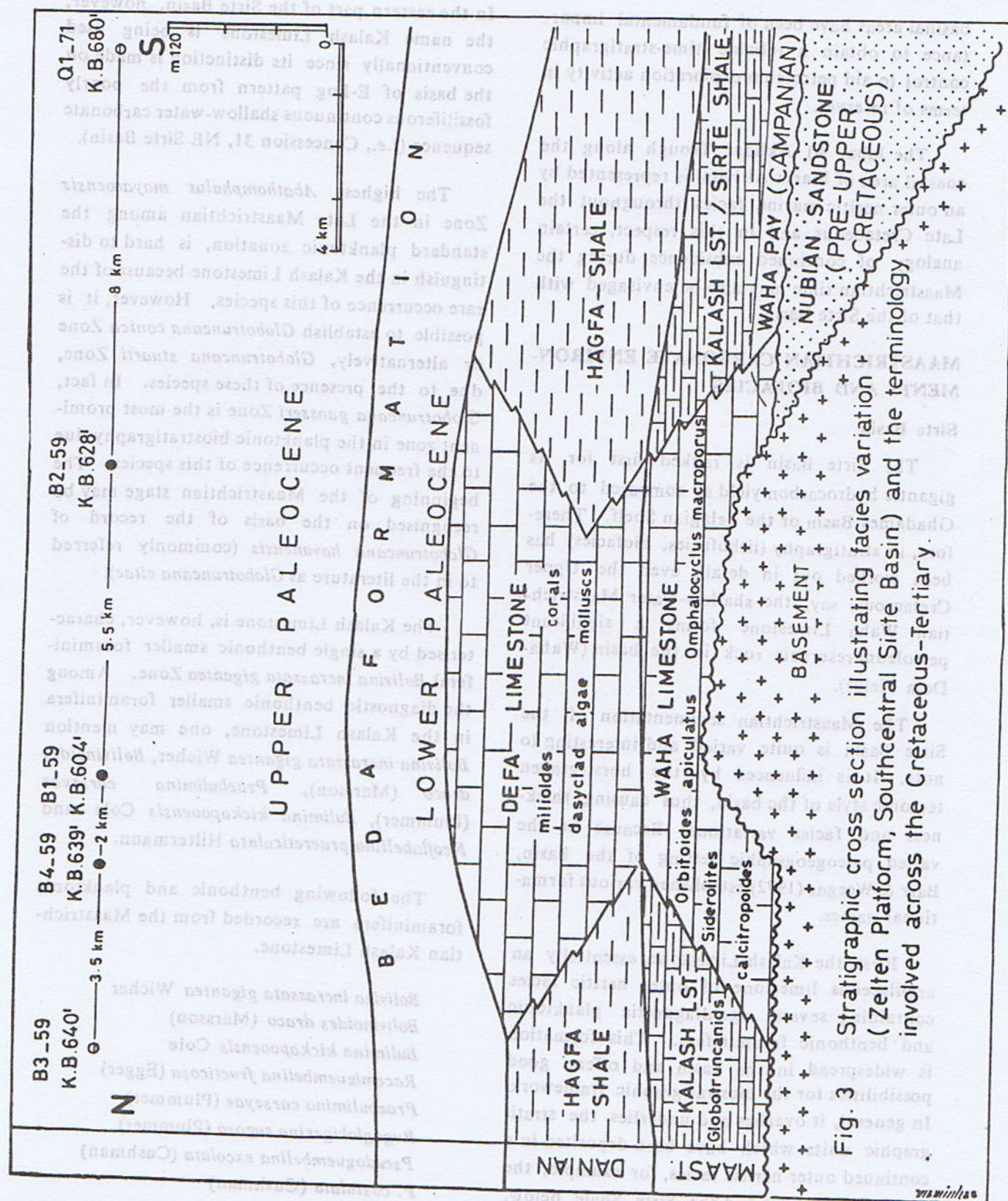
The highest *Abathomphalus mayaroensis* Zone in the Late Maastrichtian among the standard planktonic zonation, is hard to distinguish in the Kalash Limestone because of the rare occurrence of this species. However, it is possible to establish *Globotruncana conica* Zone or alternatively, *Globotruncana stuarti* Zone, due to the presence of these species. In fact, *Globotruncana gansseri* Zone is the most prominent zone in the planktonic biostratigraphy due to the frequent occurrence of this species. The beginning of the Maastrichtian stage may be recognised on the basis of the record of *Globotruncana havanensis* (commonly referred to in the literature as *Globotruncana citae*).

The Kalash Limestone is, however, characterised by a single benthonic smaller foraminiferal *Bolivina incrassata gigantea* Zone. Among the diagnostic benthonic smaller foraminifera in the Kalash Limestone, one may mention *Bolivina incrassata gigantea* Wicher, *Bolivinoidea draco* (Marsson), *Praebulimina carseyae* (Plummer), *Bulimina kickapooensis* Cole and *Neoflabellina praereticulata* Hiltermann.

The following benthonic and planktonic foraminifera are recorded from the Maastrichtian Kalash Limestone.

- Bolivina incrassata gigantea* Wicher
- Bolivinoidea draco* (Marsson)
- Bulimina kickapooensis* Cole
- Racemiguembelina fructicosa* (Egger)
- Praebulimina carseyae* (Plummer)
- Rugoglobigerina rugosa* (Plummer)
- Pseudoguembelina excolata* (Cushman)
- P. costulata* (Cushman)







*Planoglobulina acervulinoides* (Egger)  
*P. carseyae* (Plummer)  
*Heterohelix globulosa* (Ehrenberg)  
*H. striata* (Ehrenberg)  
*H. striata* var. *aegytiaca* Ansary & Tewfik  
*H. ultimatimida* (White)  
*H. planata* (Cushman)  
*H. glabrans* (Cushman)  
*H. pseudotessera* (Cushman)  
*H. reussi* (Cushman)  
*H. dentata* Stenestad  
*Globotruncana gansseri* Bolli  
*G. conica* White  
*G. aegytiaca* Nakkady  
*G. mariei* Banner & Blow  
*G. arca* (Cushman)  
*G. havanensis* Voorwijk  
*G. contusa* (Cushman)  
*G. stuarti* (de Lapparent)  
*G. plummerae* Gandolfi  
*G. stuartiformis* Dalbiez  
*G. ventricosa* White  
*Pseudotextularia elegans* (Rzehak)  
*Neoflabellina praereticulata* Hiltermann

Second, the Waha Limestone, a shallow-water calcarenitic facies developed in the central part of the basin (Zelten Platform) containing stratigraphically important benthonic larger foraminiferal species, *Orbitoides apiculatus*, *Omphalocyclus macroporus* and *Siderolites calcitrapoides*. In view of its lithofacies characters, this formation is an important petroleum reservoir rock in the Zelten Platform. In its type subsurface section, it overlies the basement and is overlain by an unusually thin Maastrichtian Kalash Limestone. In the Defa area, however, the Waha Limestone is overlain by the Danian (Paleocene) Defa Limestone in a continued shallow-water carbonate facies. The carbonate complex of the Waha Limestone and the Defa Limestone grades laterally into argillaceous facies and as such the Maastrichtian Waha Limestone represents a lateral facies

equivalent of the Kalash Limestone (Fig. 3).

The time-transgressive nature of the Waha limestone (Fig. 4), either in the eastern or the southern side of the Waha-Defa Fields, draws attention towards the formation of a continued shallow-water facies of reservoir character during their continuous transgression by lapping onto the high areas in course of the Campanian and Maastrichtian times. This would produce rock of reservoir character of greater geographical extent. However, according to the present knowledge, the Maastrichtian Waha Limestone is of fundamental importance for petroleum reserves due to the favourable structural setting.

In northeastern Sirte Basin (Concession 103 "IDR1s" Oilfield) the continuous section of the Maastrichtian and Danian carbonate complex has been illustrated by the "Heira Carbonate" grading laterally into the "Heira Shale" (Fig 7; Terry & Williams, 1969). Such stratigraphic setting has also been illustrated in Figure 6.

Third, the Lower Satal Formation encountered in the Dahra-Hofra region in the north-western basin. It is developed as a thick carbonate sequence forming the basal succession to the Carbonate Platform province which actually got well-defined during the Danian (Paleocene) time, when shelf to basin transition (shallow-water carbonate complex bordered by basinal shales) produced Carbonate Rim. This unique paleogeographic setting and the mode of deposition involving varied stratigraphic terminology has been illustrated (Fig. 5). The Maastrichtian Lower Satal Formation demonstrates trend of shallowing of the facies upward, when the upper chalky facies of "back-reef" character contains age-diagnostic *Orbitoides apiculatus*, *Omphalocyclus macroporus* and *Siderolites calcitrapoides*. It is a biofacies similar to that of the Waha Limestone.



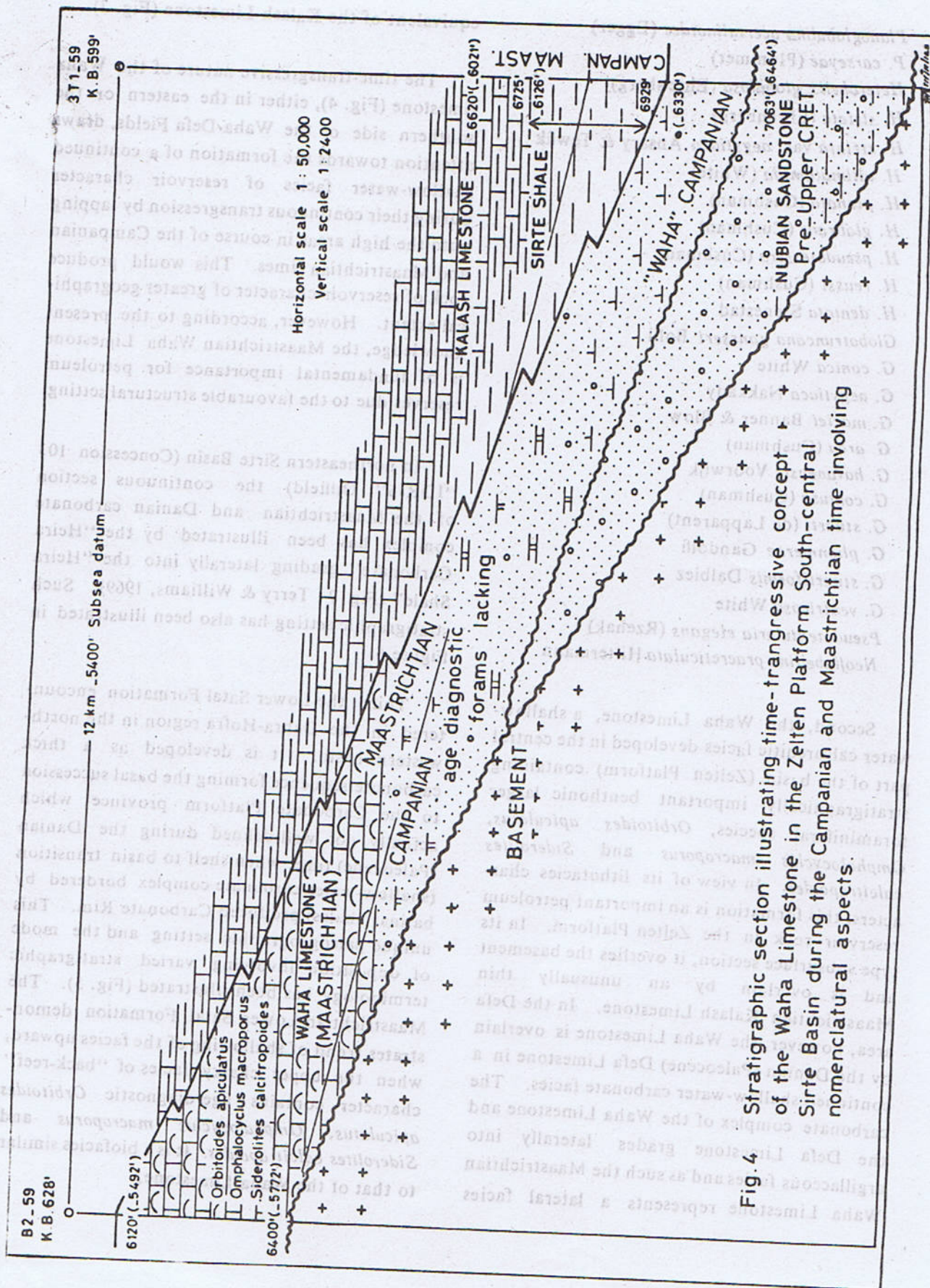


Fig. 4 Stratigraphic section illustrating time-transgressive concept of the Waha Limestone in the Zelten Platform South-central Sirte Basin during the Campanian and Maastrichtian time involving nomenclatural aspects.



Finally, the Samah Dolomite in the Samah area of the Beda Platform, is developed as a shallow-water dolomite facies of limited geographical extent but a principal reservoir rock in the Samah Field.

#### Ghadames Basin

The Maastrichtian stratigraphy of this region is classified into a stratigraphic unit, the Lower Tar Marl. This unit contains, in its lower part, abundant planktonic foraminifera and assigned to the *Globotruncana gansseri* Zone, while the upper part of this formation contains the benthonic larger foraminiferal species, *Omphalocyclus macroporus* and *Siderolites calcitrapoides* (Barr & Weegar, 1972). The faunal distribution shows that the outer neritic open marine facies is succeeded by the shallow-water facies, a trend of shallowing of the sea in the Late Maastrichtian. This is analogous to the paleogeographic setting of the Sirte Basin as demonstrated by the deposition of the Waha Limestone or the upper portion of the Lower Satal Formation.

The following planktonic foraminiferal species have been reported from the Lower Tar Marl (Barr & Weegar, 1972).

*Globotruncana gansseri* Bolli  
*G. stuarti* (de Lapparent)  
*G. arca* (Cushman)  
*G. contusa* (Cushman)  
*G. mariei* (Banner & Blow)  
*Rugoglobigerina rugosa* (Plummer)  
*Heterohelix* spp.

#### Cyrenaica Platform

As mentioned previously, the Cyrenaica Shelf acted as a shallow-water carbonate deposition during the Upper Cretaceous time, while greater subsidence took place in the adjoining Sirte Basin. This created basinal deposition of the Kalash Limestone. However, the same stratigraphic name has been extended towards the

Cyrenaican region where the distinction from the continuous K-T carbonate succession follows E-Log criteria. The 'Kalash Limestone' (Fig. 6) contains *Bolivina incrassata gigantea*, while rare minute size globotruncanids suggestive of shallower paleobathymetry are also encountered.

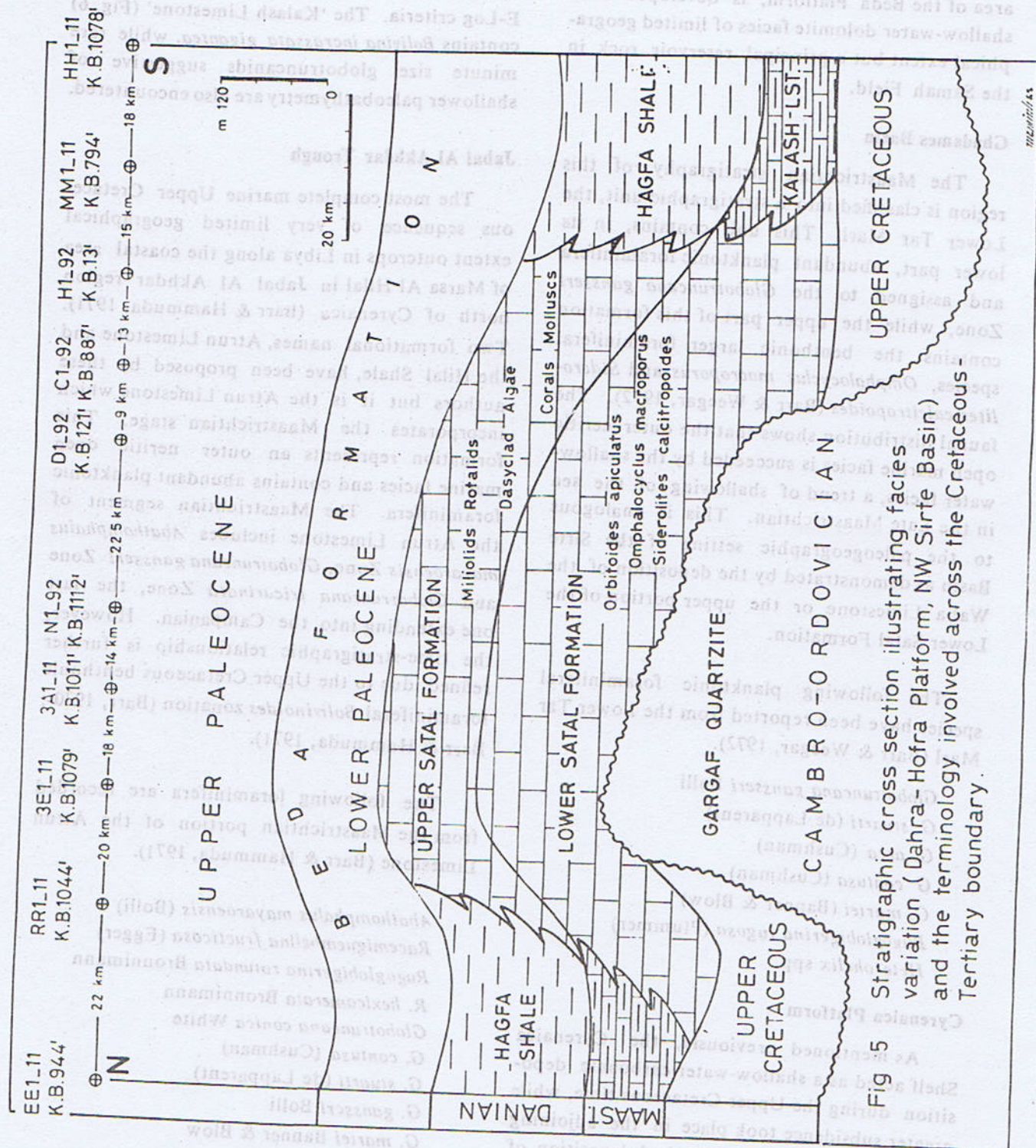
#### Jabal Al Akhdar Trough

The most complete marine Upper Cretaceous sequence of very limited geographical extent outcrops in Libya along the coastal area of Marsa Al Hilal in Jabal Al Akhdar region north of Cyrenaica (Barr & Hammuda, 1971). Two formational names, Atrun Limestone and the Hilal Shale, have been proposed by these authors but it is the Atrun Limestone which incorporates the Maastrichtian stage. This formation represents an outer neritic open marine facies and contains abundant planktonic foraminifera. The Maastrichtian segment of the Atrun Limestone includes *Abathomphalus mayaroensis* Zone, *Globotruncana gansseri* Zone and *Globotruncana tricarinata* Zone, the last one extending into the Campanian. However, the time-stratigraphic relationship is further refined due to the Upper Cretaceous benthonic foraminiferal *Bolivina* zonation (Barr, 1970 ; Barr & Hammuda, 1971).

The following foraminifera are recorded from the Maastrichtian portion of the Atrun Limestone (Barr & Hammuda, 1971).

*Abathomphalus mayaroensis* (Bolli)  
*Racemiguembelina fruticosa* (Egger)  
*Rugoglobigerina rotundata* Bronnimann  
*R. hexamerata* Bronnimann  
*Globotruncana conica* White  
*G. contusa* (Cushman)  
*G. stuarti* (de Lapparent)  
*G. gansseri* Bolli  
*G. mariei* Banner & Blow  
*G. arca* (Cushman)  
*G. falsostuarti* Sigal







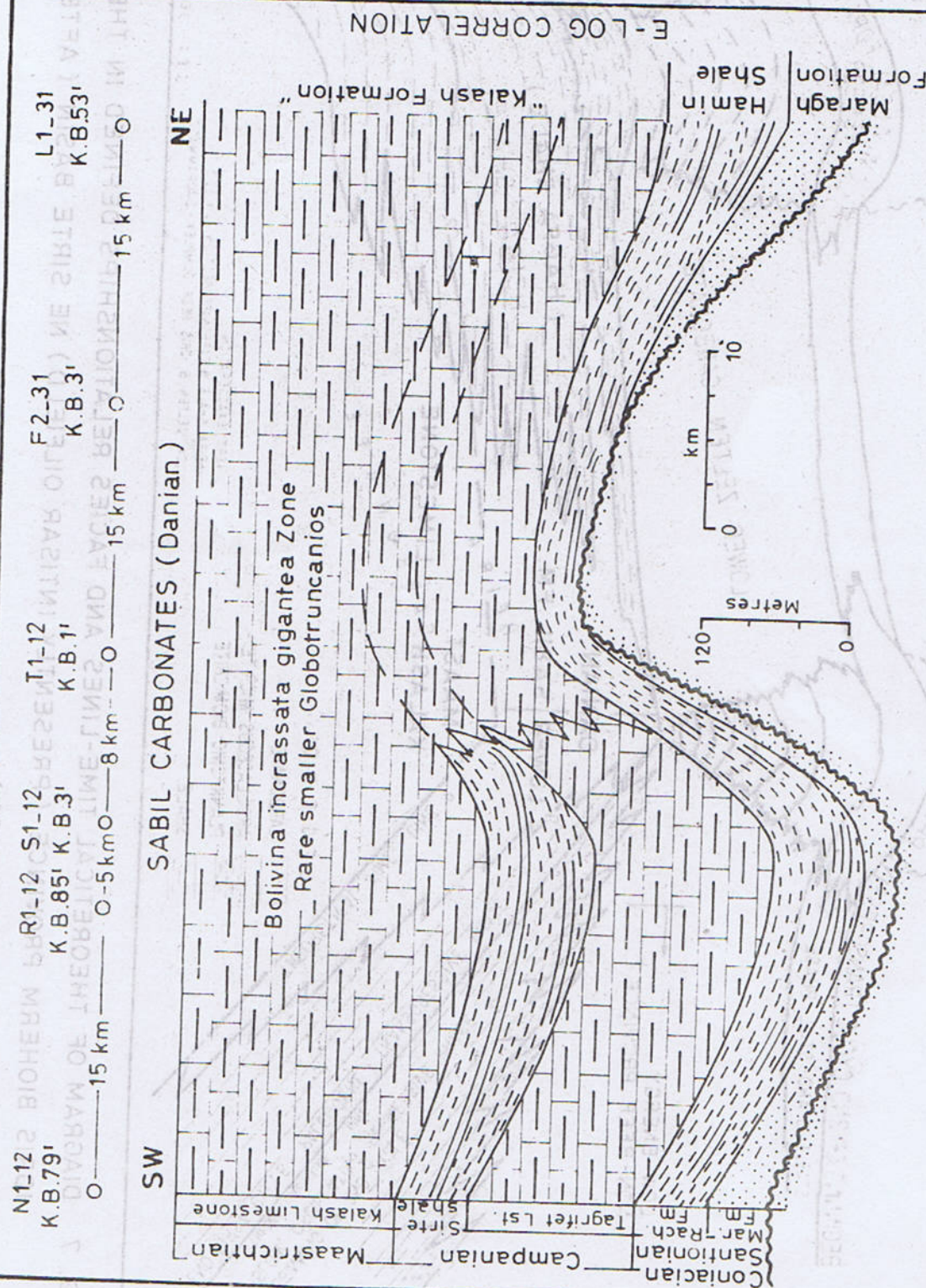


Fig.6 Diagrammatic Upper Cretaceous stratigraphic cross section of Northeast Sirte Basin ( Amal Oilfield ) and the adjoining Cyrenaica Platform showing facies variation nomenclatural problems. Oasis terminology of the Hamin Shale is incorporated.

maximise







*Globotruncanella havanensis* (Voorwijk)  
*Rugoglobigerina rugosa* (Plummer)  
*Globotruncana gagnebini* Tilev  
*G. duwi* Nakkady  
*G. rosetta* (Carsey)  
*G. ventricosa* White  
*G. obliqua* Herm  
*G. subcircumnodifer* Gandolfi  
*G. stuartiformis* Dalbiez  
*G. tricarinata* (Quereau)  
*G. fornicata* Plummer  
*Hedbergella holmsdelensis* Olsson  
*Bolivinoidea paleocenicus* (Brotzen)  
*B. peterssoni* Brotzen  
*B. draco* (Marsson)  
*B. giganteus* (Hiltermann & Koch)  
*B. miliaris* Hiltermann & Koch  
*B. decoratus* (Jones)  
*B. cyrenaicus* Barr  
*B. strigillatus* (Chapman)

## HYDROCARBON HABITAT

The factors which govern oil source capacity of a sedimentary rock are the quality of organic material in the rock, the oil-generative quality of that organic matter, its transformation into hydrocarbon in the deep subsurface under the influence of both subsurface temperature and geologic time, and the oxygen-depleted environments of deposition with high sedimentation rate. Generally, the source rock potential quality is attributed to the shales or micrites, provided they have favourable stratigraphic and structural setting as well as the anoxic depositional environments.

In the Sirte Basin, the Upper Cretaceous Sirte Shale (mainly Campanian in age) is the source rock of prime importance because of its favourable geological conditions for the petroleum source bed deposition. This stratigraphic level in the adjacent Ghadames Basin to the west and the Cyrenaica Platform to the east, does not meet the favourable geological indices

because of change in sedimentary facies and, therefore, their source potential quality is precluded. This is primarily due to the structural setting of the entire region during the Upper Cretaceous period (Fig. 2), when active subsidence began in the Sirte Basin creating favourable structural setting for promoting the source capacity of the Sirte Shale, in contrast to the adjoining shallow oxygenated shelf regions offering least favourable geological conditions for source bed deposition. On the other hand, the Silurian shales in the Ghadames Basin are the prime candidate as a source rock because of favourable stratigraphic and structural setting, while in the Cyrenaican region, much older strata (Jurassic-Lower Cretaceous) meet the favourable geological requirements.

It is, therefore, believed that the structural configuration of these basins and the stratigraphic control is a key factor to evaluate the hydrocarbon habitat in these regions. Therefore, close proximity of the Campanian Sirte Shale in the Hagfa Trough (also named as the Marada Trough) and the Maastrichtian Waha Limestone in the adjacent Zelten Platform establishes a closely situated source rock—reservoir rock stratigraphic relationship involving short distance hydrocarbon migration and entrapment (Waha-Defa Oilfields). The other example is from the Beda Platform where the Maastrichtian Samah Dolomite is a reservoir rock (Samah Oilfield). This factor makes the shallow-water Maastrichtian carbonate environments of great economic significance.

## CONCLUSIONS

In terms of standard Maastrichtian planktonic zonation, *Globotruncana gansseri* Zone has a regional significance in Libya. The *Abathomphalus mayaroensis* Zone has restricted application (i.e., Jabal Al Akhdar).

Benthonic smaller foraminiferal *Bolivina incrassata gigantea* Zone can be established in



the Cyrenaican region and the Sirte Basin. In view of the variation in paleogeographic setting and depositional style in these regions, *Bolivina incrassata gigantea* seems to have greater range of depth distribution (from inner neritic to outer neritic).

The shallow-water facies, whether developed in the Ghadames Basin or in the Sirte Basin, is characterised by diagnostic Upper Cretaceous

benthonic larger foraminiferal species, *Orbitoides apiculatus*, *Omphalocyclus macroporus* and *Siderolites calcitrapoides*.

The shallow-water Maastrichtian carbonate environments have contributed towards promoting sedimentary facies of great reservoir potentials in the Sirte Basin (Waha Limestone, Samah Dolomite).

#### HYDROCARBON HABITAT

The factors which govern oil source capacity of a sedimentary rock are the quality of organic material in the rock, the oil-generative quality of that organic matter, its transformation into hydrocarbon in the deep subsurface under the influence of both subsurface temperature and geologic time, and the oxygen-depleted environments of deposition with high sedimentation rate. Generally, the source rock potential quality is attributed to the shales or micrites, provided they have favourable stratigraphic and structural setting as well as the anoxic depositional environments.

In the Sirte Basin, the Upper Cretaceous Sirte Shale (mainly Campanian in age) is the source rock of prime importance because of its favourable geological conditions for the petroleum source bed deposition. This stratigraphic level in the adjacent Ghadames Basin to the west and the Cyrenaica Platform to the east, does not meet the favourable geological indices

#### CONCLUSIONS

In terms of standard Maastrichtian planktonic zonation, Globotruncana gurgensis Zone has a regional significance in Libya. The *Cheloniceras mayanensis* Zone has restricted application (i.e., Jabal Al Akhdar).

Benthonic smaller foraminiferal *Bolivina incrassata gigantea* Zone can be established in



## REFERENCES

- Barr, F.T., 1968 (a). Late Cretaceous planktonic foraminifera from the coastal area east of Susa (Apollonia), northeastern Libya. *Jour. Paleontology*, 42 (2), 308-321.
- Barr, F.T., 1968 (b). Upper Cretaceous biostratigraphy of Jabal Al Akhdar, northern Cyrenaica, Libya. In : Barr, F. T., (Ed.), *Geology and Archaeology of northern Cyrenaica, Libya. Petrol. Explor. Soc. Libya, Publ., Tripoli*, 131-147.
- Barr, F.T., 1970. The foraminiferal genus *Bolivinoidea* from the Upper Cretaceous of Libya. *Jour. Paleontology*, 44 (4), 642-654.
- Barr, F.T., 1972. Cretaceous biostratigraphy and planktonic foraminifera of Libya. *Micropaleontology*, 18 (1), 1-46.
- Barr, F.T. and Hammuda, O.S., 1971. Biostratigraphy and planktonic zonation of the Upper Cretaceous Atrun Limestone and Hilal Shale, northeastern Libya. *2nd Internat. Conf. Plank. Microfossils, Proc. Rome*, 27-40.
- Barr, F.T. and Weegar, A.A., 1972. Stratigraphic nomenclature of the Sirte Basin, Libya. *Petrol. Explor. Soc. Libya, Publ., Tripoli*, 1-179.
- Butt, A.A., 1984. Upper Cretaceous biostratigraphy of the Sirte Basin, northern Libya (ABSTRACT) *IX African Micropal. Colloque, Paris*. (1983) *Geologie Mediterranee (France)*, XI (1-2), 237-238.
- Eliagoubi, B.A., 1979. Systematic paleontology of Maastrichtian foraminifera (Upper Cretaceous) from northcentral and northwestern Libya. *Arab. Dev. Inst. Publ., Tripoli*, 1-79.
- Eliagoubi, B.A. and Powell, J.D., 1980. Biostratigraphy and paleoenvironment of Upper Cretaceous (Maastrichtian) foraminifera of northcentral and northwestern Libya. In : *Geology of Libya* (Eds. M.J. Salem and M.T. Busrewil), Vol. 1, Academic Press, London, 137-153.
- Massa, D. and Delort, T., 1984. Evolution du bassin Syrté (Libye) du Cambrien au Crétacé basal. *Bull. Soc. Geol. France, Ser. 7*, 26 (6), 1087-1096.
- Terry, C.E. and Williams, J.J., 1969. The Idris "A" Bioherm and Oilfield, Sirte Basin, Libya—its commercial development, regional Paleocene geologic setting and stratigraphy. *Inst. Petrol. Publ., London*, 31-48.



# MIOPORE FORMS FROM THE UPPER DEVONIAN DEPOSITS OF NEW YORK STATE AND PENNSYLVANIA U.S.A.

BY

SARFRAZ AHMED

Institute of Geology, University of the Punjab, Lahore, Pakistan.

**Abstract :** Palynological studies have been made of six sections extending over 4000 Sq. Km. through the Upper Devonian in western New York State and northern Pennsylvania, U.S.A. Sediments from this region, which represents the stratotype for the Devonian of North America, have disclosed profuse assemblages of spores and microplanktons, the former constituting the basis of the present investigations.

Thirty nine spore forms have been encountered which can be attributed to twenty genera of trilete spores; of these four species are new; seven new combinations and one new name is proposed; six other forms are present but are insufficient numerically to be proposed as new. The lithology of the material investigated is mainly composed of shale, siltstone and siltysandstone.

## INTRODUCTION

Sixty four samples from six sections namely the Walnut Creek the Brick Quarries, the Bush Hill, the Hamlet Quadrangle, the Pope Hollow and Lewis Run (see Ahmed 1986, Fig. 1) have been analysed, all of which contained palynomorphs. The sequence of these palynomorphs indicates complex relationships between marine and continental facies. Acritarchs have been recorded from throughout the sequence apart from the lower part of the Ellicott Member of the Chadakoin Formation but these are used only as environmental indicators and have not been dealt with monographically. Spore forms which have been described in this paper belong to the following eight infraturmae; *Laevigati*, *Retusotrileti*, *Apiculati*, *Murornati*, *Cingulati*, *Crassiti*, *Zonati*, and *Monopseudosaccati*.

Suprageneric Classification of the Anteturma Sporites follows the scheme of Potonie & Kremp (1954), with certain revisions and innovations proposed by Dettmann (1963) Smith & Butterworth (1967) and Streel (in Becker *et al*

1974). The term of Grebe (1971) are used here, most of which are defined in the glossary of Kremp (1965).

The size range given in the dimensions is the maximum diameter of the spore and does not include the ornament unless otherwise stated. Micron is abbreviated to ' $\mu\text{m}$ '. Scanning electron microscope is abbreviated to 'SEM'.

An effort has been made to illustrate the morphological variations within a species or a genus described here. Some species have been studied with the help of the scanning electron microscope (SEM). SEM photomicrographs have been useful in understanding the surface sculpture of miospores, whereas the light photomicrographs are essential to illustrate the sporewall structure below the surface.

Spores having appendages of bi- and multifurcate processes are also present but these are not included in this work.



The species *synorisporites flexuosus* (Juscho) Richardson & Ahmed has frequently been observed in younger part of the sequence investigated. It has been found in the Chadakoin and the Cattaraugus Formations and also in the Northeast Shale Member of the Canadaway Formation (from Sample No. US10A to US7 see Ahmed 1980, Fig. 2). The species could be considered as an index fossil of middle Famennian (Fa2b-Fa2c), since it has been reported from almost equivalent stratigraphical levels in many parts of the world e.g. western Europe, North Africa and North America. For stratigraphic and Palaeontologic details of the area the readers are referred to Ahmed 1986.

#### SAMPLE PREPARATION

The rock samples were prepared by means of standard palynological techniques using hydrofluoric acid to remove the mineral matter, followed by oxidation of the organic residue with conc. nitric acid. Various stages of oxidation were applied with maximum time of approximately 24 hours for the best results. No alkalis were used strew mounts were made using 'cellosize' dispersal agent and Canada balsam as a mounting medium.

All holotypes and figured specimens are housed in the Palynology Laboratory, Geology Department, King's College, University of London. The specimen co-ordinates were obtained on Nikon microscope No. 84368.

#### SYSTEMATIC DESCRIPTION

Anteturma	SPORITES (Potanie 1893)
Turma	TRILETES (Reinsch 1891)
Subturma	AZONOTRILETES (Luber 1935)

Infraturma RETUSOTRILETI Streel (in Becker *et al*) 1974.

Genus RETUSOTRILETES (Naumova) Richardson 1965.

*Type Species* : *R. pychovii* Naumova 1953  
(lectotype species of Richardson 1965)

*Remarks.* Naumova (1953) established a genus (subgroup) *Retusotriletes* embracing sub-circular trilete miospores with distinct contact areas, possessing both laevigate and sculptured exines. This author did not designate a genotype and therefore the genus was regarded as *nomen nudum*. Though Potonie (1958) did not formally emend this genus he selected type species *R. simplex* Naumova (1953, pl. 2, Fig. 9), the first described of Naumova's ten species, and restricted the use of taxon to forms with smooth exine. Since then many workers have commented upon the circumscription of *Retusotriletes* including Chibrikova (1959), Chaloner (1963), Playford (1964), Streel 1964, 1967, Richardson 1965, Mortimer (1967), Lanning (1968), Schultz (1968), Riegel (1968), Cramer (1969), Richardson & Lister (1969), Owens (1971), McGregor (1973) and Tiwari & Schaarschmidt (1975). At present there are two schools of thought and palynologists may follow either of them concerning the delimitation of the genus *Retusotriletes*. First, Streel (1964) emended the genus and followed Potonie in using *R. simplex* Naumova as type species. Richardson & Lister (1969, p. 214) pointed out that Potonie's arbitrary selection of Naumova's *R. simplex* was unfortunate in that Naumova's illustrations pl. 2, Fig. 9 and pl. 15, Fig. 14 lack *curvaturae perfectae* and therefore distinct contact area. *R. simplex* is therefore not characteristic of this genus. Secondly, Richardson (1965) independently of Streel, emended the genus suggesting *R. pychovii* Naumova (p. 953, pl. 1, Fig. 5) as the type species. The present writer follows Richardson (loc. cit. p. 564) on the grounds that the lectotype possesses well defined contact areas delimited by *curvaturae perfectae*. The emendation proposed by Streel (1964) is not followed here as the lectotype of Potonie lacks the diagnostic features of the genus.



**Comparison.** *Retusotriletes* (Naumova Richardson (1965) differs from *Apiculiretusispora* (Streel 1967, p. 32) and *Verruciretusispora* Owens (1971, p. 20) by having laevigate exine.

*Retusotriletes* sp. cf. *R. concinnus*  
Kedo 1955 in Lanninger 1968

Plate 1, Figs. 1-3

? 1955 *Retusotriletes concinnus* Naumova in lit. Kedo pl. 1, Fig. 13.

1968 *Retusotriletes concinnus* Naumova in lit; Lanninger pl. 1, Fig. 4.

1972 *Retusotriletes* cf. *R. concinnus* Naumova in lit; Kemp p. 109, pl. 52, Fig. 1.

**Occurrence.** Rare. Chadakoin Formation, Pennsylvania, U.S.A.

**Description.** Miospores radial trilete; amb circular to oval with rounded apices and convex sides. Margin smooth. Exine laevigate and up to  $4\mu\text{m}$  thick. Contact areas delineated by curvaturae that may be confined entirely to the proximal surface, or may be confluent with the equator along most of their length. In the latter case the curvaturae show as Y-like invaginations at the ends of the laesurae. On some specimens the terminations of the suturae are connected by curvaturae that appear interradially as a thin line. Occasionally a lighter, thinner zone is present on or in the vicinity of the proximal pole. Trilete mark distinct; laesurae sinuous, or rarely straight, extending to the spore radius, accompanied by a narrow labra  $1.5\text{--}2.5\mu\text{m}$  raised, rays terminating in curvaturae.

**Size range.**  $36\text{--}56\mu\text{m}$  mean  $48\mu\text{m}$  (25 specimens measured).

**Remarks and comparison.** The specimens described above appear to be closely akin to those recorded from Germany (Lanninger 1968)

and Antarctica (Kemp 1972). Decisive allocation is not made here to the previously described forms, however, owing to the different (smaller) size range of the miospores recorded during this study. The dimensions given by Lanninger (loc. cit.) and Kemp (loc. cit.) are  $65\mu\text{m}$  and  $63\text{--}84\mu\text{m}$  respectively.

*Retusotriletes concinnus* Naumova in Kedo (1955, pl. 1, Fig. 13) is different from those observed from Germany, Antarctica and U.S.A. with respect to morphographic circumscriptions and in the nature of laesurae. Present examples also bear some resemblance to *Retusotriletes leptocentrum* Higgs (1975) described from southeast Ireland. In the Irish specimens a lighter apical area is, however, a feature not normally associated with the present form.

*Retusotriletes concretus* nom. nov.,

Plate 1, Fig. 4

**Derivation of name.** Latin, concretus, meaning thick, referring to the thick triangular apical area.

1963 *Retusotriletes novus* Shepeleva p. 98 (invalid. I.C.B.N. article 33).

1969 *Retusotriletes* cf. *triangulatus* Streel in Richardson & Lister p. 217, pl. 37, Figs. 3-5.

**Occurrence.** The Canadaway, Chadakoin and Cattaraugus Formations; New York State and Pennsylvania, U.S.A.

**Description.** Miospores radial trilete; amb circular to subcircular. Exine laevigate and  $1\text{--}2\mu\text{m}$  thick; in some specimens folds are present along the part of the equatorial margin. Contact areas delimited by distinct curvaturae which usually follow the equatorial margin except in the radial areas in polar compression. Curvaturae  $1\text{--}1.5\mu\text{m}$  thick and raised. Trilete mark distinct, surrounded by a thickened distinctly triangular area in the apical region; the apical area extends almost to the tip of the



rays; laesurae straight, frequently splayed open, continued as dark lines to the curvaturae, total length of suturae  $\frac{3}{4}$  of the spore radius.

*Size Range.* 44-60  $\mu$ m, mean 51  $\mu$ m (30 specimens measured).

*Remarks and Comparison.* Markedly triangular apical area and dark, raised curvaturae are the distinguishing features of the species described above.

*Retusotriletes* sp.

Plate 1, Figs. 5-6

*Occurrence.* Rare, Canadaway and Chadakoin Formations, New York State and Pennsylvania, U.S.A.

*Description.* Miospores radial, trilete; amb subcircular to roundly triangular. Exine up to 2  $\mu$ m thick, laevigate to shagrinata, which may be the result of corrosion pitting. Contact areas laevigate, frequently and distinctly darkened (thickness), one-half to two-thirds of spore radius. Trilete mark distinct; laesurae straight, simple or labarate, rarely gaping, extending  $\frac{1}{4}$  of spore radius. End of the rays connected by curvaturae within 2-3  $\mu$ m of the equator.

*Size range.* 36-79  $\mu$ m, mean 54  $\mu$ m (30 specimens measured)

*Remarks and comparison.* Exine appears to be corroded in the areas of laesurae and curvaturae perfectae. The specimens referred to *phyllotheotriteles* sp. in Lanzoni & Magloire (1969) are probably identical to the present form. Miospores similar to *Retusotriletes* sp. were also found dispersed in Southern Ireland by Higgs (1975, p. 395, pl. 1, Figs. 9-13).

#### Genus ANEUROSPORA Streel 1964

*Type species.* *Aneurospora goensis* Streel 1964.

*Remarks.* The genus *Aneurospora* was diagnosed to embrace laevigate and sculptured miospores equipped with comprehensive equatorial to subequatorial crassitude formed from curvatural thickenings.

*Aneurospora greggsii* (McGregor) Streel in Becker *et al.* 1974.

Plate 1, Figs. 7-16.

*Occurrence.* In all four of the formations investigated; abundant in the Chadakoin Formation; New York State and Pennsylvania, U.S.A.

*Size range.* 31-67  $\mu$ m, mean 48  $\mu$ m (110 specimens measured).

*Remarks.* The species has been represented in profusion from the material investigated and agrees closely with the Canadian specimens described by McGregor (1964) from the Ghost River Formation, Alberta. It differs in the nature of the ornament which, unlike the present examples, possesses sculptural elements, in some of the specimens as long as 2  $\mu$ m.

*Apiculiretusispora nitida* Owens appears to be identical in terms of size and general organization. Owens (1971, p. 17) interprets that "Representatives of this species are frequently preserved in lateral or oblique compression and commonly occur in large sporangial masses". During the current investigation identical characters have also been observed and illustrated on pl. 3, Figs. 2-8.

The present author regards *Cyclogranisporites* sp. of Warg & Traverse (1973) to be identical with the species described above (see remarks under the species *Pulvinispora quasibrata* Higgs 1975).

Another taxon *Apiculiretusispora granulata* Owens (1971, p. 15) appears to possess banded curvaturae in addition to the granular ornament of the distal hemisphere. Some of the speci-



mens subsequently attributed to the Canadian species (e.g. *A. granulata* recorded by Higgs 1975 from southeast Ireland) are tentatively placed in synonymy with the species under consideration. Although Owens (loc. cit.) himself intimated that after having determined precise enunciation of the morphological details the species could be transferred to an appropriate genus. In the writer's opinion, however, the examination of the holotype would be necessary to establish conclusively the structure of the miospores.

Infraturma APICULATI (Bennie & Kidston)  
Potonie 1956.

Genus ACANTHOTRILETES (Naumova)  
Potonie & Kremp 1954.

Type species. *A. ciliatus* (Knox) Potonie & Kremp 1954.

Remarks. This category incorporates circular and triangular trilete miospores ornamented on distal, proximal and equatorial hemispheres with spinae which are at least twice as long as their basal diameter.

Comparison. The genus *Acanthotriletes* is differentiated from *Lophotriletes* (Naumova) Potonie & Kremp (1954) and *Apiculatisporis* Potonie & Kremp (1956) by its ornament of spinae.

*Acanthotriletes horridus* var. *minutus* var. nov.

Plate 1, Figs. 17-18.

Derivation of name. Latin. *minutus*, little or small, referring to the small size of miospores and ornamentation elements.

Holotype. Plate 1, Fig. 17, U. S. A. 19 1240412.

Type locality. Brick Quarries, East of Jamestown; Dexterville Member, Chadakoin Formation, New York State, U.S.A.

Occurrence. Chadakoin and Cattaraugus Formations, New York State and Pennsylvania, U.S.A.

Diagnosis. Exine of miospores thin, usually torn, ornamented with spines of various shapes and size; spines straight occasionally bent, up to  $13\mu\text{m}$  in height and  $5\mu\text{m}$  in basal diameter; suturae extend almost to the radius of the spore.

Description. Miospores radial trilete; amb circular to subcircular to convexly triangular, irregular due to torn nature of exine. Exine up to  $2.5\mu\text{m}$  thick at equator, frequently thinner in centre; occasionally folded, laevigate to slightly infrapunctate apart from the ornament of spinae. The latter may reach  $13\mu\text{m}$  in height and  $5\mu\text{m}$  basal width. Spinae taper uniformly to sharply pointed apices. Spinae often bent, non-coalescent and number thirty-five to forty around the equator. Trilete mark distinct but in a few cases indiscernible due to the partly ruptured nature of exine; laesurae (when seen) straight or sinuous, extending almost to the equator, exine folded above the rays: folds up to  $3\mu\text{m}$  high.

Size range.  $45-104\mu\text{m}$ , mean  $75\mu\text{m}$  (35 specimens measured).

Remarks and Comparison. The most closely comparable species described to date appears to be *A. horridus* Hacquebard (1957, p. 309, pl. 1, Fig. 20). Apart from the size of the miospores ( $124-170\mu\text{m}$ ), the length of sculptural elements ( $12-33\mu\text{m}$ ) also tend to be larger in the Canadian specimens. These differences are selected as suitable criteria for the erection of a new taxon at varietal level. *A. hacquebardi* Playford (1964, p. 20, pl. 4, Figs. 1-4) differs in possessing simple and short laesurae ( $2/5-1/2$  spore radius) and occasionally fused spines at the bases only for some distance along their length.

*Acanthotriletes* sp.

Plate 1, Fig. 19.



**Occurrence.** Chadakoin Formation, New York State and Pennsylvania, U.S.A.

**Description.** Miospores radial, trilete; amb subcircular, subtriangular to oval, margin smooth (exclusive of ornament). Exinal sculpture developed predominantly on distal and equatorial regions (reduced proximally within areas bounded by laesurae). Ornament irregular (on a given specimen) in terms of size of elements, their disposition and proportional representation: spinae, occasionally conical having circular or subcircular bases, spaced up to  $7\mu\text{m}$  apart. Dimensions of sculptural features: length  $1-4\mu\text{m}$ , basal diameter  $0.5-2\mu\text{m}$ . Apart from projections, exine laevigate to infrapunctate,  $2-3\mu\text{m}$  thick; conspicuous compression folds developed on some specimens. Trilete mark distinct; laesurae simple, occasionally accompanied by folds, suturae extending  $\frac{1}{2}$  to  $\frac{3}{4}$  spore radius.

**Size range.**  $48-55\mu\text{m}$  (17 specimens measured).

**Remarks.** The patterns of folding developed on the exine, sometimes give an impression of curvaturae. The sculptural elements observed on the present forms are preponderantly spines and therefore aptly placed in *Acanthotriletes*. Clearly, however, the number of specimens so far recovered is insufficient for formal taxonomic naming (i.e. species level). Partial separation of exine layers has been observed in only 20% of the specimens.

**Comparison.** Of previously described taxa, the Russian Frasnian species *Acanthotriletes grandispinus* Naumova (1953, pl. 5, Fig. 77) seems to be closest morphologically to the specimens attributed here to *Acanthotriletes* but lacks compression folds and is of distinctly smaller size ( $25-35\mu\text{m}$ ).

Genus *DIBOLISPORITES* Richardson 1965

**Type species.** *D. echinatus* (Eisenack) Richardson 1965.

**Remarks.** The genus was instituted to incorporate azonate miospores ornamented with dominantly biform elements, other features such as spines, cones, pila, verrucae and rod-like processes are also borne on the exine.

**Comparison.** *Acinosporites* Richardson 1965 comes closest but differs from *Dibolisporites* in having ornament of different types superimposed on convolute and anastomosing ridges.

*Dibolisporites* sp.

Plate 1, Figs. 20-21.

**Occurrence.** Chadakoin and Cattaraugus Formations, Pennsylvania, U.S.A.

**Description.** Miospores radial trilete; amb subtriangular to oval with convex sides and rounded apices. Exine  $2-3\mu\text{m}$  thick at equator, but possibly thinner in centre. Contact areas smooth or with reduced ornament. Remainder of proximal surface, distal and equatorial hemispheres conspicuously sculptured with biform elements; consisting of broad based (dome shaped) cones, superimposed on which are very fine spines; width of cones  $3\mu\text{m}$ , height  $1.5-3\mu\text{m}$ , basal width of spines  $1\mu\text{m}$  or less, height  $2-3\mu\text{m}$ ; elements spacing up to  $20\mu\text{m}$ ; (text Fig. 1). Sculptural processes normally discrete and straight, occasionally coalesced at their bases and bent. Equatorial region fairly densely sculptured with ornament, polar region frequently sparsely ornamented; usually 14-19 elements project from the equator. Trilete mark distinct; laesurae straight, extending full spore radius, sometimes exine folded above the suturae, folds up to  $2-5\mu\text{m}$  raised.

**Size range.**  $40-43\mu\text{m}$  (5 specimens measured).



**Remarks.** The spores occur sporadically and are not well enough preserved for precise identification at specific level. It cannot be established conclusively, at present, whether the equatorial thickening is a structural feature (zona) or merely exine thickness. The present examples are tentatively placed in *Dibolisporites* Richardson because azonate forms sculptured with bifurcated elements undoubtedly correspond to Richardson's genus (see Allen 1965, p. 702).

**Comparison.** The studied form bears a superficial resemblance to *Acanthotriletes* aff. *ignotus* Kedo (1953, pl. 2, Fig. 47). Although close comparison is impeded by the fairly generalized nature of Kedo's description and line-drawn illustration, it seems that, in lacking distinct spines surmounted by cones, *A.* aff. *ignotus* is distinct from *Dibolisporites* sp.

**Infraturma MURORNATI** Potonie & Kremp 1954.

**Genus CONVOLUTISPORA** Hoffmeister, Staplin & Malloy 1955.

**Type species.** *C. florida* Hoffmeister, Staplin & Malloy 1955.

**Remarks.** *Convolutispora* is a trilete genus covering azonate miospores that are ornamented with overlapping ridge-like processes which do not form a well-defined reticulum.

*Convolutispora* sp. aff. *Verrucosisporites congestus* Playford 1964  
Plate 2, Fig. 1

**Occurrence.** Rare, Canadaway and Cattaraugus Formations, New York State and Pennsylvania, U.S.A.

**Description.** Miospores radial trilete; amb subcircular to circular. Exine 3-4  $\mu$ m thick with coalescent verrucate or low muri, features ill-defined, elements 2-12  $\mu$ m wide, 1-3  $\mu$ m high, intervening space 1-3  $\mu$ m in maximum diameter.

Trilete mark distinct; laesurae obscured to perceptible, simple, straight; length  $\frac{1}{2}$  to  $\frac{3}{4}$  of amb radius.

**Size range.** 50-61.2  $\mu$ m (5 specimens measured).

**Remarks and Comparison.** The form described above is a borderline case between *Convolutispora vermiformis* and *verrucosisporites-congestus* Playford (1954) since the features used for separation overlap. Differs slightly from *V. congestus* in lacking discrete verrucae; the size range recorded by Playford ranges from 56-101  $\mu$ m. The form is also rather distinct from *C. vermiformis* Hughes & Playford (1961) in not having a well-defined reticulate pattern of ridges. *V.* cf. *congestus* Playford in Lanzoni & Maglorie (1969, pl. 1, Figs. 11-12) recorded from the Sahara Algeria could be identical to the present form.

**Genus EMPHANISPORITES** McGregor 1961

**Type species.** *E. rotatus* McGregor 1961.

**Remarks.** *Emphanisporites* is a well illustrated trilete genus embracing azonate miospores sculptured with well-defined radial ribs on the proximal hemisphere. Distal surface laevigate, with annulate thickening or distally sculptured with grana, conuli, or verrucae. The taxon is typical of Lower to Middle Devonian rocks but occasional examples have also been observed from Upper Devonian and Lower Carboniferous sediments. The form is rare and sporadic in its occurrence in the area studied.

**Comparison.** Some forms of *Hystricosporites* also exhibit proximal radial ribs but it differs, however, in having prominent grapple tipped appendages.

*Emphanisporites* cf. *annulatus* McGregor 1961  
Plate 2, Fig. 2.

**Occurrence.** Rare, Cattaraugus Formation, New York State, U.S.A.



**Size Range.** A single specimen seen measuring 39 $\mu$ m.

**Remarks.** This form seems to be the most closely similar to *E. annulatus* described by McGregor (1961, 1973). Firm attribution is not here made to McGregor's species, however, owing to the indistinct nature of the annulus on the distal hemisphere.

#### Genus DICTYOTRILETES (Naumova)

Smith & Butterworth 1967

**Type species.** *D. bireticulatus* (Ibrahim) Potonie & Kremp 1954.

**Remarks.** Smith & Butterworth (1967, p. 194) emended the diagnosis propounded by Potonie & Kremp to embrace only acingulate miospores which were formerly attributed to *Reticulatisporites* (Ibrahim) Neves (1964). The exine of *Dictyotriletes* is sculptured with a well defined or poorly defined reticulum which may be restricted to distal surface. Lumina regular or variable in shape, usually greater than 6 $\mu$ m in diameter.

*Dictyotriletes* cf. *trivialis* Naumova in litt.  
in Kedo 1963  
Plate 2, Fig. 3.

**Occurrence.** Chadakoin Formation, New York State, U.S.A.

**Size range.** A single specimen recorded measuring 80 $\mu$ m.

**Remarks.** The only example observed during the present investigation superficially resembles that illustrated by Kedo (1963, pl. 4, Fig. 88). Despite its morphological simplicity the form described above is not directly assigned to the Russian species on account of the corroded nature of its exine and absence of trilete mark. Probably, if enough specimens are examined, these factors do not hinder or prevent identification.

#### *Dictyotriletes* sp.

Plate 2, Fig. 4.

**Occurrence.** Rare, Chadakoin and Cattaraugus Formations, New York State, U.S.A.

**Description.** Miospores radial trilete, amb subcircular to broadly triangular. Exine 2-4 $\mu$ m thick at the equator. Proximal surface laevigate, distal hemisphere reticulate. Lumina of reticulum 6-18 $\mu$ m in greatest diameter, usually polygonal in outline, may be somewhat irregular; lumina commonly (but not always) slightly larger toward the distal pole. Number of lumina per specimen up to seventeen. Muri of reticulum 2-4 $\mu$ m thick, 3-6 $\mu$ m high, normally project at the amb; rounded to pointed in profile, distinct and strongly developed. Laesurae simple, straight extending  $\frac{1}{2}$  to almost spore radius, commonly not detectable.

**Size range.** 51-76.5 $\mu$ m mean 64 $\mu$ m (20 specimens measured).

**Remarks and Comparison.** The specimens were observed which at a first approximation are identical to *D. emsiensis* (Allen) McGregor (1973, p. 42, pl. 5, Fig. 15). However, careful examination reveals the absence of grana or small verrucae on the proximal surface. The muri, in Spitsbergen and Canadian specimens, are commonly widened or papillate at their junctions. Another taxon described by McGregor, *D. subgranifer* McGregor (1973, p. 43, pl. 5, Figs. 16, 18-20) would appear to be very close to the present form but differs in having narrower and lower muri that are serrated along the upper edge and in Canadian specimens the proximal surface is granulate.

Subturma ZONOTRILETES Waltz 1935

Infraturma CINGULATI Potonie & Kalus 1954

Genus KNOXISPORITES Potonie & Kremp emend. Neves 1961

**Type species.** *K. hageni* Potonie & Kremp 1954.



**Remarks.** Neves 1961 formulated the emended diagnosis of the genus to include miospores having a cingulum of uniform thickness which tapers slightly towards the equator and the distal hemisphere, in this category, is sculptured with radial or concentric thickened bars.

**Comparison.** *Reticulatisporites* (Ibrahim) Neves 1964 differs in having a differentiated cingulum.

*Knoxisporites literatus* (Waltz) Playford 1963  
Plate 2, Figs. 5-6.

**Occurrence.** Chadakoin and Cattaraugus Formations, New York State and Pennsylvania, U.S.A.

**Size range.** 54-78  $\mu\text{m}$ , mean 66  $\mu\text{m}$  (35 specimens measured).

**Remarks and Comparison.** The specimens observed during the present investigation comply with Playford's description except in the width of cingulum which is wider (8-19  $\mu\text{m}$ ) in the Spitsbergen specimens,

*K. hederatus* (Ishchenko) Playford (1963), originally recorded from the western extension of the Donetz Basin in sediments of Tournaisian—Lower Viséan age, is structurally identical but differs, however, in having simple laesurae.

Identical forms have widely been reported from Famennian to Viséan throughout the world. Allen (in Gayer *et al.* 1973) illustrated two specimens of *K. literatus* from the Lower Tournaisian of Taff Gorge, Glamorgan. In the writer's opinion a specimen in Plate 14, Fig. 1 seems best excluded from the Russian species because its distal ornament is not well delineated. The specimen can well be accommodated within the circumscription of *K. pristinus* Sullivan 1968.

*Knoxisporites pristinus* Sullivan 1968

Plate 2, Figs. 7-8.

**Occurrence.** Chadakoin and Cattaraugus Formation, New York State and Pennsylvania, U.S.A.

**Size range.** 53-76.5  $\mu\text{m}$ , mean 62  $\mu\text{m}$  (50 specimens measured).

**Remarks.** The specimens incorporated in the foregoing description are more frequently distributed in the area studied than the specimens attributed to *Knoxisporites literatus*. The present representatives are somewhat smaller than those described by Sullivan 1968 (62-103  $\mu\text{m}$ ).

**Comparison.** Morphologically and dimensionally *K. pristinus* Sullivan is more or less identical to *K. literatus* (Waltz) Playford (which Sullivan did not in fact record). Sullivan (1968, p. 123) erected a new species on the seemingly slight grounds that it exhibits non-polar compression and ill defined distal thickenings. During the present study, forms assignable to these two species have been recovered and the fact that a few morphographic intermediates were found enables me to uphold Sullivan's speciation. It can also be suggested that forms with an almost irregular amb (due to non-polar orientation), vaguely defined distal muri and with relatively thin contact areas should be confined to *K. pristinus* Sullivan.

A form assigned to *K. literatus* by Allen in Gayer *et al.* (1973, pl. 14, Fig. 1), can easily be accommodated within the circumscription of *K. pristinus* Sullivan.

*Knoxisporites* sp. aff. *Reticulatisporites crassus*  
Winslow 1962  
Plate 2, Fig. 9.

**Occurrence.** Canadaway Formation, Northeast Shale Member, New York State, U.S.A.

**Size range.** Two specimens seen measuring 76.5  $\mu\text{m}$  and 81.6  $\mu\text{m}$  respectively.



**Remarks and Comparison.** The morphology of above described form appears to be distinct from previously described forms attributable to *Knoxisporites*. *K. cinctus* (Waltz) Butterworth & William (1958 p. 370, pl. 2, Figs. 11-13) somewhat resembles *K. sp. aff. R. crassus* from which it can be distinguished as it possesses three pairs of proximal muri, each enclosing a laesura.

A positive assignment to *Reticulatisporites crassus* Winslow (1962 p. 58, pl. 14, Figs. 8-10a and Pl. 22, Fig. 23) must be withheld since the differentiated cingulum and the nature of the distal ornament are common in the forms from both areas. A firm attribution is not here made to Winslow's species, however, owing to the presence of muri along rays. Winslow's specimens have a greater size range (94-147 $\mu$ m).

Genus *LOPHOZONOTRILETES* Naumova 1953  
**Type Species.** *L. lebedianensis* Naumova 1953.

**Remarks.** The miospores attributed to this genus are acavate, cingulate, sculptured with verrucate and/or conate ornament.

Richardson & Ioannides (1953, p. 280) remarked that the holotype of *Lophozonotriletes lebedianensis* Naumova selected by Potonie (1958, pl. 2, Fig. 21) does not possess a distinctive cingulum while in the customary sense this feature is well defined. In consequence the type species is not a true representative of the taxon. Playford (1976, p. 28) also seems to be unsatisfied with the present status of the genus. In the present work the miospores are attributed to the above genus on the ground that they contain a well-developed cingulum.

*Lophozonotriletes curvatus* in Naumova 1953  
 Plate 2, Figs. 10-11.

**Occurrence.** Rare. Chadakoin Formation, Pennsylvania, U.S.A.

**Size range.** 39-55 $\mu$ m, mean 47 $\mu$ m (25 specimens measured).

**Remarks and Comparison.** Specimens are sparingly represented and conform with the Russian illustrations except in the nature of the laesurae which are rather labrate in some of the examples observed during the present investigation.

Recombination of the species with *Converrucosisporites* Potonie & Kremp (1954) suggested by Turnau (1975, p. 510) is rather doubtful. Some of the specimens illustrated by Naumova (1953, pl. 15, Fig. 45; pl. 19, Fig. 27) and Turnau (loc. cit. pl. 2, Fig. 1) are not distinctly triangular, a characteristic which is a significant factor in assigning the species to the genus *Converrucosisporites*. In terms of ornament, which seems to be biform, the Polish specimens may belong to a different species.

In addition to the Russian Platform identical specimens have also been recorded from the Pripyat Depression (Kedo 1957, 1963).

Genus *VALLATISPORITES*  
 (Hacquebard) 1957 Sullivan 1964b

**Type Species.** *V. vallatus* Hacquebard 1957.

**Diagnosis.** See Sullivan 1964b, p. 370.

**Remarks.** Originally described by Hacquebard, the genus has been modified by Sullivan (1964), Staplin & Jansonius (1964, p. III) and Dolby (Ph. D. Thesis 1970, p. 108). In present work *Vallatisporites* is used in the sense implied by Sullivan (1964, p. 370) i.e. for trilete zonate miospores that have equatorial border internally vacuolate, cuniculus located at the equator of the spore cavity, distal exoexine possessing cones, verrucae and spinae.

*Vallatisporites vallatus* var. *hystricosus*

(Winslow) Clayton (et al. 1977)

Plate 2, Figs. 12-15, 17.



**Occurrence.** Frequently observed in the Cattaraugus and upper part of the Chadakoin Formations, New York State and Pennsylvania, U.S.A.

**Size range.** Exoexine 40-70 $\mu$ m, mean 55 $\mu$ m; intexine 30-55 $\mu$ m, mean 42 $\mu$ m (105 specimens measured).

**Remarks and Comparison.** Due to the restricted vertical range in the present study, the first appearance of *V. vallatus* var. *hystricosus* is used to define the base of the HL Assemblage Zone (Ahmed 1978). The sculptural elements of this form are shown in text Fig. 2.

It has been observed during the present investigation that the specimens examined from the higher part of the sequences (Cattaraugus Formation) are densely sculptured when compared with the older, Chadakoin Formation. It is evident from text Fig. 3, that specimens having sculptural elements more than sixteen have not been found occurring in the Chadakoin Formation; whilst up to 47 ornamentation elements have been observed on the specimens from the younger, Cattaraugus Formation.

It is of interest to note that the size of the sculptural elements of *Cirratiradites hystricosus* of Winslow recorded from the Bedford, Cuyahoga and Logan Formation, Ohio, range in length from 2 to 5.2 $\mu$ m. The identical specimens have also been observed from New York State and Pennsylvania and the maximum size of the sculptural elements have been recorded up to 12 $\mu$ m.

*Vallatisporites vallatus* var. *major* (Kedo)  
comb. nov.

Plate 2, Fig. 16.

1963 *Hymenozonotriletes pusillites* var. *major* (Kedo) pl. 16, Fig. 143.

**Occurrence.** Rare, Cattaraugus Formation, New York State, U.S.A.

**Size range.** Two specimens encountered measuring 85 and 90  $\mu$ m respectively.

**Remarks.** The specimens observed during this study comply with the description of *V. vallatus* var. *hystricosus* excepting the size range, which tends to be greater in the present form. *V. vallatus* var. *major* has a restricted vertical range when compared with its mother species.

Subturma ZONOTRILETES Waltz 1955

Infraturma CRASSITI Bharadwaj & Venkatachala 1961.

Genus AMBITISPORITES Hoffmeister 1959

**Type species.** *A. avitus* Hoffmeister 1959.

**Remarks and Comparison.** The taxon *Ambitisporites* was founded by Hoffmeister from Libyan Lower Silurian sediments and embraces laevigate, trilete miospores coupled with an equatorial crassitude. The category could be placed in synonymy with *Stenozonotriletes* Hacquebard (1957). Richardson (1969), however, indicated that the interest in Hoffmeister's spores is that they are from "high Lower Silurian" strata. The genus is treated here as a coherent generic entity.

*Ambitisporites* cf. *avitus* Hoffmeister 1959

Plate 3, Figs. 1-2.

**Occurrence.** Rare, Canadaway, Chadakoin and Cattaraugus Formations, New York State and Pennsylvania, U.S.A.

**Size range.** 38-56 $\mu$ m, mean 47 $\mu$ m (20 specimens measured).

**Remarks.** The specimens observed during the present investigation are tentatively left in the species *Ambitisporites avitus* Hoffmeister 1959 because of the identical nature of crassitude. A difference such as folds along laesurae is not regarded, at present, sufficient ground for separation. They are grouped together for convenience until enough specimens are found upon which to select criteria



for separation. A specimen illustrated by Richardson and Lister (1969, pl. 40, Fig. 2) is most probably assignable to the present form. A more or less identical specimen has also been reported by Cramer (1966, pl. 2, Fig. 34) from some Silurian-Devonian rocks of northwest Spain.

### Genus STREELISPORE

Richardson & Lister 1969

*Type Species.* *S. newportensis* (Chaloner & Streel) Richardson & Lister.

*Remarks and Comparison.* The diagnosis of *Streelispora* propounded by Richardson & Lister covers crassitudinous trilete miospores, ornamented with granulate, conate, spinose and/or bifurc elements, proximal surface laevigate or with interrational papillae. The genus is distinct from *Aneurospora* Streel 1964 since the latter does not possess an equatorial thickening.

*Streelispora catinata* (Higgs) comb. nov.

Plate 3, Figs. 3-5.

*Crassispora catinata* (Higgs) P. 396, Pl. 2, Figs. 1-3.

*Occurrence.* Almost in all the samples studied.

*Description.* Miospores radial trilete; amb subcircular, subtriangular to oval. Proximal surface laevigate, contact areas bounded by distinct to barely distinguishable crassitude, up to 5  $\mu$ m wide, width differs from place to place even on a single specimen. Distal and equatorial hemispheres covered with spinae, conic and grana; elements with rounded to pointed apices, up to 1  $\mu$ m in width and 2  $\mu$ m in height, sometimes characteristically coalesced to form irregular ridges. Specimens rarely thrown into fine folds of irregular orientation. Trilete mark distinct, laesurae straight, extending  $\frac{2}{3}$  to full spore radius, terminating in

curvaturae imperfectae; rays usually masked with folds 1-2.5  $\mu$ m in height and width.

*Size range.* 40-65  $\mu$ m, mean 52  $\mu$ m (95 specimens measured).

*Remarks and Comparison.* The specimens here assigned to *Streelispora* (*Crassispora*) *catinata* comb. nov. are closely comparable to the specimens from the Upper Devonian of southwest Ireland illustrated by Higgs (1975), although the structural interpretations placed on the present specimens differ considerably from those made by Higgs in the original description of the species. Although Higgs (1975) made no specific reference to equatorial thickening (crassitude), it seems probable from interpretation of (at least the one) illustrated specimen (Higgs loc. cit. pl. 2, fig. 2) that such a feature (structure) is in fact present. Therefore, allocation of the species to *Streelispora* is preferred. Both the genera *Crassispora* and *Streelispora* are crassitudinous but inclusion of the present form within *Streelispora* is justified since *Crassispora* lacks granulate ornament. Apical papillae, in the latter are probably constant feature (see Sullivan 1964, pl. 375).

*Streelispora distincta* sp. nov.

Plate 3, Figs. 6-11.

*Derivation of name.* Latin, distinctus, meaning separate, referring to the discrete nature of ornament.

*Holotype.* Plate 3, Figs. 6-7 US6H 319 1195581.

*Type locality.* Pope Hollow Section; along boundary between Carroll and South valley Townships, Jamestown quadrangle, New York State.

*Occurrence.* Canadaway, Chadakoin and Cattaraugus Formations, New York State and Pennsylvania, U.S.A.



**Diagnosis.** Miospores with distinct equatorial crassitude of uniform width, distally and equatorially ornamented with conic and grana, suturae terminating in curvaturae perfectae.

**Description.** Miospores radial trilete; amb subtriangular to rounded triangular, sides distinctively convex. Exine 0.5-1.5  $\mu$ m thick distally, contact areas highly distinctive and smooth. Well delineated equatorial crassitude 2-4  $\mu$ m wide with uniform width. The examples bear a loosely set ornament of grana, conic and/or spinae which are confined to the equatorial margin and distal hemisphere; ornamentation elements 0.5-2  $\mu$ m high, up to 1.5  $\mu$ m in diameter, circular in plan, pointed or rounded in profile. Spores usually compressed in polar views. Trilete mark distinct; laesurae straight, simple or accompanied by lips 0.5-1.5  $\mu$ m wide, length of rays  $\frac{2}{3}$  to full spore radius, terminating in curvaturae perfectae, which coincide through most or all of their length with the equator of the spore.

**Size range.** 35-60  $\mu$ m, mean 45  $\mu$ m (60 specimens measured).

**Remarks.** On the grounds of characters described above, the species seems to be best left in *Streelisporea*.

**Comparison.** *S. catinata* (Higgs) comb. nov. somewhat resembles *S. distincta* sp. nov. from which it can be differentiated by being populated by vaguely defined equatorial thickening and by having coalescent ornamentation elements. *S. newportensis* (Chaloner & Streel) Richardson & Lister bears three interrarial papillae and in *S. granulata* Richardson & Lister crassitude is thicker in the interrarial areas than in the radial region.

#### Genus SYNORISPORITES

Richardson & Lister 1969

**Type Species.** *S. downtonensis* Richardson & Lister.

**Remarks.** *Synorisporites* Richardson & Lister 1969 is a trilete miospore genus equipped with equatorial crassitude and curvaturae perfectae. Distal surface comprehensively ornamented with verrucate and/or murornate elements.

**Comparison.** *Synorisporites* is distinguishable fairly readily from *Streelisporea* as it has sculptural elements of verrucae and muri rather than grana, conic and spinae. *Ambitisporites* Hoffmeister (1959) is a laevigate crassitudinous taxon.

*Synorisporites flexuosus* Richardson & Ahmed 1988 (Jusch in Kedo & Golubtsov).

Plate 4, Fig. 1-9

Non 1953 *Hymenozonotriletes famenensis* Naumova p. 77 (French transl.) pl. 17, fig. 17.

Non 1953 *Hymenozonotriletes mirandus* Naumova p. 36 (French transl.) pl. 18, fig. 34.

Non 1963 *Hymenozonotriletes famenensis* Kedo pl. 5, fig. 109.

1966 ? *Perotriletes* sp. McGregor & Owens, pl. 28, fig. 25.

1967 *Hymenozonotriletes famenensis* Kedo; Neves & Dolby pl. 2, fig. 3.

1970 *Rugospora miranda* (Naumova) Dolby M.S. p. 103, pl. 9, figs. 8-10

1971 *Trachvtriletes flexuosus* Jusch. in Kedo & Golubtsov pl. 5, fig. 1.

1974 *Rugospora flexuosus* (Jusch. in Kedo & Golubtsov) Streel in Becker *et al.* pl. 21, figs. 8-11.

For description and occurrence of this species readers are referred to Richardson & Ahmed 1988, pp. 551-552.

**Size range.** 43-67  $\mu$ m, mean 53  $\mu$ m (200 specimens measured).



**Remarks and Comparison.** The presence of a distinctive equatorial crassitude together with well defined distal murornate ornament (text fig. 4) studied under light and scanning electron microscope (SEM), renders appropriate the assignment of this species to the genus *Synorisporites* Richardson & Lister. The arrangement of muri (confined within the crassitude) on the distal region is variable but gradational from specimen to specimen and does not form a basis for further speciation. Wide geographical distribution but the restricted vertical range of *S. flexuosus* (Jusch.) Richardson & Ahmed contribute to its usefulness as an index fossil. The first appearance of this species is used to define the base of the *S. flexuosus*—*A. varia* Assemblage Zone (Ahmed 1978).

*Hymenozonotrites famenensis* in Neves & Dolby subsequently recovered from British Isles by Dolby (1970, pl. 19, fig. 8); Utting & Neves (1970, pl. 27, fig. 9); Allen in Gayer *et al.* (1973, pl. 15, fig. 5) and specimens illustrated from Canada by McGregor (1970, pl. 23, fig. 4) and from Pennsylvania by Warg & Traverse (1973) pl. 1, fig. 4 are almost certainly junior synonyms of *S. flexuosus* (Jusch.) Richardson & Ahmed. *H. famenensis* Kedo in Clayton *et al.* (1974) is probably a different form.

*Synorisporites richardsonii* sp. nov.

Plate 4, Figs. 10-12

**Derivation of name.** The species is named after Dr. J. B. Richardson, in recognition of his research on Silurian-Devonian miospores with equatorial crassitude (Richardson & Lister 1969, Richardson & Ioannides 1973).

**Holotype.** Plate 4, figs. 10-11 NY95C 37 119663.

**Type Locality.** Lewis Run, Hanley Quarries, Cattaraugus Formation, Pennsylvania, U.S.A.

**Occurrence.** Rare. Chadakoin and Cattaraugus Formations, New York State and Pennsylvania, U.S.A.

**Diagnosis.** Miospores with distinct equatorial thickening; ornament of verrucae and rare coni disposed over the entire distal and equatorial hemispheres; laesurae straight or barely sinuous, simple occasionally accompanied by lips of folds.

**Description.** Miospores radial trilete; amb subtriangular with convex sides and rounded apices, ranging from subtriangular to sub-circular. Exine proximally laevigate, thin, occasionally tending to break down. Contact areas distinct and delimited by curvaturae perfectae, forming an equatorial thickening of 3.5-6  $\mu$ m. Distal and equatorial hemispheres sculptured with verrucae and/or rare coni, 1.5-2  $\mu$ m high, 1-3  $\mu$ m wide at their base. In plan view they are circular, subcircular or irregular; in profile rounded, almost pointed or with flattened apices, ornamentation elements densely packed at the equatorial margin, but widely spaced on the distal hemisphere. Specimens occasionally occur with compression folds, whilst proximo-distal orientation frequent. Trilete mark distinct; laesurae straight or slightly sinuous, extending between  $\frac{1}{4}$  of radius and almost to spore margin, simple or accompanied by folds or lips up to 4  $\mu$ m high.

**Size range.** 38-44  $\mu$ m, mean 41  $\mu$ m (40 specimens measured).

**Remarks.** Equatorial thickening (crassitude) and ornament of mainly verrucae are the features utilized to justify the inclusion of the present specimens within the morphographic circumscription of *Synorisporites*.

**Comparison.** The species described above is distinct from all the previously described forms attributed to genus *Synorisporites*. *S. papillensis* McGregor (1973, p. 51) stands closest morphologically but differs however, by possessing



dark papillae on the proximal surface. *S. downtonensis* Richardson & Lister (1969, p. 232) is distinguished by being larger (44-78  $\mu\text{m}$ ) and possessing convolute and anastomosing muri. *S. ? libycus* Richardson and Ioannides (1973, p. 278) is merely ornamented with verrucae which "are strictly confined within the equatorial thickening"

*Synorisporites variegatus*

Richardson & Ahmed 1988

Plate 5 & Figs. 1-4.

1966 'unidentified' McGregor & Owens pl. 28, figs. 17-18, 21-22.

1970 *Hymenozonotriletes famenensis* Kedo in McGregor pl. 21, figs. 6, 16; pl. 22, fig. 5.

1975 *Hymenozonotriletes famenensis* Naumova in Higgs pl. 5, fig. 6.

For holotype, type locality, diagnosis, description and occurrence see Richardson & Ahmed 1988, p. 552.

**Size range.** 49-64  $\mu\text{m}$ , mean 55  $\mu\text{m}$  (50 specimens measured).

**Remarks and Comparison.** The species is well ornamented with muri and subordinate verrucae together with equatorial crassitude. It is therefore better accommodated by *Synorisporites*. *S. richardsonii* sp. nov. somewhat resembles *S. variegatus* Richardson & Ahmed from which it can be distinguished as it possesses distal ornament of verrucae and coni. Crassitude in *S. verrucatus* Richardson & Lister 1969 is smooth proximally and distally and the miospores are considerably smaller (16-33  $\mu\text{m}$ ).

Infraturma ZONATI Potonie' & Kremp 1954

Genus SAMARISPORITES Richardson 1965

**Type Species.** *S. orcadensis* (Richardson) Richardson 1965.

**Remarks.** In making *Samarisporites* a junior synonym, McGregor (1973, p. 58) remarked that the extent of the cavity and the degree of attachment between exine layers are insufficient criteria for generic differentiation. According to McGregor the genus therefore comes within the morphographic range of *Grandispora*. The present author departs from McGregor but concurs with Playford (1976, p. 41) in retaining this taxon as separate from *Grandispora*. *Samarisporites* is used here in the sense implied by Richardson (1965; i.e. as zonate miospores having a distal ornament of coni, short spiniae and/or verrucae.

*Samarisporites inusitatus* Allen 1965

Plate 5, Fig. 5

**Occurrence.** Abundant in the Java and Canadaway Formations; a single specimen was also found in the Chadakoin Formation, New York State U.S.A.

**Size range.** Exoexine 55-70  $\mu\text{m}$ , mean 62  $\mu\text{m}$ ; intexine 50-60  $\mu\text{m}$ , mean 55  $\mu\text{m}$  (35 specimens measured).

**Comparison.** *Samarisporites inusitatus* Allen (1965) differs from *S. triangulatus* Allen 1965 in the nature of amb which is circular to roundly triangular rather than triangular.

*Samarisporites orcadensis* (Richardson 1960, p. 58, pl. 14, fig. 12, text fig. 8) Richardson (1965) possesses an ornament merely of cones which do not support an apical spine. The size range of the Scottish species is considerably greater (96-153  $\mu\text{m}$ ).

*Samarisporites kedoae* (Riegel) comb. nov.

Plate 5, Figs. 6-7

Non 1953 *Hymenozonotriletes argutus* Naumova p. 41, pl. 4, fig. 10; pl. 9, fig. 9.

? 1955 *Kymenozonotriletes argutus* Naumova, in Kedo pl. 4, fig. 4.



1968 *Hymenozonotriletes argutus* Naumova, in Lanninger p. 144, pl. 24, fig. 15.

1973 *Hymenozonotriletes kedoe* Riegel p. 94, pl. 15, figs. 1-3.

1974 *Samarisporites* sp. cf. *Hymenozonotriletes acanthyrugosus* Chibricova in Becker et al. p. 25, pl. 18, fig. 8.

Non 1974 *Ancyrospora kedoe* (Riegel) Turnau, p. 152, pl. 9, figs. 1-3, 6, 7.

**Occurrence.** Chadakoin and Chadakoin Formations, New York State, U.S.A.

**Description.** Miospores radial trilete, zonate, amb subtriangular or oval with convex interrational sides and rounded apices; margin notched and irregular due to the distribution of ornament. Exine two layered, intexine roundly triangular 3-4 $\mu$ m thick (dark) and laevigate; exoexine 1-1.5 $\mu$ m thick, closely appressed to intexine and extended in the equatorial plane to form a zonate flange. Exoexine laevigate to infrapunctate apart from the ornament which is confined to the distal face and the equatorial hemisphere. Sculptural elements comprise spines and cones of variable shape, height and width (text fig. 5). They range 2-8 $\mu$ m in height and up to 5 $\mu$ m in basal width; isolated spines rarely borne, normally connected at their bases. Distance between tips of elements at equator 5-20 $\mu$ m, distance between intexine and equator of exoexine 7-30 $\mu$ m, occasionally more at angles than at interrational region. Trilete mark distinct; laesurae frequently masked with folds, straight or sinuous extending  $\frac{2}{3}$  to full intexine radius.

**Size range.** 67-153 $\mu$ m, mean 110 $\mu$ m, intexine 56-107 $\mu$ m, mean 81 $\mu$ m (40 specimens measured).

**Remarks.** In its current broadly defined form, the genus *Samarisporites* Richardson 1965 can reasonably accommodate the species

originally described from the Middle Devonian of the Eifel, West Germany.

**Comparison.** The intexine in *S. kedoe* is frequently thicker which stains darkly. In the specimens observed the sculptural elements appear to be darker (thicker) near the tip, this feature is evident in the figures illustrated by Riegel (1973), especially in holotype. This effect is also portrayed in Streel's (in Becker et al. 1974, pl. 18, fig. 8) photograph of *Samarisporites* sp. cf. *H. acanthyrugosus* Chibricova. *Hymenozonotriletes argutus* Naumova in Kedo (1955) is placed with question in synonymy with *S. kedoe* (Riegel) comb. nov. since apparently it seems to lack the characteristic spine structure of the latter, otherwise conspecific with Riegel's species. Another taxon *Calyptosporites angulatus* Tiwari & Schaarschmidt (1975) would appear to be very close to, if not synonymous with, *S. kedoe*. The former differs in having bifurcate spines. The thickening near the tip of the element is also evident in *Samarisporites* sp. cf. *S. kedoe*. In the latter, however, the thickenings are much more pronounced and it is conceivable that the two forms are end members of a morphological variation.

*Samarisporites* sp. cf. *S. kedoe* (Riegel)

comb. nov.

Plate 5, Figs. 8-9

**Occurrence.** Rare. Chadakoin Formation, New York State, U.S.A.

**Description.** Miospores trilete; amb subtriangular to irregular; margin notched. Exine two layered, intexine thick, circular and laevigate; exoexine thin, minutely roughened by fine, dense infrapunctation. The intexine and exoexine are closely appressed and the latter extends in the equatorial plane to form a wide zonate flange. Distal and equatorial hemispheres of exoexine conspicuously sculptured with spinae of distinctive form. Spinae show,



overall, a uniform taper from base to sharp point; but approximately two-third to three quarters of the distance from the base of each is a prominent circular swelling up to  $4\mu\text{m}$  wide. Each of these swelling is surmounted by a single spine. Elements are up to  $8\mu\text{m}$  high and  $2\mu\text{m}$  wide at the base (text fig. 5). Spinae and conical may be interspersed between the bifurcated elements. Trilete mark distinct; laesurae accompanied by straight or flexuous folds of the exoexine which extend, decreasing in height  $\frac{3}{4}$  to full intexine radius.

*Size range.* Only one specimen seen measuring  $115\mu\text{m}$ .

*Remarks.* Sculptural elements appear thicker (darker) towards the top and thinner (lighter) at the base, which may be the result of corrosion pitting.

Genus *SPINOZONOTRILETES* Hacquebard 1957

*Type Species.* *S. uncatus* Hacquebard 1957.

*Remarks.* The genus is confined to zonate miospores consisting of two wall layers; the intexine and exoexine which are closely appressed to each other. The exoexine extends equatorially to form a solid flange, ornamented with well-developed spines, otherwise it is laevigate or finely granulose.

Playford (1971, p. 45; 1976, p. 41) and McGregor (1973, p. 58), the latter apparently independently of the former, merged *Spinozonotriletes* into *Grandispora* Hoffmeister, Staplin & Malloy, the latter genus as a senior synonym takes priority over the former. In the present work *Spinozonotriletes* is treated as a genus separate from *Grandispora* on the basis of exine structure. The latter possesses cavate rather than zonate organisation. (See also remarks under *Grandispora*).

*Spinozonotriletes* sp.

Plate 5, Fig. 10

*Occurrence.* Rare. Cattaraugus Formation, New York State, U.S.A.

*Description.* Miospores radial trilete; amb subtriangular with convex sides and rounded apices. Exine two layered; the inner layer (intexine) thick, distinct, outline conformable with the amb and laevigate; the outer layer (exoexine) also thick and extends at the equator in the form of a thick flange. Exoexine partly folded, infurcate to laevigate apart from the ornament which is restricted to the distal and equatorial hemispheres. Ornament consists of relatively long, widely spaced, straight or bent spines which are parallel sided with rounded apices; sometimes the spines taper uniformly from broad bases, they are  $14-45\mu\text{m}$  long and number thirteen to eighteen around the equator. Trilete mark distinct; laesurae accompanied by elevated, sinuous lips, which may simulate exinal folds and almost attain equatorial margin; length of the laesurae equal to the radius of the body of the spore.

*Size range.* Exoexine  $82-141\mu\text{m}$ , intexine  $69-120\mu\text{m}$  (7 specimens measured).

*Remarks.* Owing to its extreme rarity, the form cannot formally be named specifically at this stage. The specimens find suitable inclusion within the genus *Spinozonotriletes* because of their non-pseudosaccate (zonate) construction.

*Comparison.* *Spinozonotriletes* sp. somewhat resembles *S. cf. naumovii* (Kedo) Richardson, originally recovered by Kedo (1955) from the Givetian of B.S.S.R. and subsequently observed by Richardson (1965, p. 583) and McGregor (1973, p. 61) from the middle Devonian of Scotland and Canada respectively. The present form differs, however, in having rounded rather than pointed tips to the spines.



Suprasubturma PSEUDOSACCITRILETES  
Richardson 1965

Infraturma MONOPSEUDOSACCITI  
Smith & Butterworth 1967

Genus GRANDISPORA Hoffmeister,  
Staplin & Malloy emend. Neves & Owens 1966

Type species. *G. spinosa* Hoffmeister,  
Staplin & Malloy 1955.

Remarks and Comparison. Neves & Owens (1966) emended the diagnosis of *Grandispora* to clarify the nature of attachment of the intexine and exoexine. These are only attached in the region of the trilete mark. The exoexine is sculptured with spinae and/or conic borne on distal and equatorial hemispheres and may encroach slightly on to the proximal surface.

The present author does not concur with Playford (1971, p. 45) and McGregor (1973 p. 58) regarding their broad generic concept of the taxon under consideration. The generic diagnosis formulated by McGregor (loc. cit.) incorporates *spinozonotriteles* Hacquebard 1957, *Calyptosporites* Richardson (1960) 1962 and *samarisporites* Richardson 1965 in synonymy with *Grandispora*. Playford (loc. cit.) failed to observe zonate miospores and regarded *spinozonotriteles* as cogenetic with *Grandispora*. However, contrary to McGregor, Playford did not include *samarisporites* within his synonymy listing for *Grandispora*.

During the present investigation a number of miospores having pseudosaccate structural organization (e.g. *Auroraspora*, *Grandispora* and *Calyptosporites*) on one hand and zonate exine (e.g. *spinozonotriteles* and *samarisporites*) on the other have been recovered, providing a way to sustain these taxa of different morphological characters as separate from each other.

The diagnosis of *Grandispora* as restated by Neves & Owens (1966) still remains the basic

circumscription of the genus, and is hence followed in this work. The features redefined by these authors are also the principal criteria used to justify the transfer of some of the Russian species to the present genus.

*Grandispora coronata* Higgs 1975

Plate 6, Fig. 1

Occurrence. Rare. Chadakoin and Cattaraugus Formations, New York State and Pennsylvania, U.S.A.

Size range. Exoexine 51-64 $\mu$ m, mean 55 $\mu$ m; intexine 44-52 $\mu$ m, mean 47 $\mu$ m (25 specimens measured).

Remarks. The cavate construction of the miospores and their distal and equatorial spinose sculpture support the generic allocation. The specimens recorded during the present investigations are only sparingly represented in the upper part of the sequence; many of them are badly preserved and the inner body is not clearly defined. However, the specimens are comparable in general organization with *G. coronata* Higgs recorded from the Upper Devonian of Hook Head, County Wexford, Ireland.

*Grandispora echinata* Hacquebard 1957

Plate 6, Figs. 2-3

Occurrence. Canadaway, Chadakoin and Cattaraugus Formations, New York State and Pennsylvania, U.S.A.,

Size range. Exoexine 41-69 $\mu$ m, mean 58 $\mu$ m; intexine 35-54 $\mu$ m, mean 45 $\mu$ m (30 specimens measured).

Remarks and Comparison. The specimens of this study are morphologically identical in terms of size, shape and nature of ornament to those recovered by Sullivan 1968 from the Tournaisian of the Cementstone Group in Ayrshire, Scotland. A Russian species recorded from the Tournaisian of Pripyat Depression, *Hymenozonotriteles flavus* Kedo (1963, pl. 5,



fig. 132) bears equivocal, possibly close, relationship with *G. echinata*.

*Grandispora echinula* (Naumova) comb. nov.

Plate 6, Figs. 4-6

1953 *Hymenozonotriletes echinulas* Naumova p. 78 (Russian transl.) pl. 17, fig. 22.

**Occurrence.** Java, Chadakoin and Cattaraugus Formations, New York State and Pennsylvania, U.S.A.

**Description.** Miospores radial trilete; amb subcircular to subtriangular. Exine double layered. Body thin, laevigate surrounded by pseudosaccus and attached to it over proximal surface, outline conformable with amb. Pseudosaccus 1-1.5  $\mu\text{m}$  thick, finely infragranulate to laevigate, proximal surface smooth, equatorial and distal hemispheres bear distinctive broad based discrete spines which taper sharply to almost pointed apices. Spines 6-16 project at the equator, 2.5-7.6  $\mu\text{m}$  high, 1-2.5  $\mu\text{m}$  wide at their bases. Trilete mark distinct; laesurae straight extending  $\frac{1}{2}$  to  $\frac{3}{4}$  spore radius, frequently accompanied by sinuous folds up to 7  $\mu\text{m}$  high.

**Size range.** Exoexine 51-70  $\mu\text{m}$ , mean 60  $\mu\text{m}$ ; intexine 42-58  $\mu\text{m}$ , mean 50  $\mu\text{m}$  (30 specimens measured).

**Remarks and Comparison.** Assignment to the present genus is endorsed because the pseudosaccate miospores having spinose ornament should eventually be attributed to *Grandispora*. The most closely comparable category seems to be *G. echinata* Hacquard (1957) which can be differentiated by having conate, as well as spinose, ornamentation elements. The Canadian species has a somewhat greater size range (62-93  $\mu\text{m}$ ). Another taxon illustrated from the Devonian-Carboniferous boundary in the central region of the Russian Platform by Umnova, *Hymenozonotriletes facilis* Kedo var. *decorus* Umnova (1971, pl. 3, figs. 53

and 74) seems to be similar in general organization and may be conspecific. However, a detailed comparison is not possible with undescribed Russian specimens. An identical form has also been recorded from the Pripyat Depression by Kedo (1957, pl. 1, fig. 3).

*Grandispora macroseta* (Kedo) comb. nov.

Plate 6, Figs. 7-9

1963 *Hymenozonotriletes macrosetus* Kedo pl. 6, figs. 149-150.

**Occurrence.** Chadakoin and Cattaraugus Formations, New York State, U.S.A.

**Description.** Miospores radial trilete; amb subcircular to subtriangular. Exine two layered, intexine (body) subcircular, virtually laevigate, covered by pseudosaccus and attached to it over proximal surface. Pseudosaccus infrapunctate. Body usually eccentrically placed, imperceptible to fairly distinct. Distance between body and pseudosaccus subequal. Pseudosaccus ornamented with gently tapering spines, 8-22  $\mu\text{m}$  high, 2.5  $\mu\text{m}$  wide at bases, 1  $\mu\text{m}$  wide at tips. Trilete mark distinct; laesurae straight, extending  $\frac{3}{4}$  to full body radius, accompanied by flexuose exoexinal folds which normally extend, decreasing in height to the pseudosaccus margin, ray folds up to 8  $\mu\text{m}$  high.

**Size range.** Exoexine 71-119  $\mu\text{m}$ , mean 90  $\mu\text{m}$ ; intexine 43-77  $\mu\text{m}$ , mean 53  $\mu\text{m}$  (30 specimens measured).

**Remarks and Comparison.** Pseudosaccate organization and spinose ornament makes inclusion within *Grandispora* entirely satisfactory.

Although sharing similar sculptural and structural attributes, *Grandispora macroseta* (Kedo) comb. nov. and *G. echinula* can be differentiated from each other as the latter incorporates smaller miospores (51-70  $\mu\text{m}$ ) and sculptural elements (2.5-7.6  $\mu\text{m}$ ). Comparison



can also be drawn between *G. microseta* (Kedo) Streel in Becker *et al.* and *G. macroseta* (Kedo) comb. nov.; the former is distinct in having a smaller size range (53 and 54  $\mu\text{m}$  see Streel in Becker *et al.* 1974, p. 26) and possessing more or less parallel sided spines with non-pointed apices.

*Grandispora* sp. cf. *G. spinosa* Hoffmeister, Staplin & Malloy in Massa & Moreau-Benoit 1976

Plate 6, Figs. 10-11

cf. 1976 *Grandispora spinosa* Hoffmeister, Staplin & Malloy; Massa & Moreau-Benoit pl. 5, fig. 5.

**Occurrence.** Cattaraugus Formation, New York State, U.S.A.

**Size range.** Two specimens seen measuring 70 and 73  $\mu\text{m}$  respectively.

**Remarks.** Two specimens have been encountered during the present investigation which are comparable with those illustrated by Massa & Moreau-Benoit of western Libya from the Upper Givetian to Upper Famennian. Firm attribution to the American species is hindered by the rudimentary nature of the ornament and the extreme rarity of the examples observed in the present material.

#### Genus CALYPTOSPORITES (Richardson)

Richardson 1962

**Type Species.** *C. velatus* (Eisenach) Richardson 1960.

**Remarks.** Playford (1971, p. 45) and McGregor (1973, p. 58) interpret *Calyptosporites* as being synonymous with *Grandispora*. The present writer rejects this suggestion and uses the genus in the sense diagnosed by Richardson (1960, 1962) i.e. for pseudosaccate species ornamented with cones and spines, having subtriangular outlines to both the intexine and exoexine with prominent ray folds.

#### *Calyptosporites perclarus* sp. nov.

Plate 7, Figs. 1-7

**Derivation of name:** Latin, *perclarus*, meaning very beautiful, referring to beautiful nature of varied ornamentation elements.

**Holotype.** Plate 7, Figs. 1-2. US6E 299 125°33'N,

**Type Locality.** Pope Hollow Section, along boundary between Carroll and South Valley Townships, Jamestown quadrangle, New York State.

**Occurrence.** Chadakoin and Cattaraugus Formations, New York State and Pennsylvania, U.S.A.

**Diagnosis.** Pseudosaccate miospores, ornamented with varied elements including pila, bacula, cones 1-4  $\mu\text{m}$  high, reduced or absent on proximal hemisphere; laesurae distinct to perceptible, frequently associated with lips which simulate exinal folds.

**Description.** Miospores radial trilete; amb subtriangular with convex sides and rounded apices. Exine double layered; intexine (body) laevigate up to 3  $\mu\text{m}$  thick, subcircular to subtriangular usually conformable with amb, covered with pseudosaccus (exoexine) and attached to it over proximal surface, most probably in the region of laesurae. Pseudosaccus 1-2  $\mu\text{m}$  thick, infrapunctate to infragranulate; independent sets of concentric and arcuate compression folds commonly developed on the distal side of the pseudosaccus; distal and equatorial hemispheres bear a closely set ornament of varied elements including pila, bacula and cones. Height of elements 1-4  $\mu\text{m}$ , basal width 1-2  $\mu\text{m}$ , stalk 1  $\mu\text{m}$  thick up to 3  $\mu\text{m}$  high and spherical head (on stalk) 1.5  $\mu\text{m}$  in diameter (text fig. 6). Discrete and coalesced ornament equally developed. Representatives usually preserved in polar compressions.



Trilete mark distinct; laesurae straight extending full body radius, rarely proceed further. frequently associated with lips which simulate exinal folds, 2-3 $\mu$ m wide, up to 5 $\mu$ m high.

*Size range.* Exoexine 48-65 $\mu$ m, mean 56 $\mu$ m, intexine 34-45 $\mu$ m, mean 39 $\mu$ m (50 specimens measured).

*Remarks and Comparison.* Subtriangular amb together with ray folds are regarded as sufficient criteria to warrant their inclusion within the genus *Calypptosporites*.

This species shows certain similarities to some previously described forms, but in no instance could identity with them be established confidently. *G. inculta* Allen (1965) is ornamented with cones only which are 1-2 $\mu$ m in height and width and possesses longer laesurae; moreover, it has a greater size range 51-86 $\mu$ m. *G. setosa* Clayton & Graham (1974, p. 578) is somewhat comparable with *C. perclarus* sp. nov. from which it can be differentiated by having smaller ornament (up to 2 $\mu$ m high). Should the Irish species prove to have larger ornament then it would be conspecific. A miospore from *Endoculeospora gardzinskii* Turnau (1975, p. 518, pl. 7, figs. 1-3), described from Lower Carboniferous deposits of northern Poland, appears to be closely akin to the species under consideration. The Polish species differs, however, in having weakly developed lips, as is suggested by the photographs (measurement not given), smaller ornamentation elements (up to 1 $\mu$ m long) and a circular to subcircular amb. *Hymenozonotrilete acanthyrugosus* Chibrikova (1959, pl. 11, fig. 11) appears to be similar. The Russian description is insufficiently explicit (e.g. about sculptural detail) for a close comparison to be made, but it is much larger (90-110 $\mu$ m) than *C. perclarus* and its sculptural elements probably comprise spines and cones.

Genus RHABDOSPORITES Richardson 1960

*Type Species.* *R. langi* (Eisenach) Richardson.

*Remarks.* *Rhabdosporites* is instituted to accommodate trilete pseudosaccate miospores. Pseudosaccus (exoexine) sculptured with closely spaced minute rods, that are parallel sided elements with almost truncated tips. Intexine (body) laevigate, pseudosaccus is frequently collapsed into folds, perhaps acquired during preservation.

*Comparison.* *Remysporites* Butterworth and Williams 1958 differs in having laevigate to microreticulate pseudosaccus. *Calypptosporites* Richardson 1962 is also sculptured but the latter has an ornament of cones and spines. *Auroraspora* Hoffmeister Staplin and Malloy, Richardson (1960) is a laevigate pseudosaccate taxon.

*Rhabdosporites langi* (Eisenach)

Richardson 1960

Plate 7, Figs. 11-12

*Occurrence.* Rare, Chadakoin Formation, New York State, U.S.A.

*Size range.* Exoexine 150-170 $\mu$ m, mean 160 $\mu$ m; intexine 102-114 $\mu$ m, mean 108 $\mu$ m (7 specimens measured).

*Remarks and Comparison.* The population measured from the Dexterville Member of the Chadakoin Formation comprised only 7 specimens which conform with those described by Richardson (1960) from the Lower Givetian, Middle Old Red Sandstone, Cromarty, Scotland, differing only in the nature of body which appears to be thicker in the studied material. *Hymenozonotriletes platyrugosus* Naumova (1953, pl. 8, fig. 10) differs in possessing larger body, simple and longer laesurae.

*Rhabdosporites parvulus* Richardson 1965

Plate 7, Figs. 8-10



**Occurrence.** Rare, in the Chadakoin, abundant in the Cattaraugus Formation, New York State and Pennsylvania, U.S.A.

**Size range.** Exoexine 62-80 $\mu$ m, mean 70 $\mu$ m; intexine 42-60 $\mu$ m, mean 52 $\mu$ m (30 specimens measured).

**Remarks.** The examples recovered during the present investigation resemble those described from the Orcadian Basin, Scotland by Richardson (1965). This species has sporadically been encountered in the Chadakoin and Cattaraugus Formations.

Genus RETISPORA Staplin 1960

**Type Species.** *R. florida* Staplin 1960.

**Remarks.** The genus *Retispora* embraces two layered miospores consisting of an intexine and anexoexine. The latter is strongly reticulate on the distal surface.

*Retispora lepidophyta* (Kedo) Playford 1976  
Plate 8, Figs. 1-4

**Occurrence.** Cattaraugus and upper part of the Chadakoin Formations, New York State and Pennsylvania, U.S.A.

**Size range.** Exoexine 50-114.7 $\mu$ m, mean 70 $\mu$ m; intexine 30-60 $\mu$ m, mean 45 $\mu$ m (15 specimens measured).

**Remarks.** The species has been described under various disguises by many palynologists. Because of its inordinately wide geographical distribution and restricted vertical range, *R. lepidophyta* is regarded as a key biostratigraphic index for the uppermost Devonian (latest Famennian, Fa2d, to Strunian, Tn1a, and lower Tn1b, interval). The remarkable geographical extent of the taxon has been summarized by many workers. Owens & Streel (1967) and Richardson (1969) outlined the previous record of the species from different parts of the world. Streel (1974, fig. 1) plotted the geographic

spread of *R. lepidophyta* on Smith, Briden & Drewry's (1973, text fig. II, map 6) continental assembly for the Lower Carboniferous. Playford (1976, p. 46) amply documented work already published on the species under consideration.

The representatives of *R. lepidophyta* that have been recorded during the present study from samples NY96B to US95 (from base of the Ellicott Member of Chadakoin Formation to top of the Cattaraugus Formation) are a few in number. In a total of eleven productive samples only 22 specimens of *R. lepidophyta* including var. *granda* have been observed. Some of the specimens are fragmentary and poor in preservation, so it was not therefore, possible to make a biometric study of the successive populations. Further, it will be evident from Table I that Streel's biometric zones are not applicable to the present material. The specimens having different size ranges are equally distributed in the sequences investigated. Nevertheless, some measurements have been taken and these are presented in Table I.

*Retispora lepidophyta* var. *granda*  
(Kedo) comb. nov.

Plate 8, Figs. 5-6

1971 *Hymenozonotriletes lepidophytus* Kedo var. *grandis* Kedo in Kedo & Goloubtsov pl. 2, fig. 4.

**Size range.** Exoexine 130-158 $\mu$ m; intexine 80-100 $\mu$ m (5 specimens measured).

**Remarks.** *R. lepidophyta* var. *grandia* is comparable in morphological characters with *R. lepidophyta*. The former diverges slightly in having a greater size range. Lacunae are 3-10 $\mu$ m in maximum diameter and muri vary in size from 3-6 $\mu$ m. Trilete mark is distinct and laesurae are found associated with folds which are straight or slightly sinuous and invaginated at the radial positions.



## Genus SPELAEOTRILETES

Neves &amp; Owens 1966

*Type Species.* *S. triangulatus* Neves & Owens 1966.

*Remarks.* *Spelaeotriletes* Neves & Owens was found to incorporate cavate trilete miospores consisting of two layers; the intexine and exoexine are in contact only in the region of the laesurae. Exoexine is sculptured with a variety of elements, including coni, grana, and verrucae which are confined to distal and equatorial quarters especially in the radial positions about the proximal surface. Contact areas and inner body laevigate.

*Spelaeotriletes densatus* sp. nov.

Plate 8, Figs. 7-9

*Derivation of name.* Latin, densus, meaning close, referring to high density of sculptural elements.

*Holotype.* Plate 8, fig. 8, US6D 296 1170718.

*Type locality.* Pope Hollow Section, along boundary between Carroll and South Vally Townships, Jamestown quadrangle, New York State.

*Occurrence.* Chadakoin and Cattaraugus Formations, New York State and Pennsylvania, U.S.A.

*Diagnosis.* Pseudosaccate miospores ornamented on distal and equatorial hemispheres with grana and coni up to  $1\mu\text{m}$  high and wide; intexine laevigate; laesurae simple or accompanied by folds, extending  $\frac{3}{4}$  to full spore radius, ray extremities joined with curvaturae imperfectae.

*Description.* Miospores radial trilete; amb subcircular to subtriangular with convex sides and rounded apices; margin smooth to finely granulate. Exine two layered; intexine laevi-

gate, up to  $1\mu\text{m}$  thick, normally eccentrically placed, distance between body and pseudosaccus equal to subequal, junction distinct. Exoexine  $1.5-2.5\mu\text{m}$  thick, bearing closely set ornament of minute grana and/or coni which do not exceed  $1\mu\text{m}$  in height and diameter, confined to distal and equatorial regions of the proximal hemispheres, contact areas laevigate. Ornamentation elements discrete, rounded to pointed in profile, circular to irregular in plan. Trilete mark distinct; laesurae straight, occasionally slightly sinuous, simple or accompanied by lips or folds up to  $2\mu\text{m}$  raised and wide; laesurae extending  $\frac{3}{4}$  to full spore radius, joined with curvaturae imperfectae at their extremities.

*Size range.* Exoexine  $38-51\mu\text{m}$ , mean  $44\mu\text{m}$ ; intexine  $23-41\mu\text{m}$ , mean  $32\mu\text{m}$  (40 specimens measured).

*Comparison.* The most closely comparable category described to date seems to be *Spelaeotriletes crustatus* Higgs (1975 p. 399, pl. 6, figs. 4-c). There is a morphological overlap between the Irish species described from Devonian and Lower Carboniferous deposits of Hook Head and *S. densatus* sp. nov., but Higgs' species is distinct in having greater size range ( $55-110\mu\text{m}$ , mode  $70\mu\text{m}$ ), prominent ray folds (up to  $7\mu$  high) and longer sculptural elements (up to  $2\mu\text{m}$ ). Moreover, apical papillae are also discernible in some of the specimens described from Ireland. *S. resolutus* Higgs (1975 p. 400, pl. 6, figs. 7-9) displays conate, baculate and pilate sculptural features.

*Spelaeotriletes microverrucosus*

(Kaiser) comb. nov.

Plate 8, Figs. 10-11

1970 *Hymenozonotriletes microverrucosus* Kaiser p. 110, pl. 23, fig. 11.

*Occurrence.* Rare. Chadakoin Formation, New York State, U.S.A.



**Description.** Miospores radial trilete; amb subcircular, Exine two layered. Intexine  $2\mu\text{m}$  thick (dark) laevigate, outline slightly more circular than the amb, eccentrically placed. Exoexine thin, infrapunctate with compression folds, attached to intexine only over proximal surface; bears an ornament of low, discrete verrucae,  $1.5\mu\text{m}$  high, up to  $2\mu\text{m}$  wide. Trilete mark distinct; laesurae hardly discernible, straight, with low folds  $2\mu\text{m}$  high. Length of rays full spore radius and terminating in curvaturae which are poorly developed and may be defined as a change in exine thickness, coincident with the equator.

**Size range.** Exoexine  $60\mu\text{m}$ , intexine  $42\mu\text{m}$  (only one specimen measured).

**Remarks.** The species is here transferred to the genus *Spelaeotriletes* Neves & Owens (1966) because of being pseudosaccate which is sculptured with discrete verrucae. The population recorded by Kaiser (1970) comprise 7 specimens which are slightly smaller ( $40\text{--}50\mu\text{m}$ ) than the only representative observed during the present investigation.

**Comparison.** The species most closely comparable to *Spelaeotriletes microverrucosus*

(Kaiser) comb. nov. appears to be *Hymenozonotriletes krestovnikovii* Naumova (1953, pl. 9, fig. 7) which occurs in the Upper Devonian of the Russian Platform. The latter is distinct, however, in possessing seemingly coarser sculpture whose height seems to be greater than the basal diameter. These are no traces of curvaturae at the ray extremities.

Another closely comparable, if not identical, form has also been illustrated by McGregor (1970) pl. 22, fig. 15) from the Sunbury Formation (? Upper Famennian) Canada.

## EXPLANATION OF PLATES

All figures are from unretouched negatives and prints. Magnifications are X500, unless stated otherwise. Transmitted light photographs were taken with Zeiss Photomicroscope under bright-field illumination. Ilford Pan-F film was used.

Scanning electron micrographs, indicated by the letters SEM, were taken with Cambridge Stereoscan scanning electron microscope, using Kodak-X film.

*Spelaeotriletes microverrucosus*  
(Kaiser) comb. nov.  
Plate 2, Figs. 10-11  
1970 Hymenozonotriletes microverrucosus Kaiser  
p. 110, pl. 2, fig. 11.  
Occurrence. Rare, Chabakoin Formation,  
New York State, U.S.A.

**Description.** Miospores radial trilete; amb subcircular to subtriangular with convex sides and rounded apices; margin smooth to finely granulate. Exine two layered; intexine laevigate, laesurae simple or accompanied by folds, extending  $\frac{1}{2}$  to full spore radius, ray extremities joined with curvaturae imperfect.

Diagnosis. Pseudosaccate miospores ornamented on distal and equatorial hemispheres with granules and conical up to  $1\mu\text{m}$  high and wide; intexine laevigate; laesurae simple or accompanied by folds, extending  $\frac{1}{2}$  to full spore radius, ray extremities joined with curvaturae imperfect.

Occurrence. Chabakoin and Cattaraugus Formations, New York State and Pennsylvania, U.S.A.



## PLATE 1

- Figs. 1-3. *Retusotriletes* sp. cf. *R. concinnus* Kedo in Lanninger.
1. NY96A 79 122858. Ellicott Member.
  2. NY96A 76 1198041. Ellicott Member.
  3. NY96A 79 1108549. Ellicott Member.
  4. *Retusotriletes concretus* nom. nov. NY960 74 1110032. Ellicott Member.
- Figs. 5-6. *Retusotriletes* sp.
5. US8A 338A 1159309. Ellicott Member.
  6. US8A 338A 1100046. Ellicott Member.
- Fig. 7-16. *Aneurospora greggsii* (McGregor) Streel.
7. NY96D 96 1104328. Ellicott Member.
  8. Distal focus, detail of 14, X 1000.
  9. Proximal focus, NY96D 96 1104328, X1000.
  10. A cluster of *A. greggsii* NY96C 74C 1157638. Ellicott Member.
  11. NY96C 74C 1202611. Ellicott Member.
  12. NY96H 148 1182407. Ellicott Member.
  13. NY96D 96 1108324. Ellicott Member.
  14. US6D 296 1250699. Cattaraugus Formation.
  15. NY96C 74C 1220065. Ellicott Member.
  16. Detail of 15, X 1000.
- Figs. 17-18. *Acanthotriletes horridus* var. *minutus* var. nov.
17. US4A 19 1240412. Dexterville Member.
  18. US4A 19 1090602. Dexterville Member.
- Fig. 19. *Acanthotriletes* sp.
- US4F 245 1254688. Dexterville Member.
- Figs. 20-21. *Dibolisporites* sp.
20. NY96G 138 1169434. Ellicott Member.
  21. Detail of 20, X1000.

## PLATE 2

- Fig. 1. *Convolutispora* sp. aff. *Verrucosisporites congestus* playford2.
- 10B 381 1145596. Northeast Shale Member.
- Fig. 2. *Emphanisporites* cf. *annulatus* McGregor.
- US6D 293 1218648. Cattaraugus Formation.
- Fig. 3. *Dictyotriletes* cf. *trivialis* Kedo.
- US8D 357 1252478. Ellicott Member.



- Fig. 4. *Dictyotriletes* sp.  
US6A 267 1210047, Cattaraugus Formation.
- Fig. 5-6. *Knoxisporites literatus* (Waltz) Playford.  
5. NY96C 73 1118335. Ellicott Member.  
6. NY96C 74C 1180505. Ellicott Member.
- Figs. 7-8. *Knoxisporites pristinus* Sullivan.  
7. NY96C 74C 1221482. Ellicott Member.  
8. US6H 319 1200588. Dexterville Member.
- Fig. 9. *Knoxisporites* sp. aff. *Reticulatisporites crassus* Winslow.
- Figs. 10-11. *Lophozotriletes curvatus* Naumova.  
10. NY96C 74C 1190379. Ellicott Member.  
11. Detail of 6, X 1000.
- Figs. 12-15, 17. *Vallatisporites vallatus* var. *hystricosus* (Winslow) Clayton et. al.  
12. US95A 11 1090531. Cattaraugus Formation.  
13. US6H 319 1198592. Cattaraugus Formation.  
14. US6G 314 1090060. Cattaraugus Formation.  
15. NY95A 11 1100462. Cattaraugus Formation.  
17. Distal surface, NY96A, SEM, X 1100. Ellicott Member.
- Fig. 16. *Vallatisporites vallatus* var. *major* (Kedo) comb. nov.  
US6B 280 1090694. Cattaraugus formation.

### PLATE 3

- Figs. 1-2. *Ambitisporites avitus* Hoffmeister.  
1. NY95A 11 1096461. Cattaraugus Fm.  
2. NY95C 36 1101051. Cattaraugus Fm.
- Figs. 3-5. *Streelispora catinata* (Higgs) comb. nov.  
3. US6E 297 1155439. Cattaraugus Fm.  
4. US6E 297 1142044. Cattaraugus Fm.  
5. US12K 129 1151323. South Wales Shale M.
- Figs. 6-11. *Streelispora distincta* sp. nov.  
6. Holotype, US6H 319 1195581. Cattaraugus Fm.  
7. Detail of holotype, X 1000.  
8. NY96D 1128679. Ellicott member.  
9. US6D 291 1251514. Cattaraugus Fm.  
10. Proximal focus, detail of 9, X 1000.  
11. US6H 319 1188591. Cattaraugus Fm.



## PLATE 4

Figs. 1-9. *Synorisporites flexuosus* (Jusch) Richardson and Ahmed  
Specimens showing variation in shape and prominence of equatorial thickening  
and nature of trilete rays.

1. US5, SEM, X 2200. Ellicott Member.
2. US5, SEM, X 1050. Ellicott Member.
3. NY96A 78 1159411. Ellicott Member.
4. NY96A 39 1213497. Ellicott Member.
5. NY96A 78 1152494. Ellicott Member.
6. Specimen with proximal wall partially collapsed.  
NY96C 74B 1231354. Ellicott Member.
7. US6E 297 1080442. Cattaraugus Fm.
8. NY96D 93 1169692. Ellicott Member.
9. NY96H 148 1219568. Ellicott Member.

Figs. 10-12. *Synorisporites richardsonii* sp. nov.

10. NY95C 37 1196063. Cattaraugus Fm.
11. Higher magnification of 10, X 1000.
12. NY96B 87 1132528. Ellicott Member.

## PLATE 5

Figs. 1-4. *Synorisporites variegatus* sp. nov.

1. Holotype, US6D 296 1200492. Cattaraugus Fm.
2. Detail of holotype, X 1000.
3. US6D 1212069. Cattaraugus Fm.
4. US6D 296 1206492. Cattaraugus Fm.

Fig. 5. *Samarisporites inusitatus* Allen.

US12L 132 1121035. South Wales Shale Member.

Figs. 6-7. *Samarisporites kedoe* (Riegel) comb. nov.

6. US8A 332 1142412. Ellicott Member.
7. US8A 333 1150043. Ellicott Member.

Fig. 8-9. *Samarisporites* sp. cf. *S. kedoe* (Riegel) comb. nov.

8. US8B 342 1166036. Ellicott Member.
9. Detail of 8, X 1000.

Fig. 10. *Spinozonotriletes* sp.

US6A 1230468. Cattaraugus Fm.



## PLATE 6

- Fig. 1. *Grandispora coronata* Higgs.  
US6C 286 1251549. Cattaraugus Fm.
- Figs. 2-3. *Grandispora echinata* Hacquebard.  
2. US4F 241 1254634. Dexterville Member.  
3. US6C 290 1258288. Cattaraugus Fm.
- Figs. 4-6. *Grandispora echinula* (Kedo) comb. nov.  
4. NY95A 11 1105618. Cattaraugus Fm.  
5. US6C 286 1229272. Cattaraugus Fm.  
6. Detail of 5.
- Figs. 7-9. *Grandispora macroseta* (Kedo) comb. nov.  
7. NY95A 11 1211271. Cattaraugus Fm.  
8. US6E 302 1249582. Cattaraugus Fm.  
9. US4E 198 1212060. Dexterville Member.
- Figs. 10-11. *Grandispora* sp. cf. *G. spinosa* in Massa & Moreau-Benoit  
10. US6F 308 1260372. Cattaraugus Fm.  
11. Detail of 10, X 1000.

## PLATE 7

- Figs. 1-7. *Calyptosporites perclarus* sp. nov.  
1. Holotype, US6E 299 1250339. Cattaraugus Fm.  
2. Detail of Holotype, X 1000.  
3. US6E 299 1242062. Cattaraugus Fm.  
4. US6E 301 1190292. Cattaraugus Fm.  
5. Detail of 4, X 1000.  
7. Part of previous specimen illustrating details of ornament, X 1000.
- Figs. 8-10. *Rhabdosporites parvulus* Richardson.  
8. US6E 297 1188532. Cattaraugus Fm.  
9. US6B 297 121405. Cattaraugus Fm.  
10. US6E 297 1232029, 1000. Cattaraugus Fm.
- Figs. 11-12. *Rhabdosporites langi* Richardson.  
11. US4A 198 1098662, X 300. Dexterville Member.  
12. Part of previous specimen showing details of ornament, X 500.



## PLATE 8

- Figs. 1-4. *Retispora lepidophyta* (Kedo) Playford.
1. NY96C 57 1198518. Ellicott Member.
  2. A small specimen showing ill-defined reticulum, NY95C 38 1152592. Cattaraugus Fm.
  3. NY96C 69 1080342. Ellicott Member.
  4. NY96B 85 1190692. Ellicott Member.
- Figs. 5-6. *Retispora lepidophyta* var. *granda* (Kedo) comb. nov.
5. NY96B 87 1148361. Ellicott Member.
  6. NY96B 90 118240. Ellicott Member.
- Figs. 7-9. *Spelaeotriletes densatus* sp. nov.
7. US6C 290 1256296. Cattaraugus Fm.
  8. Holotype, US6D 296 1170718. Cattaraugus Fm.
  9. US6D 296 1211339. Cattaraugus Fm.
- Figs. 10-11. *Spelaeotriletes microverrucosus* (Kaiser) comb. nov.
10. US5 255 1162332. Ellicott Member.
  11. Detail of 10, X 1000.

## PLATE 9

- Fig. 1. *Tasmanites* sp.  
US6E 299 1242498. Cattaraugus Formation.
- Figs. 2-5. *Cymatiosphaera* sp.
2. US4E 235 1161055. Dexterville Member.
  3. US4E 235 1118319. Dexterville Member.
  4. US4E 235 1119309. Dexterville Member.
  5. US4E 235 1108312. Dexterville Member.
- Fig. 6. *Lophostridium* cf. *citrinum* Downie  
US8A 332 1158535. Ellicott Member.
- Fig. 7. *Veryhachium trispinosum* Deunff.  
US4A 198 1243519. Dexterville Member.
- Fig. 8. *Veryhachium lairdi* Cramer  
US4C 365 1129672. Dexterville Member.
- Fig. 9. *Micrhystridium* cf. *stellatum* Deflandre.  
US8B 341 121137. Ellicott Member.
- Figs. 10-11. *Electoreskos* sp.
10. US5 251 1141661. Ellicott Member.
  11. US4E 231 1098549. Dexterville Member.



Fig. 12. *Multiplicisphaeridium* sp.   
 US4E 235 1151296. Dexterville Member.

Fig. 13. *Polydrixium* sp.   
 US12U 157 1158060. Gowanda Shale Member.

Fig. 14. *Evittia* sp.   
 US4E 235 1116031. Dexterville Member.

# PLATE 10

Fig. 1. *Legenochitina* sp.   
 US12H 121 1171481. Dunkirk Shale Member.

Fig. 2. *Angochitina* sp.   
 US12Y 171 1151539. Laona Shale Member.

Fig. 3. cf. *Hoegispaera glabra* Staplin   
 US12N 142 1079486. South Wales Shale Member.

Fig. 4. *Scolecodont* sp.   
 US4A 198 1104060. Dexterville Member.

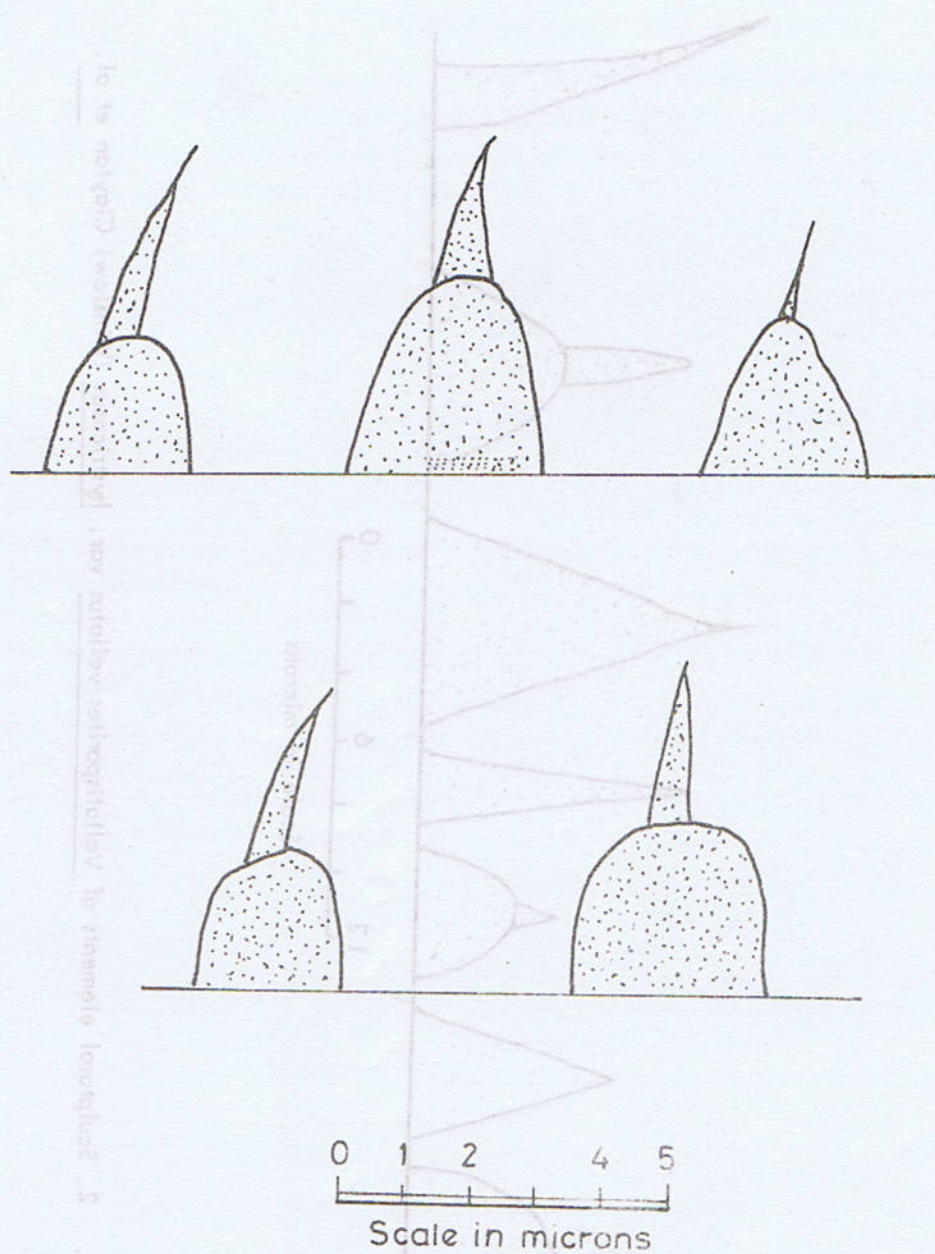
Figs. 5-7. Tracheids.   
 5. US12V 160 1182263. Gowanda Shale Member.   
 6. US4B 206 1189712. Dexterville Member.   
 7. US12L 134 1120602. South Wales Shale Member.

Fig. 8. *Auroraspora* spp. and plant fossils.   
 A sample from the Bush Hill Section.   
 Fig. 9. *Auroraspora* spp. and plant fossils.   
 NY96C 74 1172558. Ellicott Member.

Fig. 10. *Veryhachium* spp. and plant fossils.   
 US8A 332 1142552. Ellicott Member.

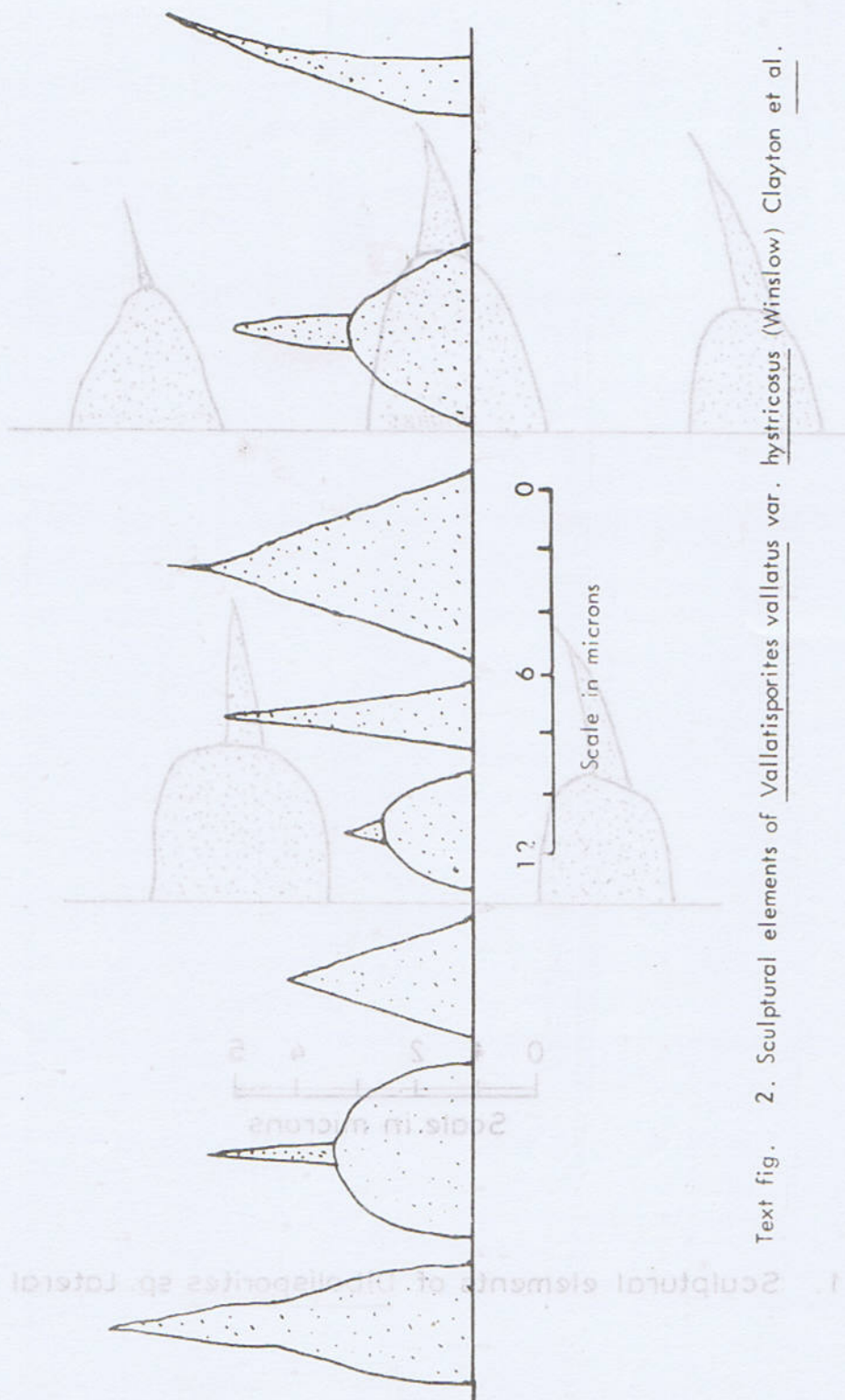
Fig. 11. *Veryhachium* spp. and *Micristidium* sp. with plant fossils.   
 US8A 332 1142559. Ellicott Member.





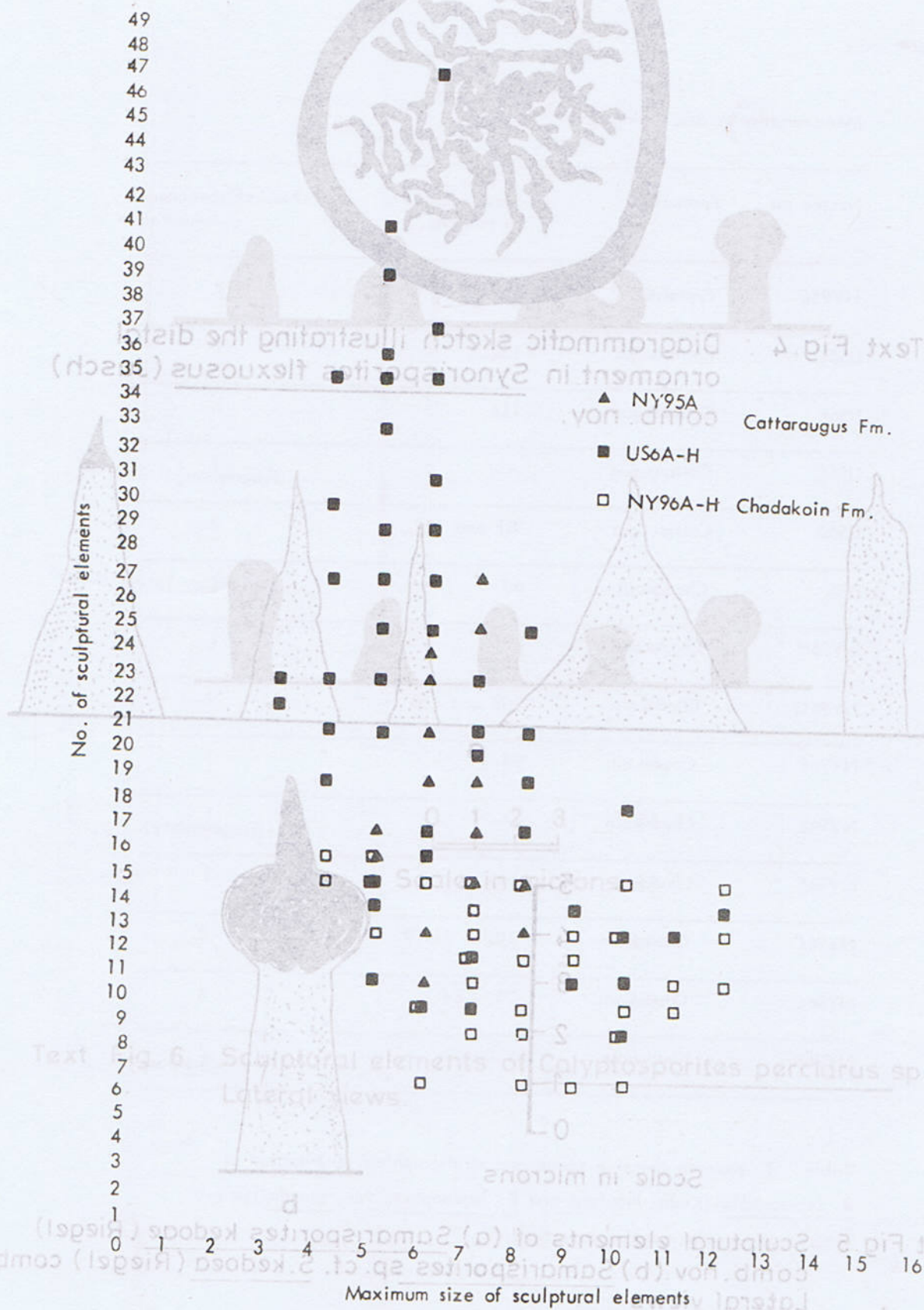
Text Fig. 1. Sculptural elements of *Dibolisporites* sp. Lateral views.





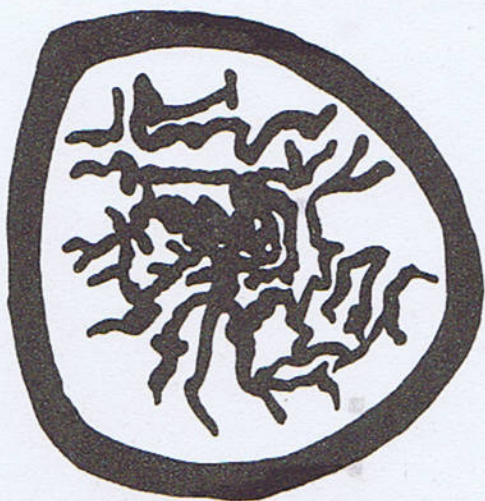
Text fig. 2. Sculptural elements of *Vallatisporites vallatus* var. *hystricosus* (Winslow) Clayton et al.



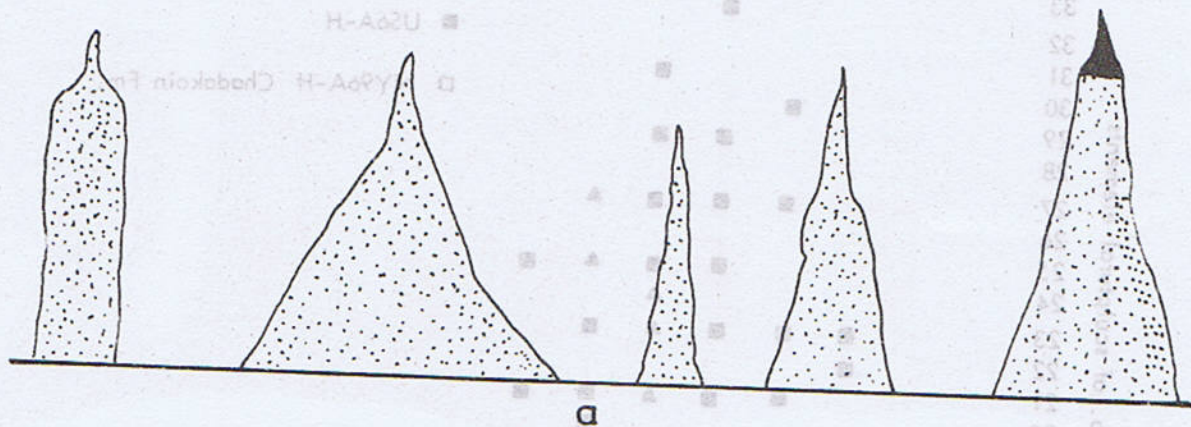


Text fig. 3. Distribution of sculptural elements in *V. vallatus* var. *hystricosus* (Winslow) Clayton.





Text Fig. 4 . Diagrammatic sketch illustrating the distal ornament in Synorisporites flexuosus (Jusch) comb. nov.



a

5  
4  
3  
2  
1  
0

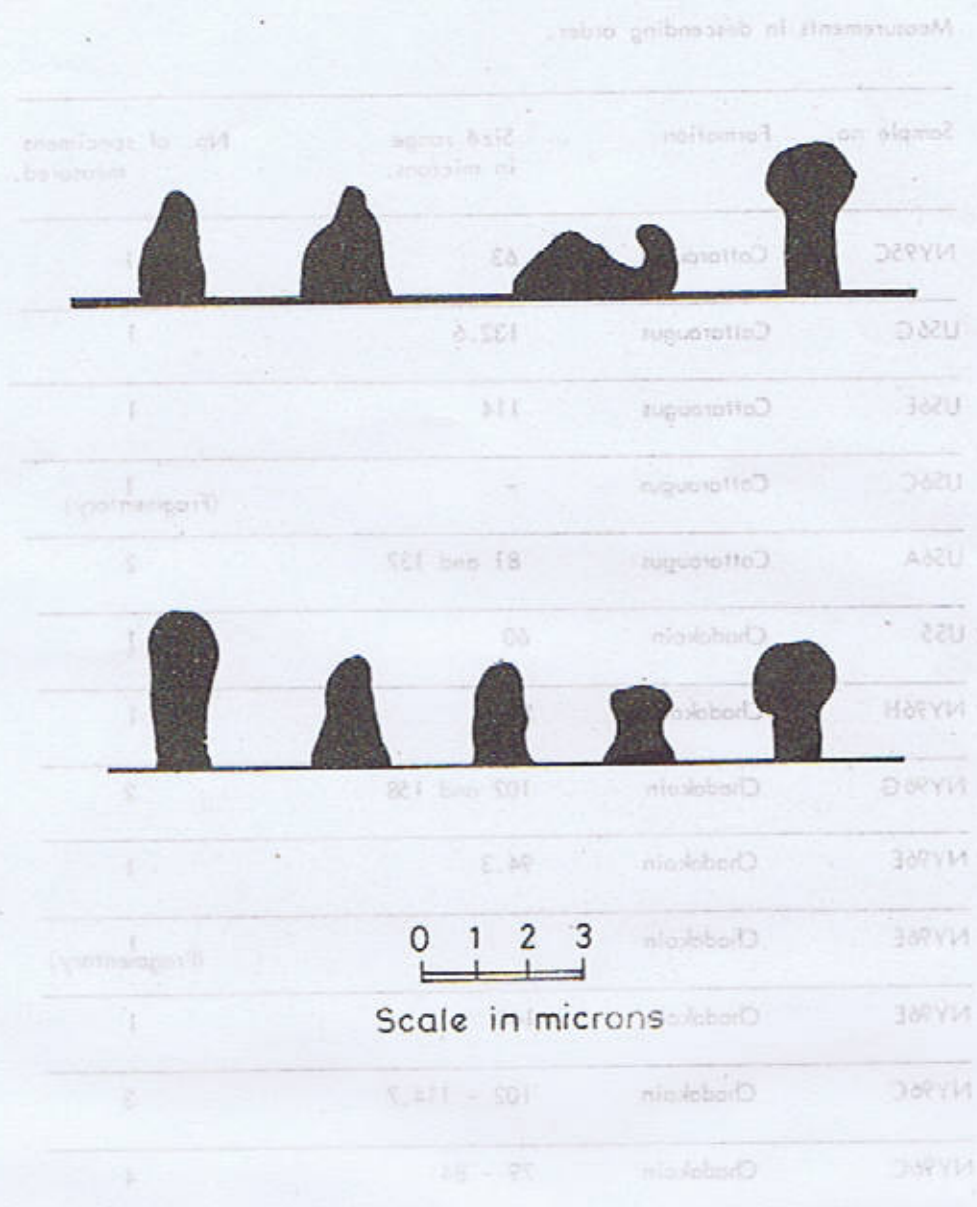
Scale in microns



b

Text Fig. 5 . Sculptural elements of (a) Samarisporites kedoeae (Riegel) comb. nov. (b) Samarisporites sp. cf. S. kedoeae (Riegel) comb. nov. Lateral views





Text Fig. 6. Sculptural elements of Calyptosporites perclarus sp. nov. Lateral views.

Table 1. Showing the size range and stratigraphical distribution of R. lapidophorus (Kudo) Pflüger and R. lapidophorus var. gracilis (Kudo) comb. nov. in the samples investigated.



Measurements in descending order.

Sample no.	Formation	Size range in microns.	No. of specimens measured.
NY95C	Cattaraugus	63	1
US6G	Cattaraugus	132.6	1
US6E	Cattaraugus	114	1
US6C	Cattaraugus	-	1 (Fragmentary)
US6A	Cattaraugus	81 and 137	2
US5	Chadakoin	60	1
NY96H	Chadakoin	50	1
NY96G	Chadakoin	102 and 158	2
NY96E	Chadakoin	94.3	1
NY96E	Chadakoin	82.1	1 (Fragmentary)
NY96E	Chadakoin	140	1
NY96C	Chadakoin	102 - 114.7	3
NY96C	Chadakoin	79 - 84	4
NY96B	Chadakoin	130	2 (1 Fragmentary)

Table 1. showing the size range and stratigraphical distribution of *R. lepidophyta* (Kedo) Playford and *R. lepidophyta* var. *granda* (Kedo) comb. nov. in the samples investigated.



## PLATE 1

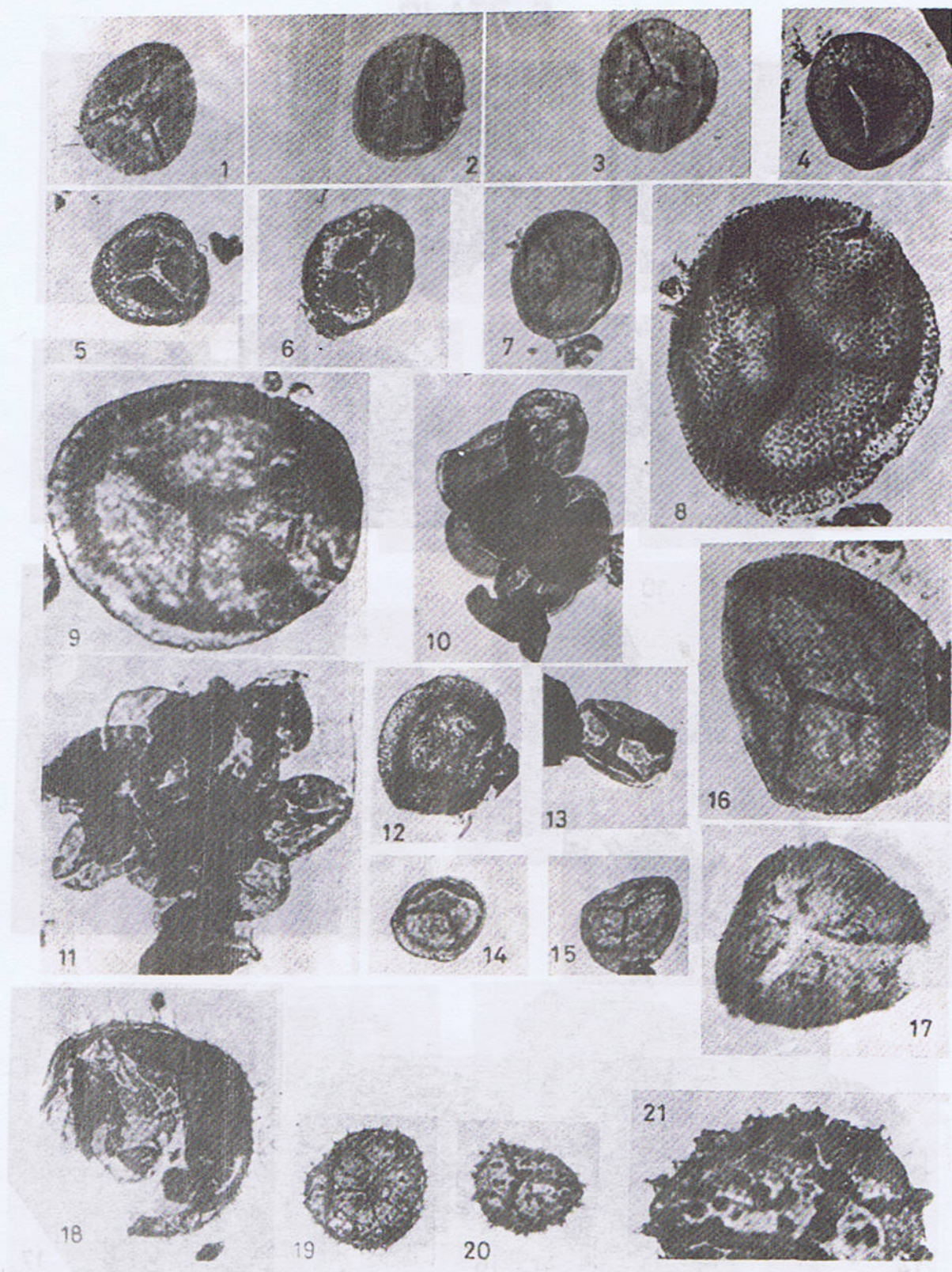




## PLATE 219

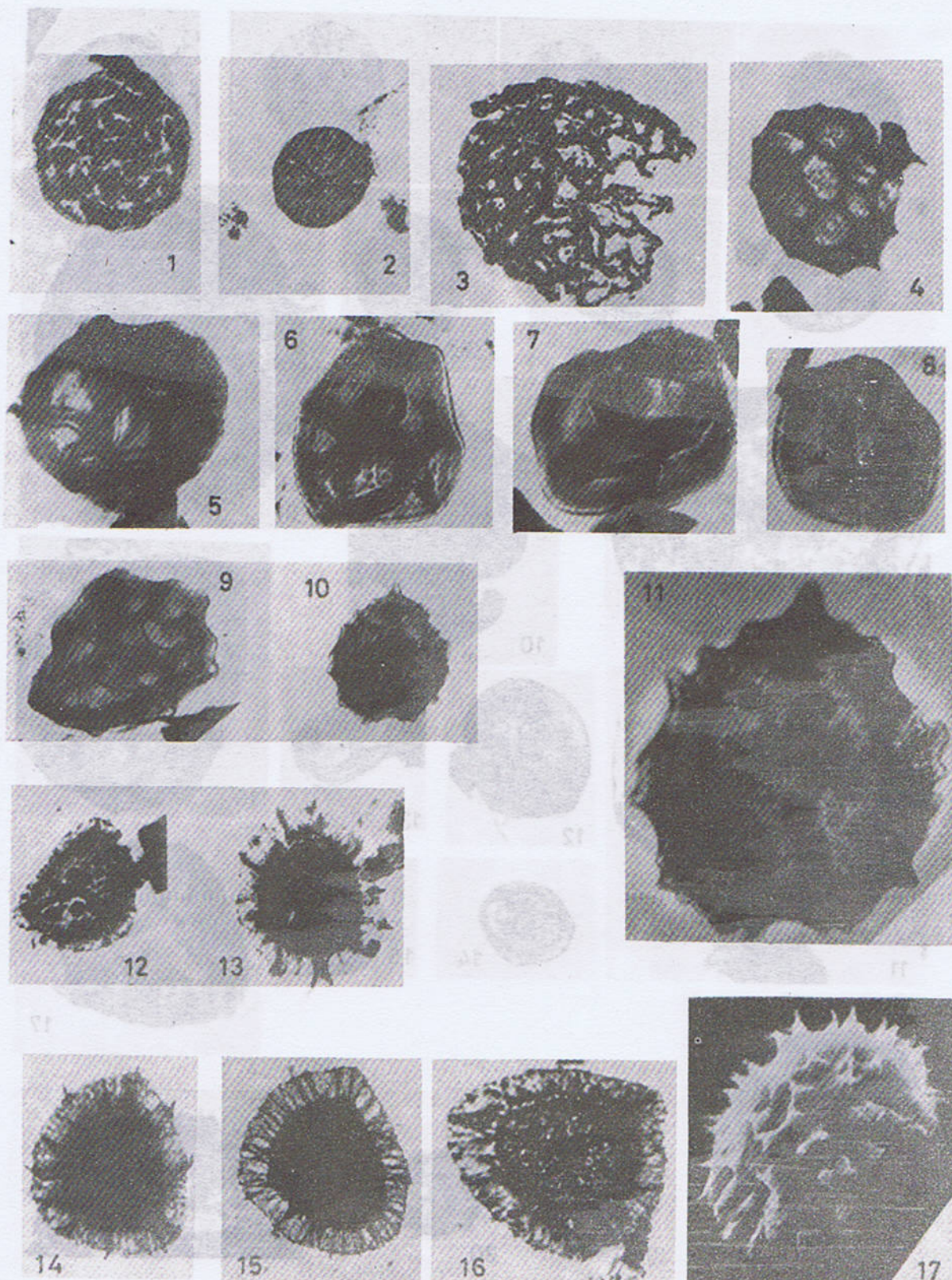




## PLATE 3

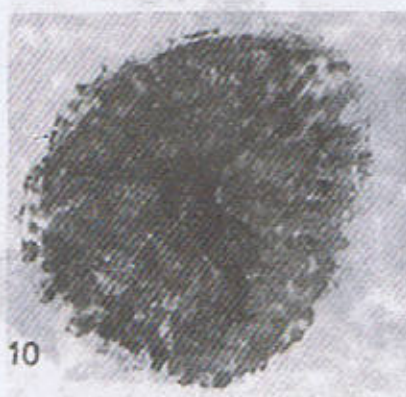
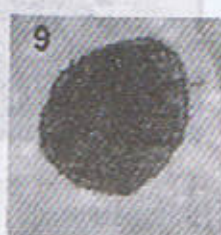
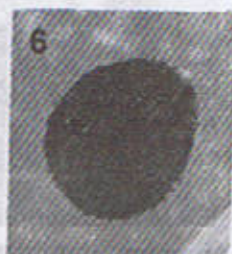
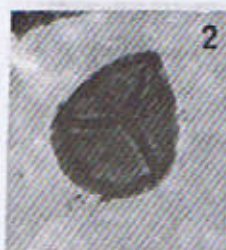




## PLATE 4

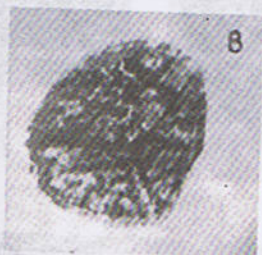
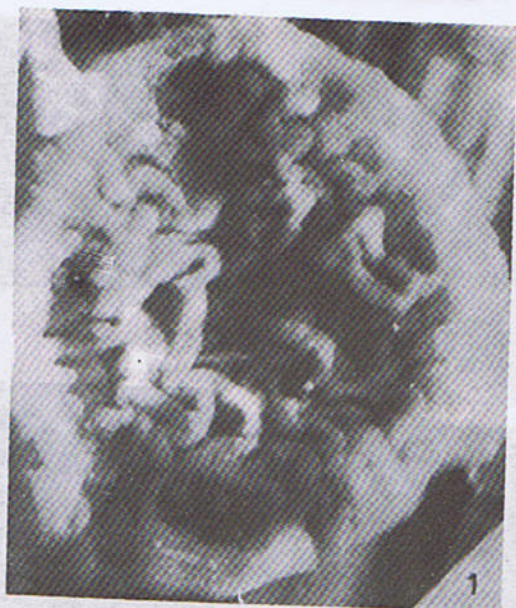




## PLATE 5

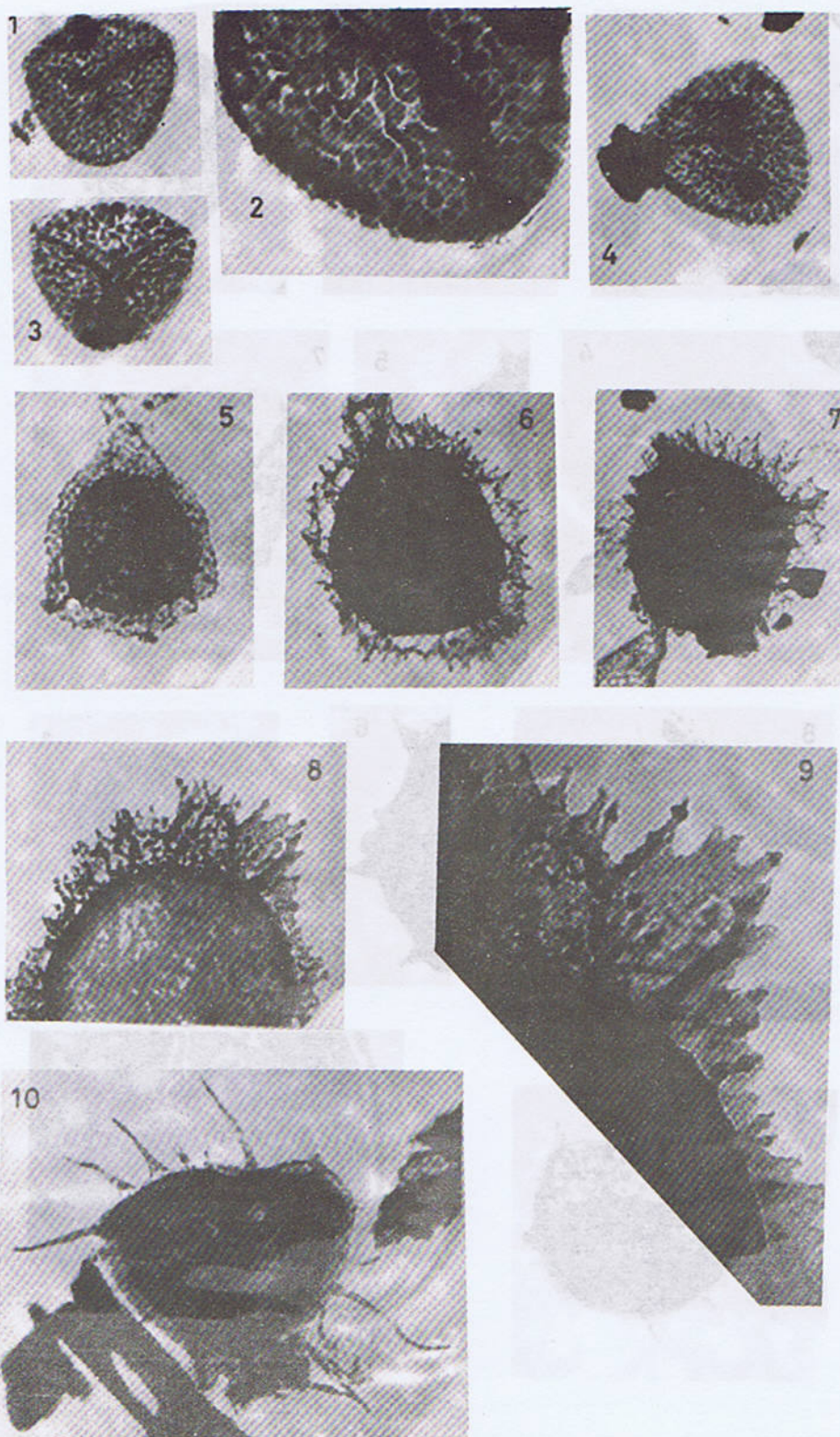




## PLATE 6

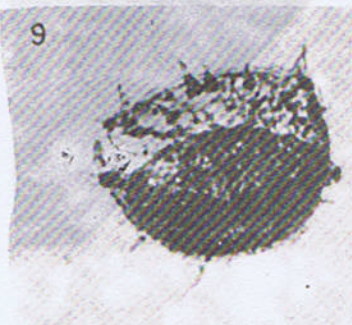
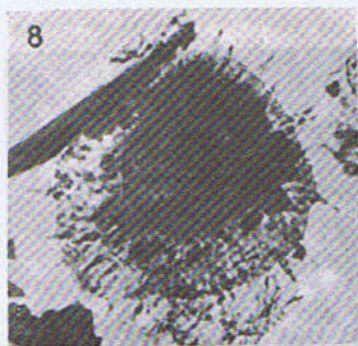




## PLATE 7

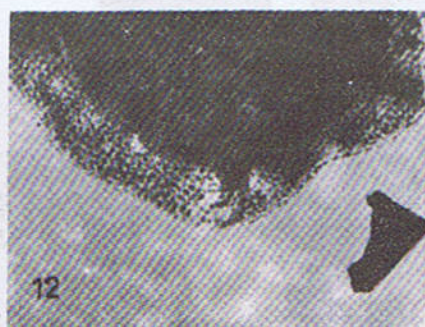
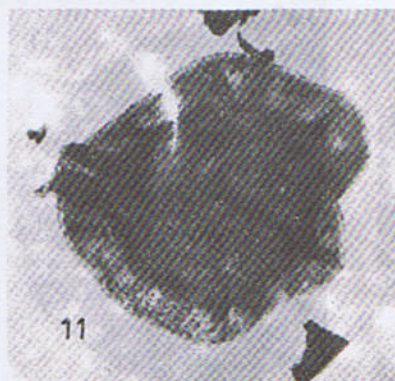
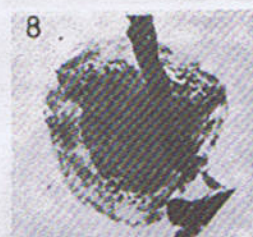
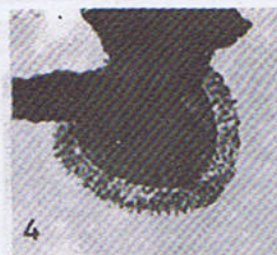
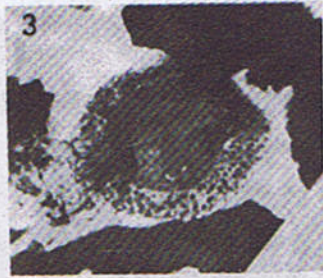
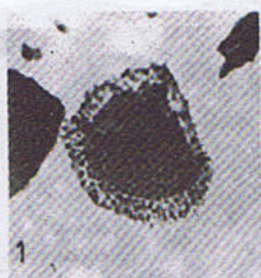




## PLATE 8

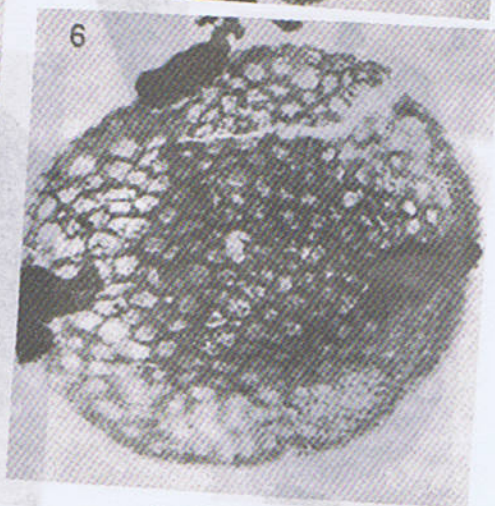
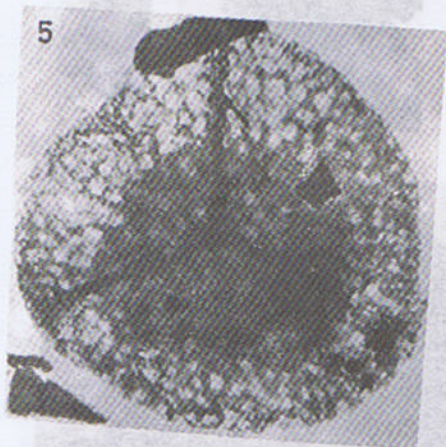
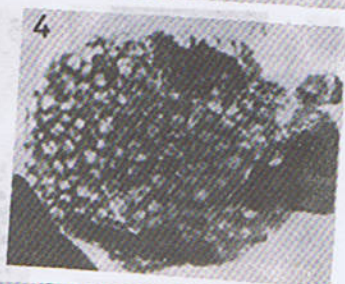
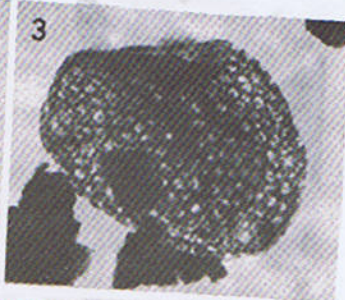




## PLATE 9

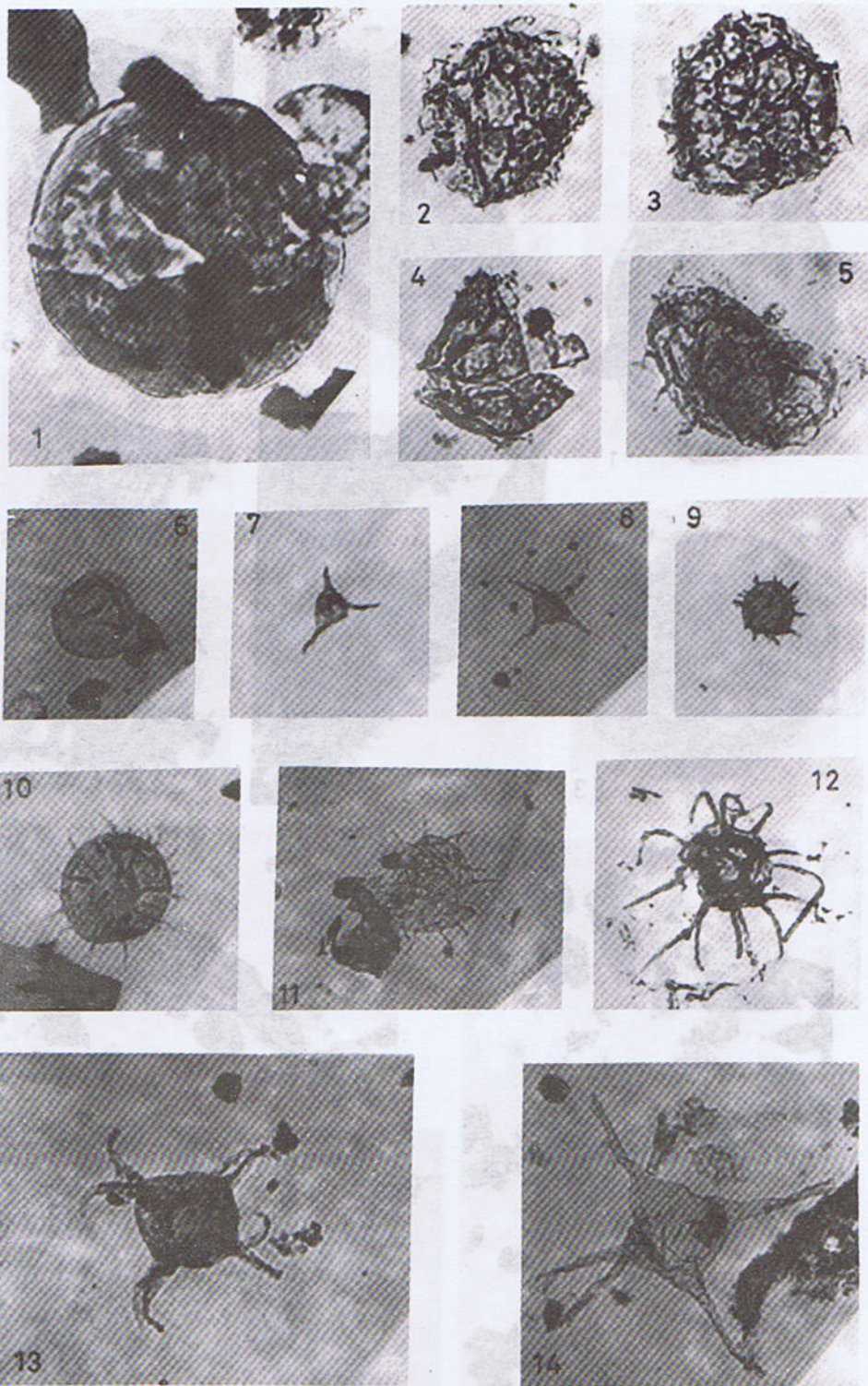
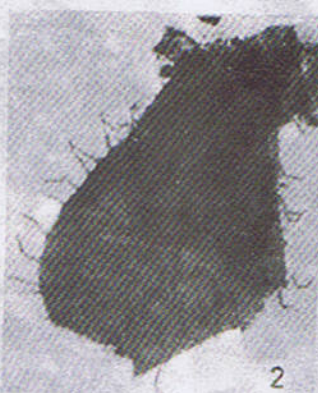




# PLATE 10



1



2



5



3



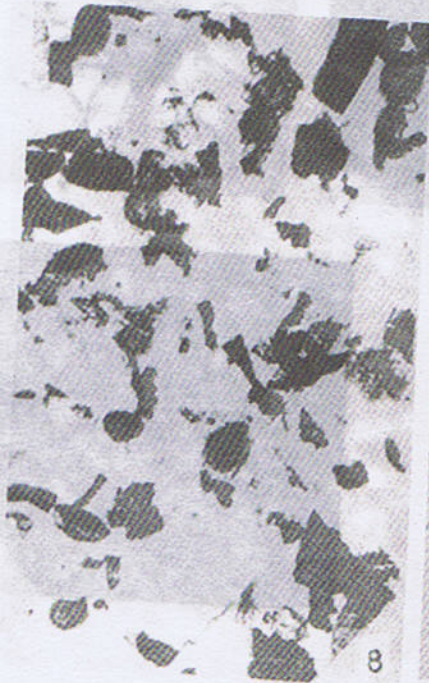
4



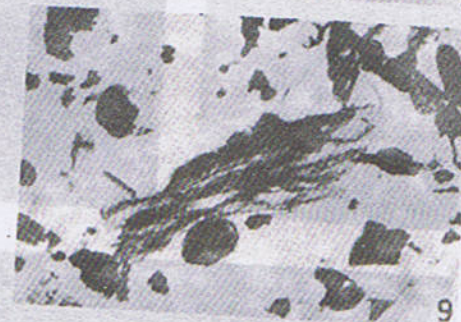
6



7



8



9



10



11



## REFERENCES

- Ahmed, S. 1978. Palynology and biostratigraphy of some upper Devonian deposits of Western New York State and northern Pennsylvania, U.S.A., London University. Ph. D. Dissert., Thesis, 1-355.
- Ahmed, S. 1980. Some forms of the genus *Auroraspora* from the Upper Devonian of New York State and Pennsylvania, U.S.A., *Journal of the Univesity of Kuwait (Science)* 7, 227-244.
- , 1985. Comparison of the upper Devonian miospore assemblages of New York State and Pennsylvania with different areas of the world. *Geol. Bull. Punjab University*, 20, 60-70.
- , 1986. Comparison of the upper Devonian miospore assemblages of New York State and Pennsylvania with those from other parts of North America. *Acta Mineralogica Pakistanica*, 2, 134-143.
- Allen, K.C., 1965. Lower and Middle Devonian spores of north and central Vestspitsbergen. *Palaeontology*, 8, 687-748.
- Becker, G. ; Bless, M.J.M. ; Streel, M. & Thorez, J. 1974. Palynology and Ostracod distribution in the Upper Devonian and basal Dinantian of Belgium and their dependence of sedimentary facies. *Meded. Rijks. Geol. Dienst, n. s.*, 25, 9-99.
- Bharadwaj, D.C. & Venkatachala, B.S., 1971. An upper Devonian mioflora from New Albany Shale, Kentucky, U.S.A. *The Palaeobotanist*, 19, (1), 29-40.
- Bouckaert, J. et al., 1969. Biostratigraphic chart of the Famennian stage (Upper Devonian) in the type localities of Belgium : A preliminary report. *J. Pal.*, 43, 727-734.
- Butterworth, M.A. & Williams, R.W., 1958. The small spore floras of coals in the Limestone Coal Group and Upper Limestone Group of the Lower Carboniferous of Scotland. *Trans. Roy. Soc. Edin.*, 63 (2), 353-392.
- Chaloner, W.G., 1963. Early Devonian spores from a bore-hole in southern England. *Grana Palynologica*, 4 (1), 100-110.
- Chibrikova, E.V., 1959. Spores from the Devonian and older rocks of Bashkiria. Acad. Sci. USSR, Bashkir. filial, Data on Palaeont. & Stratig. of Dev. & Older Depos. *Bashkiria* 3-116.
- Clayton, G. ; Higgs, K. ; Gueinin, K.J. & Van Gelder, A., 1974. Palynological correlations in the Cork Beds (Upper Devonian ? Upper Carboniferous) of southern Ireland. *Proc. R. Ir. Acad.* 74B, 145-155.
- Clayton, G & Graham, J.R., 1974. Miospore assemblages from the Devonian Sherkin Formation of south-west Country Cork, Republic of Ireland. *Pollen et Spores*, 16 (4), 565-588.
- Clayton, G. et al., 1977. *Vallatisporites Vallatus* var. *hystricosus* - C.I.M.P. working group.
- Combaz, A. & Streel, M., 1970. Microfossiles vegetaux du Tournaisien inferieur dans le 'core drill' de Brevillers (Pas-de-Calais, France). *Congress et Colloques Univ. Liege*, 55, 227-241.
- Cramer, F.H., 1969. Plant spores from the Eifelian to Givetian Gosseletia Sandstone Formation near Candas, Asturias, Spain. *Pollen et Spores*, 11 (2), 425-447.



- Dolby, G., 1970. Spore assemblages from the Devonian-Carboniferous transition measures in south-west Britain and southern Eire. *Congres et Colloques Univ. Liege*, 55, 267-274.
- , 1970. A palynological investigation into the Devonian-Carboniferous transition measures in south-west Britain and southern Eire. Ph. D. thesis, (Sheffield Univ.).
- Dolby, G. & Neves, R., 1970. Palynological evidence concerning the Devonian-Carboniferous boundary in the Mendips, England. *C. r. 6th Cong. Avanc. Etud. Stratigr. Geol. Carb.*, Sheffield (1967), 2, 631-646.
- Gayer, R.A.; Allen, K.C.; Bassett, M.G. & Edwards, D. 1973. The Taff Gorge area, Glamorgan, and the stratigraphy of the Old Red Sandstone Carboniferous Limestone transition. *Geol. J.* 8 (2), 345-374.
- Hacquebard, P.A., 1957. Plant spores from the Horton group (Mississippian) of Nova Scotia. *Micropalaeontology*, 3 (4), 301-324.
- Hacquebard, P.A. & Barss, M.S., 1957. A Carboniferous spore assemblage, in coal from the South Nahanni River area, Northwest Territories. *Bull. Geol. Surv. Can.*, 40, 63.
- Higgs, K., 1965. Upper Devonian and Lower Carboniferous miospore assemblages from Hook Head, County Wexford, Ireland. *Micropalaeontology*, 21 (4), 393-419.
- Hoffmeister, W.S., 1959. Lower Silurian plant spores from Libya. *Micropalaeontology*, 5 (3), 331-334.
- Hoffmeister, W.S.; Staplin, F. L. & Malloy, L.E., 1955. Mississippian plant spores from the Hardisburg formation of Illinois and Kentucky. *J. Paleont.* 29 (3), 372-399.
- Hughes, N.F. & Playford, G., 1961. Palynological reconnaissance of the Lower Carboniferous of Spitsbergen. *Micropalaeontology*, 7, 27-44.
- Ishchenko, A.M., 1956. Spores and pollen from the Lower Carboniferous sediments of the western extension of the Donetz Basin and their stratigraphic importance. *Trudy Inst. geol. Nauk, Kiev, Ser. strat. pal.*, 11, 185.
- Kaiser, H., 1970. Die Oberdevon-Flora der Bareninsel. 3, Microflora des höheren Oberdevons und des Unterkarbons. *Palaeontographica, Abt. B.* 129, 71-124.
- Kedo, G.I., 1955. Spores of the Middle Devonian of the north-eastern Byelorussian S.S.R.—Acad. Sci. B.S.S.R., *Inst. Geol. Sci., Palaeont. Stratigr. B.S.S.R., Sbornik* 1, 5-59. (In Russian).
- , 1957a. Stratigraphic significance of *Hymenozonotriletes pusillites* sp. n. *Dokl. Akad. Nauk. BSSR*, 1, 21-23.
- , 1957b. Spores from the supra-salt Devonian deposits of the Pripyat Depression and their stratigraphical significance. *Rep. Palaeont. Strat. Byelorussian SSR*, 2, 3-43. (pp. 1-69 English Translation).
- , 1963. Spores of the Tournaisian stage of the Pripyat Basin and their stratigraphic significance. *Rep. Palaeont. Strat. Byelorussian SSR*, 4, 3-121. (In Russian).
- , & Goloubtsov, V.K., 1971. Palynological criteria for determination of boundaries between Devonian and Carboniferous in the Pripyat Basin. In: Palynology research in Byelorussia and other regions of the U.S.S.R., *Nauka i Tekhnika, Minsk*: 5-34. (In Russian).



- Kemp, E.M., 1972. Lower Devonian palynomorphs from the Horlick Formation, Ohio Range, Antarctica. *Palaeontographica, Abt. B.* 139, 105-124.
- Lanninger, E.P., 1968. Sporen-Gesellschaften aus dem Ems der SW-Eifel (Rheinisches Schiefergebirge). *Palaeontographica*, 122, Abt. B. 95-170.
- Lanzoni, E. & Magloire, L., 1969. Associations palynologiques et leurs applications stratigraphiques dans le Devonien superieur et Carbonifere inferieur du Grand Erg occidental (Sahara algerien). *Rev. Inst. francais du Petrole*, 24, 441-469.
- Massa, D. & Moreau-Benoit, A., 1976. Essai de synthese stratigraphique et palynologique du systeme Devonien en Libye occidentale. *Revue de L'institut Francais du Petrol.* 31 (2), 287-333.
- McGregor, D.C., 1961. Spores with proximal radial pattern from the Devonian of Canada. *Geol. Surv. Canada, Bull.* 76, 11.
- , 1964. Devonian miospores from the Ghost River Formation, Alberta. *Geol. Surv. Canada, Bull.*, 109, 31.
- , 1970. *Hymenozonotriletes lepidophytus* KEDO and associated spores from the Devonian of Canada. *Congres et Colloques Univ. Liege.* 55, 315-326.
- , 1973. Lower and Middle Devonian spores of eastern Gaspé, Canada'. Systematics. *Palaeontographica, Abt. B.* 142, 1-77.
- Molyneux, S.G., Manger, W.L. and Owens, B., 1984. Preliminary account of Late Devonian palynomorph assemblages from the Bedford Shale and Berea Sandstone Formation of Central Ohio, U.S.A. *J. micropalaeontol.*, 3 (2), 41-51.
- Mortimer, M.G., 1967. Some Lower Devonian microfloras from southern Britain. *Rev. Palaeobot. Palynol.*, 1 (1-4), 95-109.
- Naumova, S.N., 1953. Spore-pollen assemblages of the Upper Devonian of the Russian Platform and their stratigraphic significance. *Trans. Inst. Geol. Sci., Acad. Sci. U.S.S.R.* 143 (Geol. Ser. 60) : (In Russian), 128 French Trans).
- Neves, R., 1961. Namurian plant spores from the southern Pennines, England. *Palaeontology*, 4, 247-279.
- , 1964. *Knoxisporites* (Potonie & Kremp). Neves 1961. *C.R. 5th Congr. Avanc. Etud. Stratig. Carb. Paris.*, 1, 1063-1069.
- Neves, R. & Owens, B., 1966. Some Namurian camerate miospores from the English Pennines. *Pollen et Spores*, 8, 337-360.
- Owens, B., 1971. Miospores from the Middle and early Upper Devonian rocks of the western Queen Elizabeth Islands, Arctic Archipelago. *Pap. Geol. Surv. Can.*, 70 (38), 157.
- Owens, B. & Streel, M., 1967. *Hymenozonotriletes lepidophytus* KEDO, its distribution and significance in relation to the Devonian-Carboniferous boundary. *Rev. Palaeobot. Palyn.* 1, 141-150.
- Paris, F., Richardson, J.B., Riegel, W., Streel, M. and Vanguetstaine, M., 1985. Devonian (Emsian-Famennian) Palynomorphs. *J. micropalaeontol.*, 4 (1), 42-82.



- Playford, G., 1964. Miospores from the Mississippian Horton Group, eastern Canada. *Bull. Geol. Surv. Can.*, 107, 47.
- Playford, G., 1976. Plant microfossils from the Upper Devonian and Lower Carboniferous of the Canning Basin, Western Australia. *Palaeontographica, Abt. B.*, 158, 1-71.
- Potonie, R., 1956. Synopsis der Gattungen der sporae dispersae. Teil 1-V. *Beih. Geol.* 23.
- Potonie, R., 1958. Synopsis der Gattungen der sporae dispersae. Teil 1-V. *Beih. Geol.* 31.
- Potonie, R., 1960. Synopsis der Gattungen der sporae dispersae. Teil 1-V. *Beih. Geol.* 39.
- Potonie, R., 1966. Synopsis der Gattungen der sporae dispersae. Teil 1-V. *Beih. Geol.* 72.
- Potonie, R., 1970. Synopsis der Gattungen der sporae dispersae. Teil 1-V. *Beih. Geol.* 87.
- Potonie, R. & Klaus, W., 1954. Einige Sporengattungen des alpinen Salzgebirges. *Geol. Jb.* 8, 517-544.
- Potonie, R. & Kremp, G.O.W., 1954. Die Gattungen der palaeozoischen Sporae und ihre Strati-graphic. *Geol. Jb.*, 69, 111-194.
- Potonie, R. & Kremp, G.O.W., 1955-1956. Die Sporae des Ruhrkarbons. *Palaeontographica Abt. B.* 98, B. 99.
- Richardson, J.B., 1960. Spores from the Middle Old Red Sandstone of Cromarty, Scotland. *Palaeontology*, 3 (1), 45-63.
- Richardson, J.B., 1962. Spores with bifurcate processes from the Middle Old Red Sandstone of Scotland. *Palaeontology*, 5 (2), 171-194.
- Richardson, J.B., 1965. Middle Old Red Sandstone spore assemblages from the Orcadian Basin, north-east Scotland. *Palaeontology*, 7 (4), 559-605.
- Richardson, J.B., 1969. Devonian spores. In: Tschudy, R.H. and Scott, R.A., *Aspects of Palaeontology*, Wiley-Interscience, 193-222.
- Richardson, J.B., and Ahmed, S., 1988. Miospores, Zonation and Correlation of Upper Devonian sequences from western New York State and Pennsylvania. "Devonian of the World" *Canadian Society of Petroleum Geologists, Memoir* 14, 541-558.
- Richardson, J.B. & Lister, T.R., 1969. Upper Silurian and Lower Devonian spore assemblages from the Welsh Borderland and South Wales. *Palaeontology*, 12 (2), 201-252.
- Richardson, J.B. and McGregor, D.C., 1986. Silurian and Devonian spore zones of the Old Red Sandstone Continent and adjacent regions. *Geological Survey of Canada Bulletin* 364, 1-79.
- Riegel, W., 1968. Die Mitteldevon-Flora Von Lindlar (Rheinland). 2. Sporeae dispersae. *Palaeontographica, Abt. B.* 132, 76-96.
- Riegel, W., 1973. Sporenformen aus den heisdorflauch und nohnschichten (Emsium und Eifelium) der Eifel, Rheinland. *Palaeontographica, Abt. B.* 143, 78-104.
- Schultz, G., 1968. Eine unterdevonische Mikroflora aus den Klerfer Schichten der Eifel (Rheinisches Schiefergebirge). *Palaeontographica, Abt. B.* 123 (1-6) 5-42.
- Shepeleva, E.D., 1963. Spores from the Lower Devonian beds of the Podolain Dniester River area. *Data on Regional Stratig. U.S.S.R., Moscow*, 98-101. (In Russian).



- Smith, A.H.V. & Butterworth, M.A., 1967. Miospores in the coal seams of the Carboniferous of Great Britain, *Spec. Pap. Palaeontology*, 1, 324.
- Staplin, F.L., 1960. Upper Mississippian plant spores from the Golata Formation, Alberta, Canada. *Palaeontographica, Abt. B*, 107, 1-40.
- Staplin, F.L. & Jansonius, J., 1964. Elucidation of some Paleozoic densospores. *Palaeontographica, Abt. B*, 114, 95-117.
- Streel, M., 1964. Une association de spores du Givetien inferieur de la Vesdre, a Goe (Belgique). *Ann. Soc. Geol. Belgique* 87 (7), 1-30.
- Streel, M. 1965. Etude palynologique du Devonian du sandage de Boaschot (Belgique). *Societe belge de Geologie, de Palaeontologie et d'Hydrologie, Bulletin*, V. 73 (2), 172-185.
- , 1966. Criteres palynologiques pour une stratigraphie detaillee du Tria dans les bassins Ardenno-Rhenans. *Soc. Geol. Belgique Ann.*, 89, 65-95.
- , 1967. Associations de spores du Devonien interieur Belge et leur signification stratigraphique. *Ann. Soc. Geol. Belgique*, 90 (1), 11-53.
- , 1974. Similitudes des assemblages de spores d'Europe, d'Afrique du Nord et d'Amerique du Nord, au Devonien terminal. *Sci. Geol., Bull.*, 27, 25-38.
- Sullivan, H.J., 1964. Miospores from the Drybrook Sandstone and associated measures in the Forest of Dean Basin, Gloucestershire. *Palaeontology*, 7, 351-392.
- , 1968. A Tournaisian spore flora from the Cementstone Group of Ayrshire, Scotland. *Palaeontology*, 11, 116-131.
- Tiwari, R.S. & Schaarschmidt, F., 1975. Palynological studies in the Lower and Middle Devonian of the Prum Syncline, Eifel (Germany). *Adh. Senckenb. naturforsch. Ges.* 534, 1-129.
- Turnau, E., 1974. Microflora from core samples of some Palaeozoic sediments from beneath the flysch Carpathians (Bielsko-Wadowice area, southern Poland). *Ann. Soc. Geol. Pologne*, 44, 143-169.
- , 1975. Microflora of the Famennian and Tournaisian deposits from boreholes of northern Poland. *Acta Geologica Polonica*, 25 (4), 505-528.
- Utting, J. & Neves, R., 1970. Palynology of the Lower Limestone Shale Group (basal Carboniferous of Limestone series) and Portishead Beds (Upper Old Red Sandstone) of the Avon Gorge, Bristol, England. In *Colloque sur la stratigraphie du Carbonifere, Liege, Univ., Congr. Colloq.*, 55, 411-422.
- Warg, J.B. & Traverse, A., 1973. A palynological study of shales and "coals" of a Devonian-Mississippian transition zone, central Pennsylvania. *Geoscience & Man*, 7, 39-46.
- Winslow, M.R., 1962. Plant spores and other microfossils from Upper Devonian and Lower Mississippian rocks of Ohio. *U.S. Geol. Surv. Prof. Paper* 364, 1-93.
- Wray, J.L., 1964. Palaeozoic palynomorphs from Libya. In *Palynology in Oil Exploration. A symposium SEPM*, 11, 90-96.



# TECTONIC ELEMENTS AND EMPLACEMENT OF DYKES AND PLUG LIKE BODIES, AS DEMONSTRATED BY PEGMATITES OF EVJE-IVELAND AREA OF SOUTHERN NORWAY

BY

SHERJIL AHMAD KHAN LODHI

PCSIR Laboratories, Lahore, Pakistan.

**Abstract.** *Intensive field and photogeological studies of tectonic elements like foliation, rock cleavage, joints, fold, shear, beta and fold axis of the area are interpreted, which reveal that the country rock Migmatite has undergone intensive shearing and compressive stress action. This resulted into shear fractures of the joints and form cracks and fissures, which are responsible for the intrusion of pegmatites.*

## INTRODUCTION

Structural features of the investigated area are described to know how Migmatite body has tectonically behaved for the emplacement of Pegmatites. Emplacement is collectively the simultaneous process of space formation, its filling with a mobile phase and subsequent crystallization of this phase (Uebel, 1980). By shear and tear (in orogenic areas) of solid rocks, cracks are opened and mechanical pressure gradients are immediately set up, which in turn create corresponding gradients in the chemical activities. Mobilization of the rocks will migrate towards the cracks and then consolidate into new minerals. The Pegmatites of the area are lying preferably in Migmatite (Lodhi, 1983), in which the cracks formed more easily than the adjoining granitic gneisses.

## FIELD INVESTIGATIONS

The readings of the tectonic elements are taken with Freiburger Clinometer, using the topographic sheet No. M-816-Evje Blad 1:25,000. The studied area lies between the cities of Evje and Iveland in southern Norway, Longitude  $7^{\circ}52'$  to  $7^{\circ}52'$ , Latitude

$58^{\circ}31'$  to  $58^{\circ}33'$ . The country rock of Pegmatites in Evje-Iveland is Migmatite (Lodhi, 1983), which is surrounded by granitic gneisses and augen gneisses and are supposed to be of Pre-Cambrian age, forming the base of the Baltic Shield (Barth, 1947, 1960). Kahama (1982), described the investigated area as a part of Dalsandian folded region, which has an age of 800-1200 M.Y. The southern tip of Norway, most likely belong to Telemark Basement (Ofstedahl, 1980).

Migmatite of Evje-Iveland is strongly banded and is differentiated into leuco, mela- and intermediate bands, according to their hornblende composition. The leuco bands are showing very sharp contacts with mela- and intermediate bands, whereas the intermediate and mela bands are showing gradual contacts. More than 500 pegmatitic veins, dykes and bodies are observed in the area.

## PREVIOUS WORK

The previous workers have described the Migmatite of Evje-Iveland as Amphibolite and its banding nature is attributed to metamorphic differentiation.



Reitan (1956), described the fact that the pegmatitic veins and dykes stop at the boundaries of the amphibolite bands and do not penetrate into the surrounding gneisses suggest that the gneiss was not sufficiently rigid to maintain low pressure zones in which the pegmatitic veins and dykes could be formed. Barth, (1947, 1960) observed that the initial position of the elongated amphibolite body was not with its longer axis N-S as it is now, but NE-SW. During the main phase of the granitization it reacted plastically to a compression in the E-W direction and suffered at the same time a complete recrystallization. Afterwards the temperature dropped and slowly the amphibolite stiffened and became more rigid than the adjacent gneiss which remain plastic. This difference in plasticity created a rotational force which increased as the amphibolite became more rigid in the plastic surroundings. Slowly thereby the amphibolite was rotated and swung into its present position, corresponding to the fold axis of the surrounding gneisses. During this process the temperature was too low for extended recrystallization, but slippage along the long limbs of the fold took place causing a striation and grooving on the schistosity planes. The gneisses are deprived of slippage or gliding features, because of falling temperature and pressure, the gneiss could no longer react plastically to the deforming forces. These forces had already ceased to act. Barth, (1947, 1960) described that during the period of granitization, a dispersed phase of ions, molecules or atoms which diffuse towards the unstable low pressure zones of the amphibolite and consolidate there, as Pegmatites.

## TECTONIC ELEMENTS

### Foliation

Foliation is the property of rocks, whereby they break along approximately parallel surfaces. The compositional layering in metamorphic

rock is also called as foliation. The foliation of Migmatite is striking N-S with variation in dips. Readings of foliation are given in Table-I and are interpreted with 2% of contour lines, as shown in Fig. 1, which marks the general reading of Migmatite as 15/67 East.

Thin section studies reveal that this is an aptitude of the minerals to arrange themselves in thin streaks parallel to the foliation. The a-axis from hornblende often lie normal to foliation and in many rocks a megascopic b-lineation result of the parallel alignment of hornblende crystals in the schistosity of foliation planes.

### Striation and grooves

Striation and grooves are seen along the foliation plane, that show the displacement has taken place along the foliation plane.

### Rock cleavage

Rock cleavage is the property of the rocks, whereby it breaks along the parallel surfaces of the secondary origin.

Fracture cleavage is essentially closely spaced jointing, as is shown in the lower part of the Fig. 2 the minerals of the rock are not parallel to the cleavage. The distance between the individual planes of cleavage varies to a few centimeters, if the distance exceeds a few centimeters, the term jointing is more appropriately applied. When some displacements along the cleavage planes occurred, the term shear cleavage is used.

### Joints

Most rocks are broken by relatively smooth fractures known as joints. Joints are planes but some are curved surface. Different sets of joints in the investigated area, are measured and the readings are given in the Table-II and are interpreted with 2% contour lines, as is shown in Figure 3. Four different sets of joints are traced with help of Figure 3. These sets



of joints are shown in Figure 4A. With the help of the sets of joints, a beta diagram is also produced in Figure 4B.

The four different sets of joints in the figure area :

1. 35/79NW      2. 83/80N
3. 108/80N     4. 130/79NE

It is observed in the field that the pegmatitic dykes and veins that are parallel to the joint 83/80N lying, show shearing effect (Fig. 7). Due to this effect, the metamorphic bands are bended at the both contacts of the dyke along contrary directions. The shear axis is  $0/78^\circ$  towards north measured (Fig. 4B). It is also observed in field that majority of the pegmatitic dykes, bodies and veins are lying parallel to the above mentioned joints.

#### Joint Diagram

Joint diagram (Fig. 5) is produced with the help of strike directions of joints from Table-II. These strike directions are statistically distributed in equal degree amount, as is shown in Tabel-III. The percentage so obtained would be traced to a great circle with an equal distribution of  $100^\circ$ . The points so obtained would be delineated together to get a joint diagram. Figure 5 manifests that the strike values which are lying between  $30-40^\circ$ ,  $80-90^\circ$ ,  $100-110^\circ$  and  $130-140^\circ$  are the strike values of the sets of joints which are corresponding to the values of strikes in Fig. 4.

#### Photogeological Studies

The aerial photograph of Evje-Iveland area ( $E_5$ ) is stereoscopically studied and the fractures are traced. The intersecting angles of these traces with that of N-S line of the photograph are plotted in Table-IV. With the help of this table, trace diagram is produced (Fig. 6B).

#### Studies of pegmatitic dykes and veins.

In field mostly the pegmatitic bodies, dykes and veins are lying normal to the foliation of the Migmatite. It is also noted in the field that some pegmatitic dykes and veins are present parallel to the sets of joints, which are present in the area, as shown in Fig. 7.

#### Ptygmatic Folding

Ptygmatic folding is developed due to the buckling of the rock. Many of the folds that are found in deformed rocks owe their development to a compressive stress which acted along the length of the layer. If the layers have different properties, an instability is produced which leads to the buckling of the more competent layers in the material and thus produce ptygmatic folding (Fig. 10). Intra-formational faults are produced due to the strain slip joint. One limb of these small folds become a zone of weakness. The rock tends to break parallel to these zones, causing such faults.

#### Interpretation of the Tectonic Elements

The pegmatites in the investigated area are lying perpendicular to the foliation of Migmatite (Fig. 7). It is also noted in the field that the other pegmatitic dykes and veins are present parallel to the joint sytem measured in the area (Figs. 8 & 9).

The most common joints (Fig. 4) are :

1. 35/79 NW      2. 83/80N
3. 108/80N      4. 130/79NE

It is also observed in the field that the pegmatitic dykes and veins that are parallel to the joint 83/80N lying, show the shearing effect (Fig 12). As is shown in Fig. 4B that the beta axis of the joint system also presents shearing effect, therefore, it is also called as shear axis and is  $0/78^\circ$  towards north measured.



A joint diagram (Fig. 5) is also presented. Aerial photographic studies of the area also reveal that the four system (X-rupture system) are important because they are possessing the same strike values as are given in Fig. 4. The joints which are produced due to the shearing effect of the rock are known as fracture joints and when some displacement along these joints took place then they are called as shear joints. Two sets of joints (Fig. 4,  $35^\circ$  and  $130^\circ$ ) are symmetrically disposed about the strain axis, such types of joints are considered as shear fractures. Joints may be classified genetically as either shear fractures or tension fractures. The ultimate causes may be several:

1. Tectonic stresses and strain, causing fractures due to tectonic activity.
2. Residual stresses, due to events that happened long before the fracturing;
3. Contraction due to shrinkage because of cooling of dessication and
4. Surficial movements, such as downhill movements of the rocks or mountain glaciers. In the investigated area, the joints are developed due to the tectonic activity of stress and strain.

Fracture joint may be genetically called as fracture rupture. Fracture rupture is a shear phenomenon that obeys the laws of shear fractures; consequently, fracture joint is inclined to the greatest principal stress axis at an angle of  $30^\circ$ .

In Fig. 12 the fracture joint is parallel to the planes represented by FF' and F'' F'''. This figure may be called as strain ellipsoid or the deformation ellipsoid, resulting due to the deformation of a sphere. The set of joints presented in Fig. 4 could also be called as fracture joints.

In descriptive term, shear rupture may

also be known as shear joint. Shear rupture is a fracture rupture, along which some displacements have taken place, (Fig. 12). Experiments show (Billings, 1972) that the shear fractures are closer to the least strain axis. In Figs. 4 and 12, it is noted that the shear fractures are perpendicular to the foliation plane. Along this plane, cracks are opened, enabling the emplacement of small dykes.

#### Relationship between fold and joint

Many joints are systematically disposed about fold and it has generally been assumed that they have resulted from the same compressive forces as those that produced folds. Fracture joint is characteristically developed in incompetent layers. The joints (Figs 4 and 5) are fracture and shear joints. As it is noted in field due to small folds and in Fig. 8 that the fold axis is trending N-S, parallel to the foliation and banding, therefore, the joints are conjugate strike joints, as are given in Fig. 4. If the joints (Figs 4 and 5) are compared with the strain ellipsoid (Fig. 11), it would be noted that the greatest strain axis is lying N-S, whereas the least axis lying E-W direction, showing a displacement along it. The intermediate strain axis is lying parallel to the beta or shear axis. The attitude of fold indicates that the compressive force was acting along E-W direction. The joints could be interpreted as shear fractures that developed due to a compressive force in an east-west direction, but under such condition that the easiest relief was upward.

#### Phenomenon of cracks and space opening

Cracks and space are formed more easily in Migmatite of the area, because the fold axis and the system of joints are controlled by the same compressive forces. In the investigated area the greatest strain axis is lying N-S direction and normal to this lies the least strain axis, these are the zones of low pressure where



the majority of the pegmatitic dikes have introduced.

Folding, joints and faults play a great role in space opening. If competent and incompetent layers lie side by side and become folded, this results in splitting and dilation. If incompetent layers are folded, this results in expansion beyond the neutral zone, which leads to the formation of cracks and fissures. If the fold is too narrow, a conical fold can develop into a congruent fold and as a result, spaces develop both in the anticline and the syncline. Also the shearing and schistosity plane of a divergent flexure plane can open perpendicularly in the direction of the stress, thus enabling the emplacement of small dykes (Uebel, 1980).

As it is seen in Fig. 12 that the ruptures are produced due to shearing, even before this splitting takes place feather joint (Fig. 13) are developed in the rock. These feather joints lie diagonally to the direction of friction plane and can develop to a great extent, building up spaces for the formation of intrusive bodies. Generally the ruptures by shearing in any form, either by break-off, twisting or rotation of parts of moving layers, can lead to intrusive spaces (Uebel, 1980),

Larger spaces are formed by additional tectonic processes and here gravity is a contributing factor. If a rock complex is first confined under stress of biaxial tectonic deformation, with extension of joints and lateral contraction decomposed into shearing fissures, the effect of gravity can not be ruled out. As a result, blocks lose their attachment to the rock units and subside (Uebel, 1975, 1978 and 1980). This process leads to the formation of spaces at depth and the bordering planes of such blocks are the former shearing planes (Fig 14). The shearing and subsiding effect is seen at the contact of country rock. Considering one side only, it looks like a process caused by sand-

wiching of the dykes. Regarding both contact border, it is clear that the effect runs contrary to the other direction (i.e. caused by shearing). The separation of the blocks from the upper region is probably possible due to the horizontal fissures (bedding joints), which are mostly the result of uniaxial extension strain perpendicular to a sideward separation. The whole process is supported and even caused by gravity. Sometimes this separation can be caused by an upward directed shearing fissure. For instance X-rupture system of the same age or diagonal fissure of a different age can lead to a Y-rupture system. Besides these prevailing planes, folding planes, planes of schistosity and the planes parallel to the metamorphic bands can be used, (Fig. 15). The size of the formed space depends, however, on the size, shape and movement of the block (Uebel, 1980). Along such spaces, mobilizes of pegmatites intruded and crystallized there.

## CONCLUSION

Folding, joints and faults play a great role in space opening in Migmatite. When the incompetent layers are folded, they resulted in expansion beyond the neutral zone, which leads to the formation of cracks fissures. The shearing and schistosity plane of a divergent flexure plane can open perpendicularly in the direction of the stress, thus enabling the emplacement of small dykes. Shearing produced rupture and even before this splitting, feather joints are produced, diagonally to the direction of friction plane, develop to a great extent and built up spaces for intrusive bodies. The joint system of the Migmatite body is controlled by compressive stress in E-W direction. The shear ruptures are developed at an angle of 30° to this stress, along which the majority of the pegmatitic veins and dykes are lying.

Larger spaces are formed by additional tectonic processes and thereby gravity play a



great role. If rock complex is first confined under a stress of biaxial tectonic deformation, with extension joints and lateral contraction decomposed into shearing fissures, together with the effect of gravity. As a result, block lose their attachment to the rock units and subside. This process leads to the formation of

spaces at depth and the bordering planes of such blocks are the former shearplanes. The shearing and subsiding effect is seen at the contact of Migmatite with that of pegmatites. The spaces such formed, along them, mobile phases are intruded and are subsequently crystallized there.

### ACKNOWLEDGEMENT

This study is a part of approved Ph. D. thesis, submitted to Faculty of Geosciences, Technical University, Berlin, W. Germany. Author is grateful to Prof. Dr. P. J. Uebel, Prof. Dr. J. Stiefel, Dr. M. I. Ogumbajo and Dr. D. Rose for their guidance, discussions and cooperation. Thanks are also due to Faculty of Geosciences, Technical University, Berlin, W. Germany to allow me to work on this project and partly funding the field work expenses.

### CONCLUSION

Folding, joints and faults play a great role in space opening in Migmatite. When the incompetent layers are folded, they result in expansion beyond the neutral zone, which leads to the formation of cracks and fissures. The shearing and schistosity plane of a divergent flexure plane can open perpendicularly in the direction of the stress, thus enabling the emplacement of small dykes. Shearing produced rupture and even before this splitting, feather joints are produced, diagonally to the direction of friction plane, develop to a great extent and built up spaces for intrusive bodies. The joint system of the Migmatite body is controlled by compressive stress in E-W direction. The shear ruptures are developed at an angle of 30° to this stress, along which the majority of the pegmatite veins and dykes are lying.

Larger spaces are formed by additional tectonic processes and thereby gravity play a

As it is seen in Fig. 12 that the ruptures are produced due to shearing, even before this splitting takes place feather joint (Fig. 13) are developed in the rock. These feather joints lie diagonally to the direction of friction plane and can develop to a great extent, building up spaces for the formation of intrusive bodies. Generally the ruptures by shearing in any form, either by break-off, twisting or rotation of parts of moving layers, can lead to intrusive spaces (Uebel, 1980).

Larger spaces are formed by additional tectonic processes and here gravity is a controlling factor. If a rock complex is first confined under stress of biaxial tectonic deformation, with extension of joints and lateral contraction decomposed into shearing fissures, the effect of gravity can not be ruled out. As a result, blocks lose their attachment to the rock units and subside (Uebel, 1975, 1978 and 1980). This process leads to the formation of spaces at depth and the bordering planes of such blocks are the former shearing planes (Fig. 14). The shearing and subsiding effect is seen at the contact of country rock. Considering one side only, it looks like a process caused by sand-



TABLE I  
Foliation readings in Migmatite

3/66E	25/48E	178/46E	11/57E	11/66E	15/63E
24/47E	15/45E	32/55ES	1/52E	11/72E	35/SE
43/64SE	53/64SE	29/64E	17/67E	13/73E	5/76E
5/73E	3/52E	9/69E	175/76E	173/62E	17/62E
175/78E	7/72E	175/52E	17/62E	5/42E	15/50E
13/83E	12/65E	175/62E	27/62E	1/66E	1/48E
9/62E	6/62E	19/52E	16/62E	176/74E	16/62E
175/76E	14/75E	14/62E	174/81E	3/78E	3/72E
7/68E	179/55E	2/73E	176/56E	174/63E	174/46E
8/58E	3/51E	176/55E	9/69E	7/53E	14/69E
11/72E	12/72E	2/78E	14/69E	14/64E	13/48E
13/52E	12/52E	11/57E	25/73E	15/40E	15/60E
21/75E	15/74E	25/52E	23/70E	15/60E	23/48E
13/62E	23/70E	13/62E	15/55E	13/37E	13/87E
7/74E	23/73E	21/73E	23/74E	21/73E	21/74E
23/74S	24/72E	21/73E	31/65SE	11/82E	9/50E
16/62E	14/75E	2/73E	14/69E		



TABLE II  
Joints readings in Migmatite

94/74N	153/73NE	37/72NW	153/73NE	97/89N	101/77N
127/55NE	103/79N	129/80NE	113/85NE	97/87N	101/66N
121/84NE	111/84N	80/89N	129/74NE	147/74NE	103/88N
38/72NW	126/85NE	103/64N	83/89N	159/79SW	67/68NW
133/81NE	99/71N	79/84S	145/68NE	83/62S	7/58E
97/66N	29/89N	127/83NE	169/72SW	83/89N	133/30NE
171/82E	157/76NE	95/72S	93/78N	159/82NE	69/84NW
123/81NE	45/78SE	101/83N	133/84NE	153/78SW	113/89N
127/84NE	105/83N	93/78N	119/72NE	107/82N	113/75NE
67/89N	137/86NE	29/69NW	127/86NE	73/72NW	83/72SW
55/52NW	87/79N	129/78NE	89/76N	129/82NE	73/74NW
153/87NE	101/82N	89/89N	99/76N	123/84NE	81/84N
95/85N	87/69N	109/54N	63/32NW	133/75SW	81/89N
111/83NE	125/82NE	81/35N	109/89NE	82/82NW	95/87N
83/86N	130/83NE	97/85N	83/86N	126/73NE	153/62SW
131/89NE	83/37N	113/65NE	110/47NE	83/78N	72/87NW
105/84NE	136/62NE	86/69N	109/72NE	124/84NE	73/79NW
116/87NE	106/84N	80/84N	144/37NE	126/79NE	149/71N
136/59NE	103/62N	83/78N	122/72NE	166/75NE	23/78SW
126/65NE	83/76N	74/85NW	138/66NE	49/74NW	116/87NE
109/86SW	83/86N	105/76NE	131/86NE	69/84NW	112/89NE
75/86NW	109/86N	81/84N	109/84N	141/54NE	81/52N
136/72NE	83/68N	147/68NE	108/82N	142/74NE	105/82N
131/72NE	105/79N	130/69NE	87/74N	106/86N	126/86NE
102/82N	93/89N	105/86N	74/89NW	105/84N	124/89NE
101/62N	75/84NW	91/82N	141/72NE	71/62NW	109/76N
62/66NW	131/22NE	115/86NE	87/82N	136/80NE	128/68NE
118/64NE	101/82N	21/82SE	101/84N	31/84SE	111/75NE
83/87N	96/86N	90/78N	134/59NE	133/63NE	100/82N
95/54N	73/76SE	49/76NW	171/73E	139/60NE	111/84NE
117/54SW	103/82N	143/89NE	87/74SE	109/80N	143/82NE
38/72NW	85/80N	81/89N	133/86NE	95/84N	113/77NE
103/82N	93/89N	55/82NW	93/82N	55/82NW	93/82N
33/87NW	103/84N	33/82NW	153/79SW	43/65NW	45/62SE
47/75NW	115/88NE	75/50NW	9/58E	29/88SE	89/53NW
147/70NE	38/78NW	115/74SW	125/76NE	87/35S	101/89N
102/82N	113/65NE	83/85N	73/75SE	55/79NW	123/81NE
21/82SE	111/65NE	87/82N	133/63NE	109/79N	143/79NE
101/83N	113/72NE				



TABLE III

Statistical distributions of strike directions of Joint from Table II to get a Joint Diagram

Strike directions	: 0-1	10-20	20-30	30-40	40-50	50-60	60-70	70-80	80-90
Strike data amount	: 2	1	4	9	4	3	7	10	37
Percentage	: 0,87	0,43	1,74	3,91	1,74	1,30	3,04	4,35	16,09
Strike directions	: 90-100	100-110	110-120	120-130	130-140	140-150	150-160	160-170	170-180
Strike data amount	: 18	49	18	20	23	10	9	3	3
Percentage	: 7,83	21,30	7,83	8,70	10,00	4,35	3,90	1,30	1,30

TABLE IV

Statistical distribution of angles, measured due to the traces of fractures with that of N-S line of aerial photograph No. E5

Angles display	: 1-10	11-20	21-30	31-40	41-50	51-60	61-70	71-80	81-90
Angles amount in percentage	: 0	3	3	8	7	1	1	2	8
Angles display	: 91-100	101-110	111-120	121-130	131-140	141-150	151-160	161-170	171-180
Angles amount in percentage	: 3	13	10	4	14	2	2	1	18



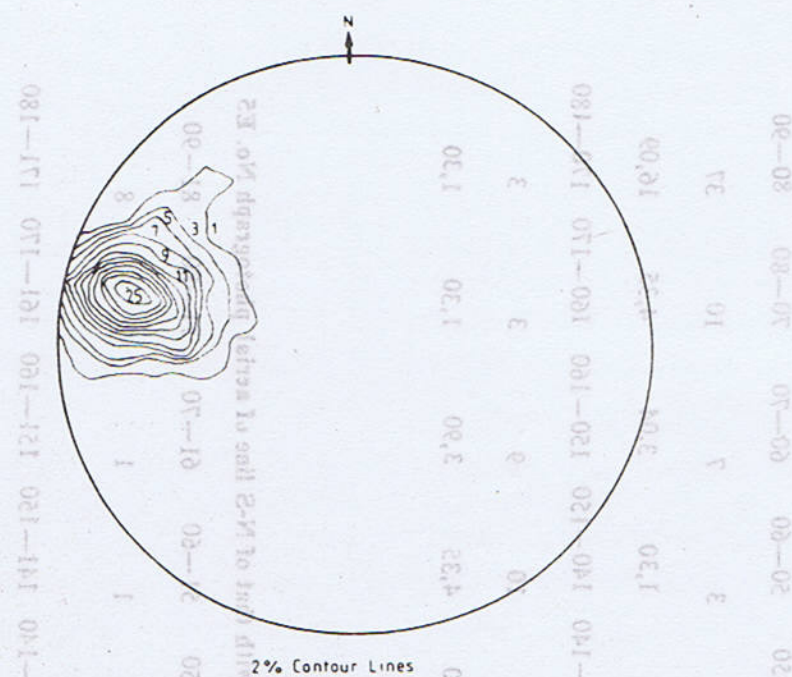


Fig. 1. 2% contour lines for the planes of poles of foliation in Migmatite are drawn due to the readings given in Table-I.

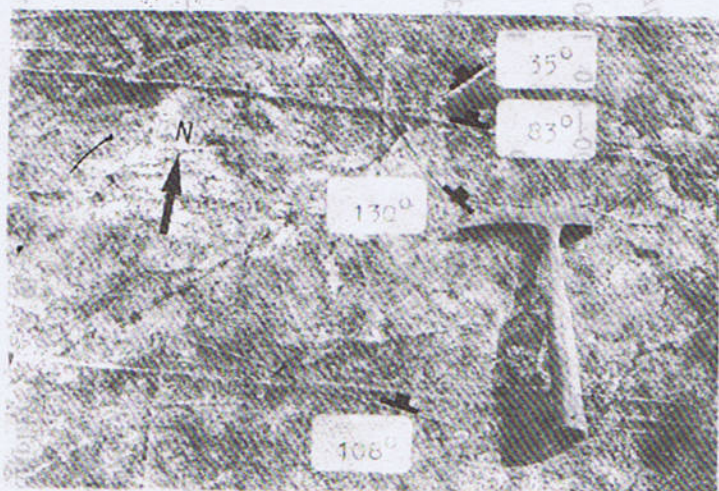


Fig. 2. Joints and Rock cleavage in Evje-Iveland Migmatite.







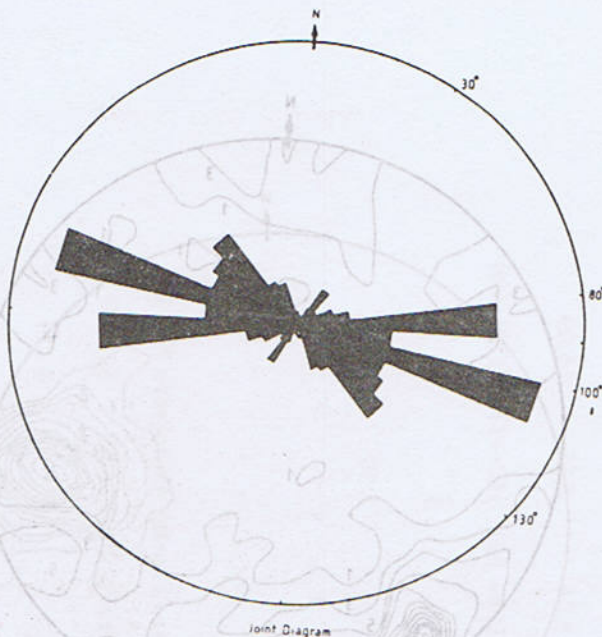
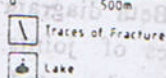
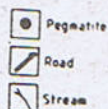


Fig. 5. Joint diagram produced due to the statistical distributions of strike directions of joints from Table-II. The percentage values are given in Table-III.



Aerial Photograph No. E5

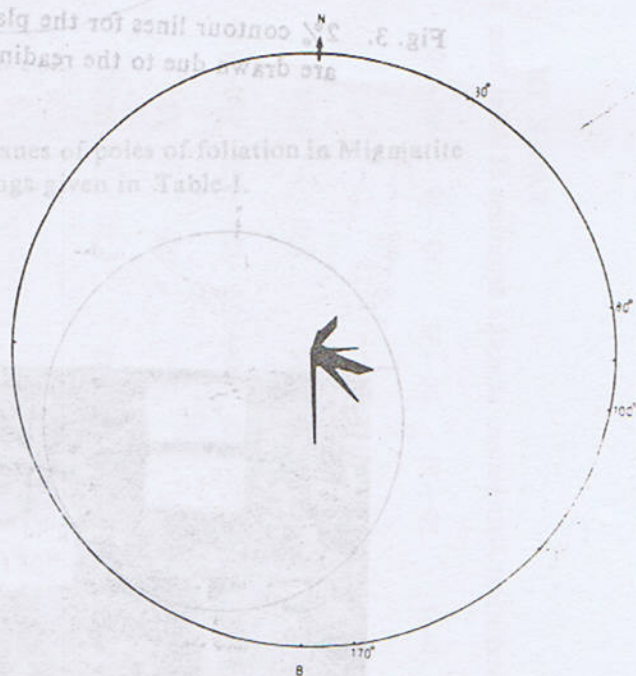


Fig. 6. A ; Traces of fractures of aerial photograph No. E5 of the investigated area. B ; Traces diagram shows that the strike value of the fractures are lying between 30-40°, 80-0°, 100-110°, 130-140° and 170-180° degrees. The first four values of the strike of the fractures are the same values as in Fig. 5 for the joints.





Fig. 7. A pegmatitic dike, about 20 centimeters thick, present in Migmatite. It is striking  $85^{\circ}$  and is dipping towards north. This dike is parallel to the joint with a strike  $85^{\circ}$ .

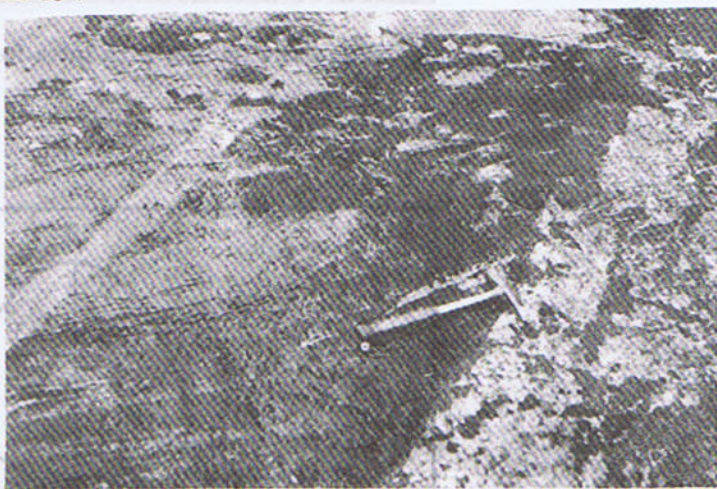


Fig. 8. Pegmatite lying with sharp contact in Migmatite. Parallel to this pegmatite a pegmatitic vein is present. Both are striking  $133^{\circ}$ .



Fig. 9. Two small pegmatitic veins in Migmatite. The old vein is striking  $100^{\circ}$  and dip is  $72^{\circ}\text{N}$ . Whereas the younger vein, which cut the older one, strikes  $137^{\circ}$  and dips  $22^{\circ}\text{NE}$ .



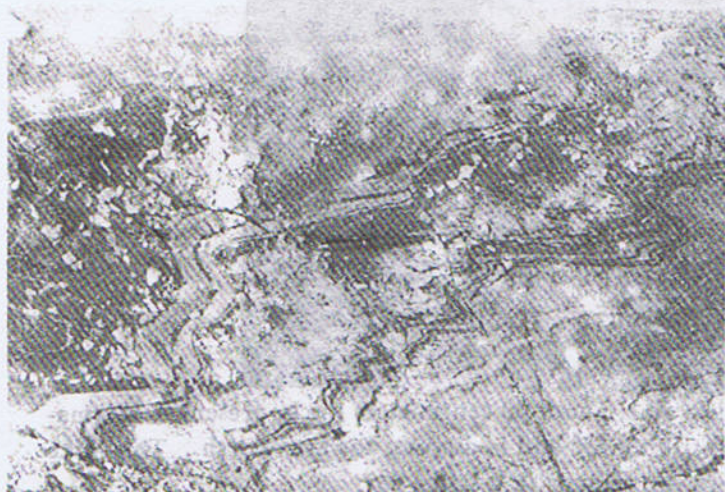


Fig. 10. Ptygmatic folding with intra-formational fault in Migmatite.

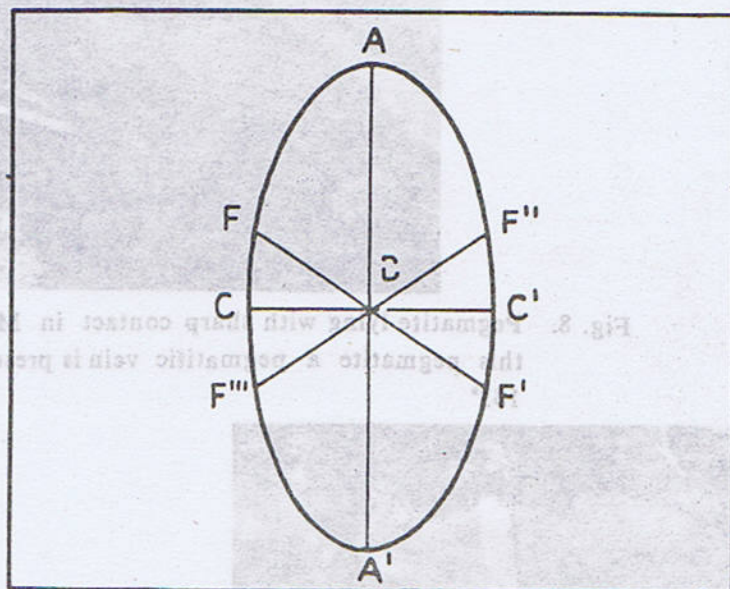


Fig. 11. Relation of joint to strain ellipsoid.  $AA'$  is the greatest strain axis ;  $CC'$  is the least strain axis and  $B$  is the intermediate strain axis, which is perpendicular to the plane of the paper. Fracture joint develop parallel to the planes represented by  $FF'$ , and  $F''F'''$ . The shear joints are produced parallel to  $CC'$ , (After Billing, 1972).



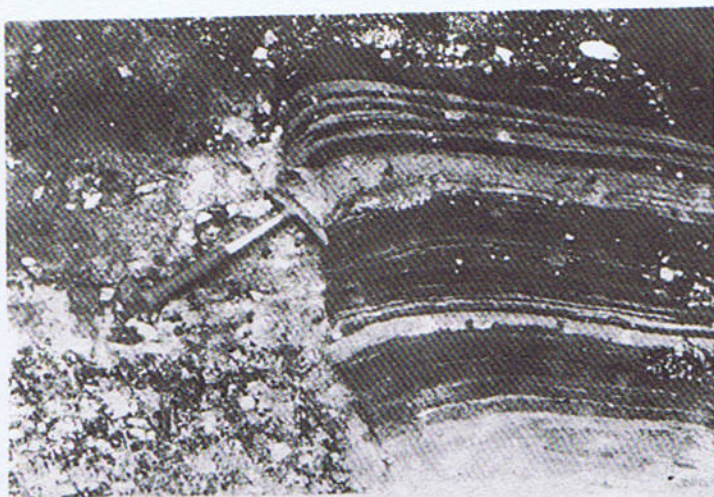


Fig. 12. Shearing rupture, recognized by the banding of the Migmatite at the contact with Peg. 2A in contrary directions at both contacts. The photo shows only one side.



Fig. 13. In the first stage of opening feather joints sometimes develop diagonally to the direction of slip. (After Uebel, 1980).





Fig. 14. The opening process has started on a great shearing rupture. This is recognized by the bending of Migmatite in contrary directions at both contacts of the dike. The photo shows only one side.



Fig. 15. The hanging-wall country rock of the flat lying pegmatite shows a vertical rupture by shearing. The contact is sharp. The continuation of the vertical dislocation in the pegmatite is caused by younger tectonics. A subsiding block separated by gravity has probably developed the space.



## REFERENCES

- Barth, T.F.W. 1947. The nickeliferous Iveland-Evje amphibolite and its relation. *N.G.U.*, 168a, 1-71.
- Barth, T.F.W., and Dons, J.A. 1960. Precambrian of southern Norway. *N.G.U.*, 208, 5-67.
- Billings, M.P. 1972. Structural Geology. Prentice-Hall, London, 1-606.
- Lodhi, S.A.K., 1983. Das Nebengestein in Pegmatite-gebiet Evje-Iveland, Sued Norwegen, (Tektonik, Gefuege, Modalbestand und gegenseitige Beeinflussung Von Nebengestein und pegmatitischen Loesungen). Dissertation Technical University, Berlin. 1-180.
- Oftedahl, Chr. 1980. Geology of Norway. (Contribution 26th International Geological Congress, Paris, 1980), *Universitetsforlaget, Trondheim, Oslo, N.G.U.*, 356, 1-167.
- Saxena, S.K., and Bhattacharjee, S. 1977. Energetics of geological processes-Springer Verlag, New York, 1-473.
- Uebel, P.J. 1975. Platznahme und Genese des Pegmatites Hangensdorf-Sued. *N.Jb. Miner. Mh.*, 318-332.
- Uebel, P.J. 1980. Emplacement of dykes and pluglike bodies, as demonstrated by Pegmatites. *N. Jb. Miner. Abh.* 138, 207-227.
- Wenk, E., 1936. Zur Genese der Baendergneise Von Orno Huvud. *Bull. Geol. Inst. Uppsala*, 26, 81-85.



## CHEMICAL QUALITY OF WATER SAMPLES FROM SAIN AREA (ANGOORI) ISLAMABAD

BY

ZAHID KARIM KHAN and SYED ALIM AHMAD

Institute of Geology, Punjab University, New Campus, Lahore-20, Pakistan

**Abstract:** Water samples collected from the Soan river and its tributaries were analysed for major anions and cations in the laboratories of the Institute of Geology, Punjab University, Lahore. To evaluate the quality for drinking purposes, sulphate ( $\text{SO}_4^{--}$ ), chlorides ( $\text{Cl}^-$ ) bicarbonate ( $\text{HCO}_3^-$ ) and total dissolved salts concentrations were compared within standard ASTM<sup>1</sup> quality limits. In order to test the suitability of water for agricultural use data was reproduced and Sodium adsorption ratios were calculated and compared with the standard SAR<sup>2</sup> ratio. It is found that all water samples were equally favourable for drinking and farm use.

The whole chemical data of all cation and anion concentrations were recalculated to 100 to represent the quality graphically.

### INTRODUCTION

The Sain area lies within the quadrangle from 33° 49' 16" to 33° 50' 22" lat. and 73° 22' 25" to 73° 23' 00" long. It is underlain by the Murree Formation which comprises alterations of sandstone, shale and claystone. The sandstones are fractured, highly jointed and permeable so acting as aquifer, conducting the water towards the foothills. Sandstone-shale contacts form because of the impermeable nature of the springs shales. As a result of increase in the population of the Islamabad metropolitan area and other developments around it, future demands for good quality drinking water are likely to increase. A related increasing demand for water for agricultural purposes, as proposed near Angoori and surrounding farms, is apparent.

The Soan stream and its tributaries may prove a suitable source of water for their future demands.

Six surface water samples were collected from different localities of the Sain area. One of them is from the main Soan river, whereas the other five are from tributaries. The main sources of the streams are springs which emerge at higher elevations in the surrounding area.

Major cation and anion concentrations are estimated and quality is determined on the basis of the A.S.T.M. recommendations. In the tables, the Soan river sample is represented by S and tributaries are represented by ST<sub>x</sub>.

1. Detailed specification for water quality according to American Standard for testing materials are given in the book "Groundwater Hydrology (Todd, 1959).
2. Sodium adsorption ratio.



## QUALITY EVALUATION FOR DRINKING AND AGRICULTURAL USE

Chemical analysis of water samples was carried out by the method given in the ASTM. Major cations and anions determined were  $\text{Ca}^{++}$ ,  $\text{Mg}^{++}$ ,  $\text{Na}^+$ ,  $\text{K}^+$ ,  $\text{HCO}_3^-$ ,  $\text{Cl}^-$  and  $\text{SO}_4^{--}$ . As far as suitability is concerned, it is found that  $[\text{Mg}^{++}]$  varies from 1.00 ml/L to 3.47 ml/L (or 12 ppm to 42 ppm) which is very much below the maximum permissible limit of 125 ppm. Sulphate ( $\text{SO}_4^{--}$ ) ionic concentration varies from 47.50 ppm (1.20 ml/L) to 57.50 ppm (1.8 ml/L), where the maximum permissible limit for drinking use is 250 ppm. Similarly chloride ranges from 10.65 ppm (0.300 ml/L to 17.75 ppm (0.500 ml/L) which is also below from the limit which is 250 ppm.

As far as the total dissolved salts are concerned, as estimated from conductivity which ranges from  $772.98 \text{ EC} \times 10^6$  (or 495.76 ppm) to  $933.66 \text{ EC} \times 10^6$  (598.50 ppm). Similarly the TDS value range is also safely below the permissible upper limit, which is 1,000 ppm.

In order to assess the suitability of water for agricultural in (Table No. 7), the ionic concentration of Ca, Mg, and Na are put into the formulae of sodium adsorption ratio SAR (Todd, 1959).

$$\text{SAR} = \frac{\text{Na meq/L}}{\frac{\text{Ca} + \text{Mg}}{2}}$$

## ACKNOWLEDGEMENTS

The authors thank Prof. F.A. Shams who provided the opportunity to work with the foreign experts. Authors also like to acknowledge the assistance of M/S Nadeem Farooq, Khurram Nawaz and Zia-ud-Din, in the collection of samples.

SAR value varies from 0.26 meq/L to 1.80 meq/L which falls below the approved maximum SAR limit of 10 meq/L for agricultural use.

## DISCUSSION

The chemical results for all samples are given in Figs. 1, 2 and 3. Fig. 1 gives the ionic concentrations, expressed in milliequivalents per litre. The base of the each figure represents the approximate ionic concentration of the water sample. The variation pattern on ionic concentration in the last three samples i.e. ST<sub>4</sub>, ST<sub>5</sub> and ST<sub>6</sub> are almost similar to each other. It may be observed that, among the cations, sodium ionic concentration is more than magnesium while calcium is the greatest among all others anion concentrations starts from zero and reaches maximum at ( $\text{HCO}_3^- + \text{CO}_3^{--}$ ) belt. The variation pattern design of the first three samples i.e. ST<sub>1</sub>, ST<sub>2</sub> compositions are not only different from last three pattern but also from each other.

The plot of concentration on Morgan and Winner (1962) (Fig. 3) triangle shows that all samples represents the bicarbonate and calcium dominancy and thus lies in the phase of  $\text{HCO}_3^- \text{Cl} + \text{SO}_4^{--} \text{Ca}$  belt in the diagram.



TABLE No. 1

Location = ST<sub>1</sub>T.D.S. = 598.50 or 933.66 EC × 10<sup>6</sup> (micromohes/cm (EC × 10<sup>6</sup>))

Cations	mg/L	meq/L	% meq	Anions	mg/L	meq/L	% meq
Ca	77.875	3.88	49.12	CO <sub>3</sub>	25.00	0.83	10.34
Mg	12.38	1.02	12.91	HCO <sub>3</sub>	336.0	5.50	68.57
Na	65.00	2.82	35.70	Cl	17.75	0.50	6.23
K	7.00	0.179	2.27	SO <sub>4</sub>	57.50	1.20	14.86
				NO <sub>3</sub>	—	—	—
				F	—	—	—
Total		= 7.899				8.03	

$$\text{Ion Balance} = \text{Cations} - \text{Anions meq/L} = 0.131$$

$$\% \text{ Discrepancy} = \frac{\text{Ion Balance}}{\text{Cations} + \text{Anions}} \times 100 = 0.82$$

TABLE No. 2

Location = S

T.D.S. = 495.76 ppm or 772.98 EC × 10<sup>6</sup>

Cations	mg/L	meq/L	% meq	Anions	mg/L	meq/L	% meq
Ca	85.312	4.25	51.27	CO <sub>3</sub>	28.00	0.93	11.43
Mg	42.18	3.47	41.86	HCO <sub>3</sub>	343.00	5.16	62.43
Na	12.00	0.52	6.27	Cl	11.18	0.315	3.87
K	2.00	0.05	0.60	SO <sub>4</sub>	53.50	1.73	21.27
Total		= 8.29				8.135	

$$\text{Ion Balance} = \text{Cations} - \text{Anions meq/L} = 0.155$$

$$\% \text{ Discrepancy} = \frac{\text{Ion Balance}}{\text{Cations} + \text{Anions}} \times 100 = 0.94$$



TABLE No. 3  
Location=ST<sub>3</sub>  
T.D.S. = 566.00 ppm or 882.98 EC  $\times 10^6$

Cations	mg/L	meq/L	% meq	Anions	mg/L	meq/L	% meq
Ca	90.127	4.49	57.56	CO <sub>3</sub>	10.00	0.33	4.35
Mg	24.87	2.04	26.15	HCO <sub>3</sub>	308.00	5.04	66.49
Na	26.00	1.13	14.49	Cl	14.20	0.400	5.28
K	5.50	0.140	1.79	SO <sub>4</sub>	57.30	1.81	23.88
Total		= 7.80				7.58	
Ion Balance = Cations - Anions meq/L						= 0.22	
% Discrepancy = $\frac{\text{Ion Balance}}{\text{Cations} + \text{Anions}} \times 100$						= 1.43	

TABLE No. 4  
Location=ST<sub>4</sub>  
T.D.S.=505.6 PPM or 787.8 EC  $\times 10^6$

Cations	mg/L	meq/L	% meq	Anion	mg/L	meq/L	% meq
Ca	88.240	4.40	62.68	CO <sub>3</sub>	24.00	0.80	12.64
Mg	12.260	1.00	14.25	HCO <sub>3</sub>	248.00	4.06	64.14
Na	36.00	1.57	22.36	Cl	10.65	0.300	4.74
K	2.000	0.051	0.712	SO <sub>4</sub>	56.40	1.17	18.48
Total	= 7.02					0.69	
Ion Balance = Cations - Anions meq/L						= 0.69	
% Discrepancy = $\frac{\text{Ion Balance}}{\text{Cations} + \text{Anions}} \times 100$						= 5.16	



TABLE No. 5

Location = ST<sub>2</sub>T.D.S. = 580.15 PPM or 905.034 EC  $\times 10^6$ 

Cations	mg/L	meq/L	% meq	Anions	mg/L	meq/L	% meq
Ca	87.351	4.36	54.16	CO <sub>3</sub>	28.00	0.93	11.77
Mg	19.149	1.57	19.50	HCO <sub>3</sub>	300.00	4.91	62.15
Na	47.00	2.04	25.34	Cl	20.65	0.300	3.79
K	3.50	0.08	0.99	SO <sub>4</sub>	54.50	1.76	22.28
Total	=	8.05				7.90	

$$\text{Ion Balance} = \text{Cations} - \text{Anions meq/L} = 0.15$$

$$\% \text{ Discrepancy} = \frac{\text{Ion Balance}}{\text{Cation} + \text{Anions}} \times 100 = 0.94$$

TABLE No. 6

Location = ST<sub>3</sub>T.D.S. = 558.5 or 871.28 EC  $\times 10^6$ 

Cations	mg/L	meq/L	% meq	Anions	mg/L	meq/L	% meq
Ca	79.632	3.97	52.65	CO <sub>3</sub>	12.00	0.40	5.35
Mg	19.85	1.63	21.61	HCO <sub>3</sub>	308.00	5.05	67.60
Na	42.00	1.82	24.14	Cl	24.20	0.40	5.35
K	5.00	0.12	1.59	SO <sub>4</sub>	47.80	1.62	21.69
Total	=	7.54				7.47	

$$\text{Ion Balance} = \text{Cations} - \text{Anions meq/L} = 0.07$$

$$\% \text{ Discrepancy} = \frac{\text{Ion Balance}}{\text{Cations} + \text{Anions}} \times 100 = 0.46$$



**TABLE No. 7**  
**Feasibility of Water Samples for Irrigation Purpose**

S. No.	Location	Ca meq/L	Mg meq/L	Na meq/L	S.A.R.
1	ST <sub>1</sub>	3.88	1.02	2.82	1.80
2	S	4.25	3.47	0.52	0.26
3	ST <sub>3</sub>	4.49	2.04	1.13	0.62
4	ST <sub>4</sub>	4.40	1.00	1.57	0.96
5	ST <sub>2</sub>	4.36	1.57	2.04	1.19
6	ST <sub>5</sub>	3.97	1.68	1.82	1.67

Formula of Sodium Adsorption Ratio  $SAR = \frac{Na \text{ meq/L}}{Ca + Mg}$

SAR = Water Class

< 10 = Excellent

10-18 = Good

18-26 = Fair

> 26 = Poor

**TABLE No. 8**  
**Feasibility of Water Samples for Drinking purpose**

S. No.	Major Constituents (in PPM)	ST <sub>1</sub>	S	ST <sub>3</sub>	ST <sub>4</sub>	ST <sub>2</sub>	ST <sub>5</sub>	Upper p. Limits
1	Mg	12.38	42.18	24.87	12.26	19.149	19.85	125
2	SO <sub>4</sub>	57.50	53.52	57.30	56.40	54.500	47.80	250
3	Cl	17.75	11.18	14.20	10.65	10.65	14.20	250
4	T.D.S.	598.50	495.76	566.00	505.60	580.15	558.50	1000

Result :—All the samples falls in the excellent quality for drinking purpose.



## Chemical Quality of water samples from Sain Area (Angoori) Islamabad.

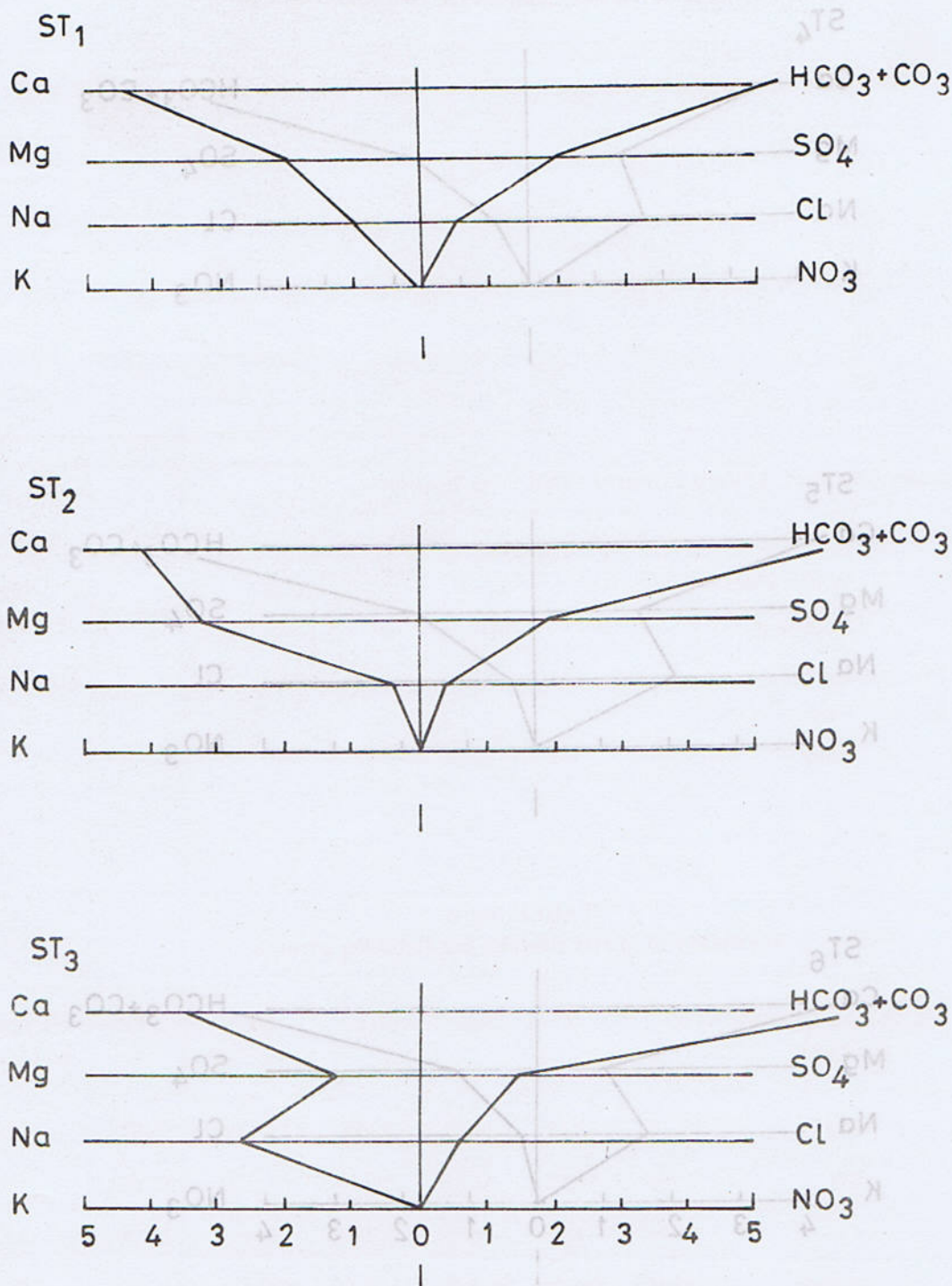


Fig. 1. Ionic concentration of the water samples from sain area, (Islamabad).



Chemical Quality of water samples from Sain Area (Angoori) Islamabad.

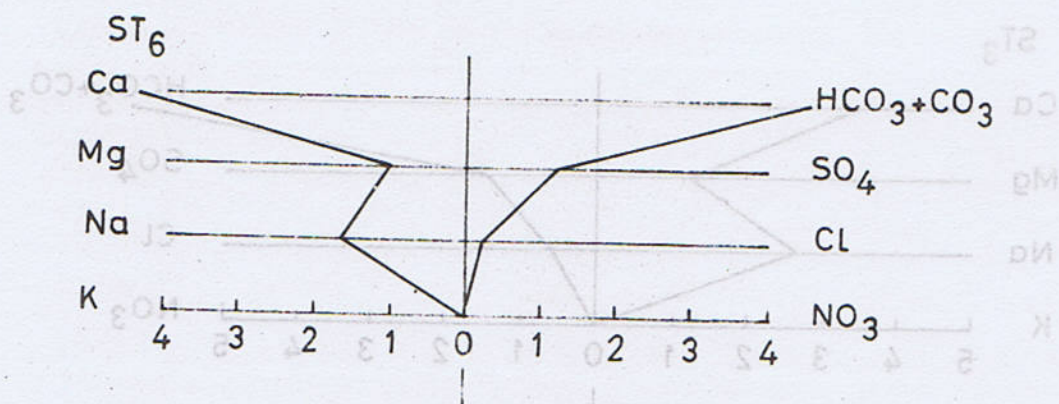
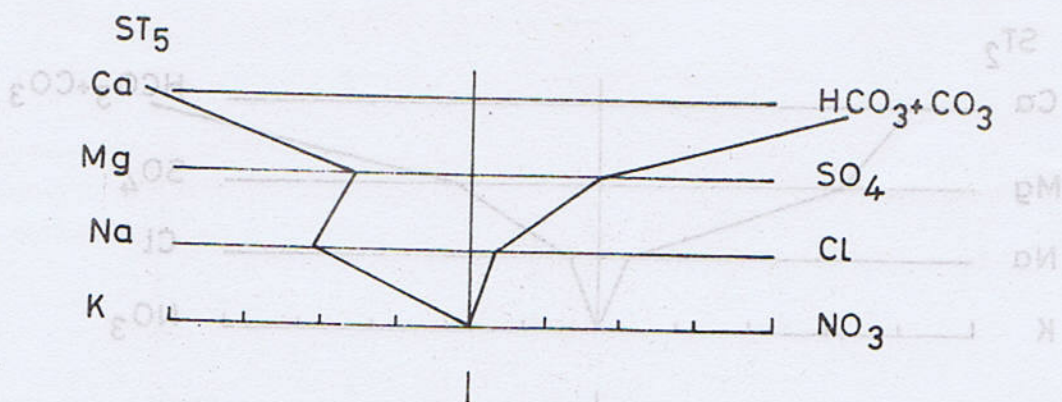
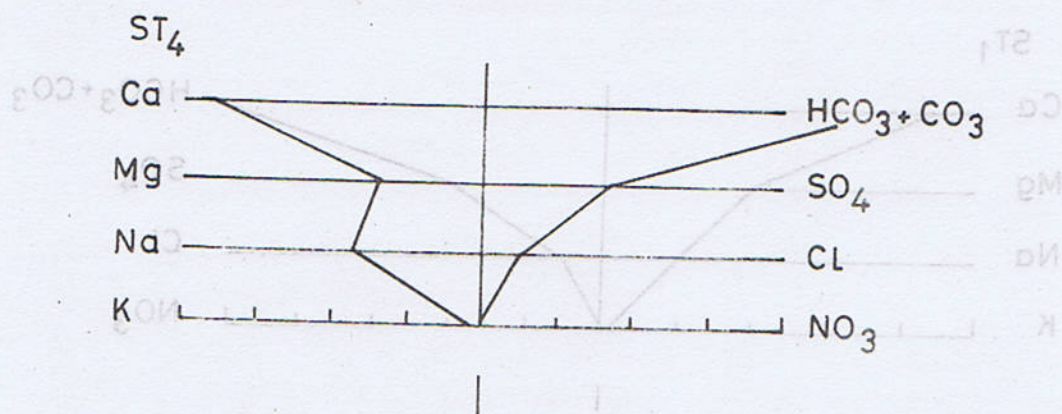


Fig. 2. Ionic concentration of the water samples from sain area (Islamabad).



## TRILINEAR PLOT

Chemical analyses of water samples represented as percentages of total equivalent per liter on diagram developed by Hill (1940) and piper (1944).

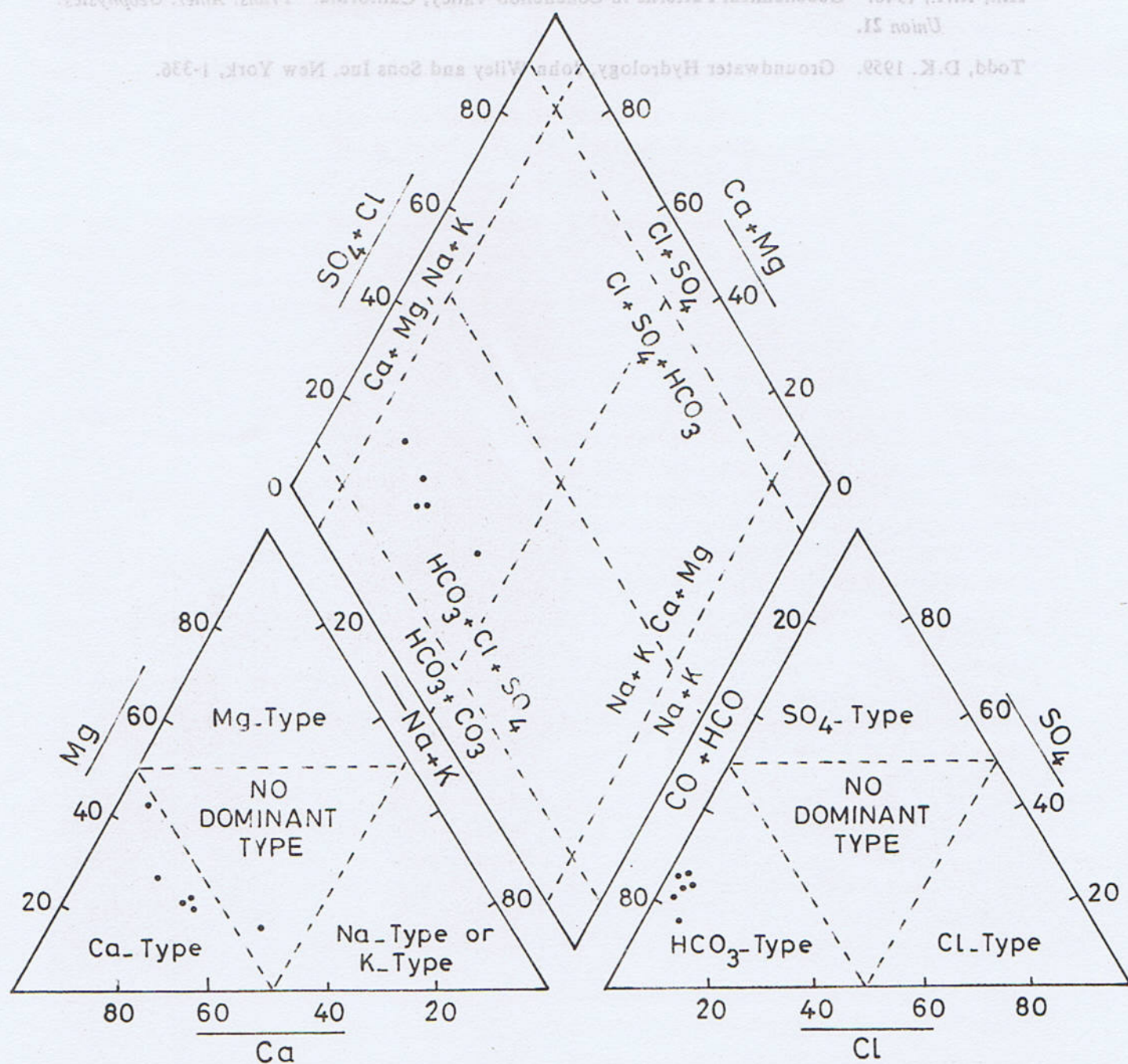


Fig. 3. Classification diagram for anion and cation facies interms of major iron percentages. Water types are designed according to the domain in which they occur on the diagram segments (after Morgan and Winner, 1962, Back, 1966 and Ahmad, Z. 1985).



## REFERENCES

- Ahmad, Z. 1985. Water Chemistry and irrigation water criteria of the Thalab Aquifer, Baluchistan, *Kashmir Jour. Geol.*, 3, 65-67.
- Hill, R.A., 1940. Geochemical Patterns in Coachello Valley, California. *Trans. Amer. Geophysics. Union* 21.
- Todd, D.K. 1959. Groundwater Hydrology, John Wiley and Sons Inc. New York, 1-336.

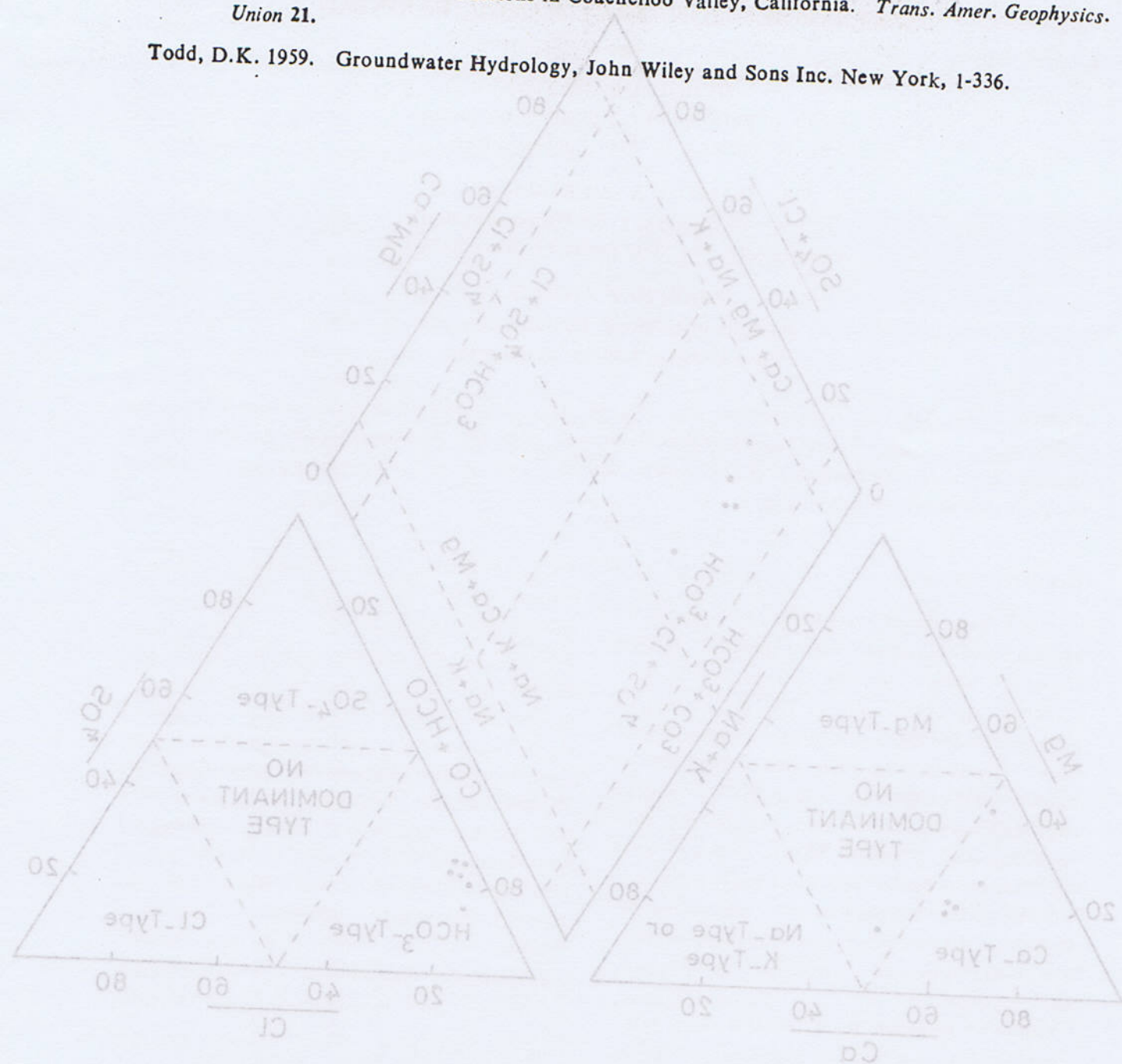


Fig. 3. Classification diagram for anion and cation facies in terms of major ion percentages. Water types are designed according to the domain in which they occur on the diagram segments (after Morgan and Winnet, 1967; Back, 1966 and Ahmad, Z. 1985).



102

**SOME DASYCLADACEAN AND GYMNOCODIACEAN ALGAE  
FROM THE WARGAL AND CHHIDRU FORMATIONS,  
SAKESAR SECTION, SALT RANGE, PAKISTAN**

BY

**OVIDIU DRAGASTAN**

Lab. of Paleontology, University of Bucharest,  
Bd. N. Balcescu 1, 70111 Bucharest, Romania.

**DOROTHEE MERTMANN**

Institute of Geology, Freie Universitat Berlin,  
Altensteinstr. 34a, 1000 Berlin 33, West Germany.

**SARFRAZ AHMED**

Institute of Geology, Punjab University,  
New Campus, Lahore 20, Pakistan.

**Abstract :** The Sakesar Section which is situated in the western Salt Range presents an almost complete rock sequence of the Wargal and Chhidru Formations up to the Permian/Triassic boundary. The macrofacies are described briefly. A few samples yielded a variety of algal species belonging to the Dasycladales and Gymnociodiaceae.

## INTRODUCTION

The Salt Range stretches out between Jhelum and Kalabagh areas (Fig. 1). Over there, the marine Permian attracted a lot of attention since the end of the last century (Waagen 1884; Wynne 1875, 1878; Middlemiss 1891; Noetling 1894, 1896, 1900; Reed 1931; Dunbar 1933). Gee (1947) mapped the entire area and modified the nomenclature of the rock sequence. Gerth (1950) defined the "Chhidruan substage" in the Upper Permian. Schindewolf (1954) marked the appearance of *Ophiceras connectens* in the basal part of the Mianwali Formation, discussing the position and significance of the Permian/Triassic boundary. Kummel & Teichert (1966, 1970) established its new position between the "White Sandstone Unit" and the Kathwai Member.

They consulted a lot of work done on conodonts (Sweet, 1970), brachiopods (Grant, 1970), ammonoids (Furnish & Glenister, 1970; Kummel, 1970), ostracods (Sohn, 1970) and palynology (Balme, 1970). In 1974, Fatmi formalized the nomenclature of the rock sequence. He divided the Zaluch Group into three formations namely from bottom to top, the Amb, the Wargal and the Chhidru. Gee's maps of the Salt Range were printed by the Geological Survey of Pakistan in 1980. Haneef *et al.* (1981) published about the Wargal of the western Salt Range. Okimura (1988) and Okimura *et al.* (1985) described smaller foraminifera assemblages of the Wargal Formation and the Late Permian Tethyan realm respectively. The Pakistan-Japanese Research Group, P.J.R.G., (1985) analysed the



Zaluch, Nammal and Chhidru areas and presented further age-assignments. The Amb Formation is correlated in part with the Late Artinskian *Misellina* Zone in the Tethys and the overlying beds are considered to be compared to the Chisian *Cancellina* Zone. The Wargal Formation ranges from the Late Murghabian *Neoschwagerina margarites* Zone to Early Dzulfian. The Chhidru Formation as a whole is supposed to be of Late Dzulfian age. The Permian/Triassic boundary is placed now in between the lower and middle unit of the partly dolomitic Kathwai Member. The latter one contains the *Ophiceras connectens* characteristic of the Lower Triassic Griesbachian.

### THE SAKESAR SECTION

The studied area is to the north of Quaidabad along road through the mountain area towards Sakesar crossing Dhoda Wahan at the southern foot of the range (Fig 2). The section is located northeast of the road, about 1.9 km south of Sarai village; Salt Range Map 2 (Gee, 1980) approx. 32°30'50"/71°54'10" – 32°30'57"/71°54'09".

The measured thickness of the rock sequence of Sakesar Section (Fig. 3) amounts to about 230 m, the part of the exposed Wargal Formation is about 165 m.

The outcrop of Wargal Formation starts with sandy, bioclastic grainstones and rudstones with a lot of echinodermal debris, brachiopod valves and spines. Fusulinids and smaller foraminifera are rarely present. Sandy or non-sandy wackestones or floatstones are intercalated. Fragments of sponges occur and corals formed small *in situ* patches on the sea-floor. Sometimes bryozoans and cyanophytes stabilized the mud building up layers of bindstone. Chert nodules appear within burrowed echinodermal limestones. This whole is correlated to the second Unit of Wargal Formation, e.g., at Zaluch (P.J.R.G. 1985).

Overlying is a 11 m. thick series of laminated, partly dolomitic carbonates representing the third Unit. Chert layers still occur. Some detrital quartz grains are distributed. The origin of lamination is due to stromatolitic growth of cyanophytes. Fragmentation of certain beds are caused by subaerial exposure within an intertidal environment. Ostracods and foraminifera show a shallow lagoon. Echinodermal fragments are washed in.

The mass of Wargal Formation, often cliff-forming, is correlated to Unit 4 and 5. It consists of a variety of open marine, shallow subtidal bioclastic grainstones and rudstones. The most basal part is an intraclastic grainstone bearing foraminifera and dasycladaceans. The latter ones are distributed throughout, in some facies dominating the faunal content. Sandy intercalations as well as micritic parts are present. Within the upper part a second phase of coral, spongal and bryozoan growth initiated. Chert nodules are again associated. Marls became frequent.

The boundary between Wargal and Chhidru Formation is not very clear. An area of about 25 m is covered by alluvium. Presumably the boundary lies at the base or within the lower part of this gap. The Chhidru Formation is characterized by the amount of detrital quartz distributed. Sandy limestones and calcareous sandstones both sparitic and micritic with gastropods, echinoderms, brachiopods and bryozoans, foraminifera and algae are interbedded. The faunal amount decreases towards the top and within each sandy part. The top of Chhidru Formation is the so-called "White Sandstone Unit" composed of sandstones with a few echinodermal and bryozoan remains. The uppermost part is already cemented with a dolomitic sparite.

The Permian/Triassic boundary presumably does not coincide with that of Chhidru/



Mianwali Formation, but may divide the lower and middle part of Kathwai Member. Its basal part yielded up to 20% quartz. Echinoderms, brachiopods and bryozoans are still present. About one m, higher up, within the middle part, the quartz content ceased almost completely. Within the echinodermal dolomite a few glauconite grains appear increasing in number towards the ammonite bearing limestone beds of upper Kathwai Member.

#### The Algal Microflora of Sakesar Section

In the Sakesar Section the Upper Permian is represented by mainly calcareous marine formations sparsely interlayered with sandstones and dolomites.

The algae reported from this section are from a few samples (Fig. 3, 4). They belong to two distinct groups, Dasycladales (Chlorophyta) and Gymnocodiaceae (Rhodophyta) respectively. The genera and species are assigned to the families Seletonellaceae, Diploporeae and Dasycladaceae.

The Dasycladales of the Upper Permian includes different and rather numerous species. During the Murghabian *Mizzia cornuta* Kochansky & Herak (Plate I-1), *Mizzia yabei* (Karpinski) Endo (Plate I-7, III-2), *Diplopore pusilla* Kochansky & Herak (Plate I-8) and *Permoperplexella wargaliae* Dragastan et al. (Plate I-2, I-9) are present. During the Djulfian this algal group diminishes progressively its

importance. The species *Mizzia cornuta* Kochansky & Herak (Plate II-5) still occur. It seems to disappear concomitantly with *Imperiella* sp. (Plate I-6) and *Atractyliopsis* sp. (Plate II-3). The species described from the Sakesar Section of Late Djulfian age is *Mizzia indusensis* Dragastan et al. (Plate I-3, I-4).

The species of the gymnocodiacean family appeared at the base of the Upper Permian (Roux, 1986), but their acme and maximum spreading interval started with the Lower Djulfian followed by a progressive decline of the group during the Upper Djulfian. The species of *Gymnocodium bellerophonitis* (Rothpletz) Pia and *Permocalculus tenellus* (Pia) Elliott appeared at the exposed base of the Wargal Formation. The former is present throughout the samples studied (Plate II-1, II-2, II-3-II-5, II-6, III-3). The latter one (Plate I-3, III-1) although closely association is not detected within the samples 119 and 24. Both species are abundant during the Lower Djulfian. *Permocalculus fragilis* (Pia) Elliott (Plate II-1, III-5) appeared at the top of Wargal Formation and reached its maximum abundance at that time and probably disappeared during the Late Djulfian. The species *Permocalculus robustus* Dragastan et al. (Plate II-4, III-4) made its appearance within the Late Djulfian. This time span is characterized by a regressive tendency of distribution of gymnocodiaceans.

#### ACKNOWLEDGEMENTS

The research work was carried out with the financial support of the "Deutsche Forschungsgemeinschaft", the "Alexander von Humboldt-Stiftung" and the "Deutsche Akademische Austauschdienst". The Government of Pakistan provided the NOC. The fieldwork would not have been possible without the help of Prof. Dr. F.A. Shams, Director Institute of Geology, Punjab University, Lahore. Mr. M. Ilyas drove the jeep throughout the campaign.



## PLATE I

1. *Mizzia cornuta* Kochansky & Herak, 1960. Sample 44.
2. *Permoperplexella wargaliae* Dragastan et al., 1989. Sample 44.
3. *Permocalculus tenellus* (Pia, 1937) Elliott, 1955. Sample 121.
4. *Mizzia indusensis* Dragastan et al., 1989. Sample 30.
5. *Mizzia indusensis* Dragastan et al., 1989. Sample 30.
6. *Imperiella* sp., Sample 121.
7. *Mizzia yabei* (Kochansky, 1909) Endo, 1956. Sample 44.
8. *Diplopora pusilla* Kochansky & Herak, 1960. Sample 44.
9. *Permoperplexella wargaliae* Dragastan et al., 1989. Sample 44.

## PLATE II

1. *Permocalculus fragilis* (Pia, 1937) Elliott 1955 and *Gymnocodium bellerophontis* (Rothpletz, 1894) Pia, 1920. Sample 121.
2. *Gymnocodium-Permocalculus* facies community and *Tuberitina* sp. (upper left corner). Sample 121.
3. *Gymnocodium bellerophontis* (Rothpletz, 1894) Pia, 1920 and *Atractyliopsis* sp. (A). Sample 124.
4. *Permocalculus robustus* Dragastan et al., 1989. Sample 24.
5. *Gymnocodium bellerophontis* (Rothpletz, 1894) Pia, 1920 and *Mizzia cornuta* Kochansky & Herak, 1960. Sample 121.
6. *Gymnocodium bellerophontis* (Rothpletz, 1894) Pia, 1920. Sample 121.

## PLATE III

1. *Permocalculus tenellus* (Pia, 1937) Elliott, 1955. Sample 56.
2. *Mizzia yabei* (Karpinsky, 1909) Endo, 1956. Sample 44.
3. *Gymnocodium bellerophontis* (Rothpletz, 1894) Pia, 1920. Sample 119.
4. *Permocalculus robustus* Dragastan et al., 1989. Sample 24.
5. *Permocalculus fragilis* (Pia, 1937) Elliott, 1955. Sample 119.

## ACKNOWLEDGEMENTS

The research work was carried out with the financial support of the "Deutsche Forschungsgemeinschaft", the "Alexander von Humboldt-Stiftung", and the "Deutsche Akademische Austauschdienst". The Government of Pakistan provided the NOC. The fieldwork would not have been possible without the help of Prof. Dr. F.A. Shams, Director Institute of Geology, Punjab University, Lahore. Mr. M. Ilyas drove the jeep throughout the campaign.



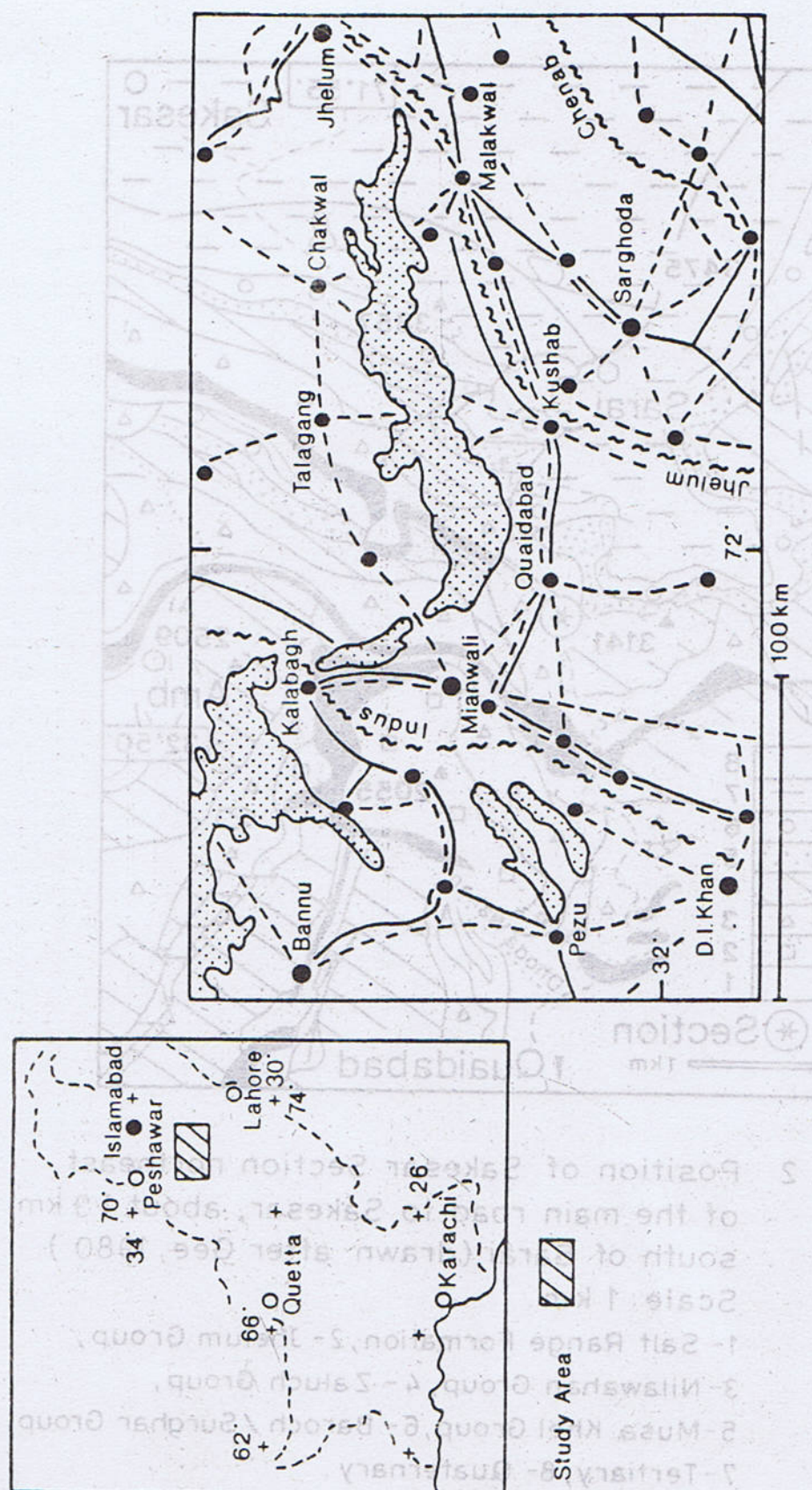


Fig. 1 Location Map of the Salt Range



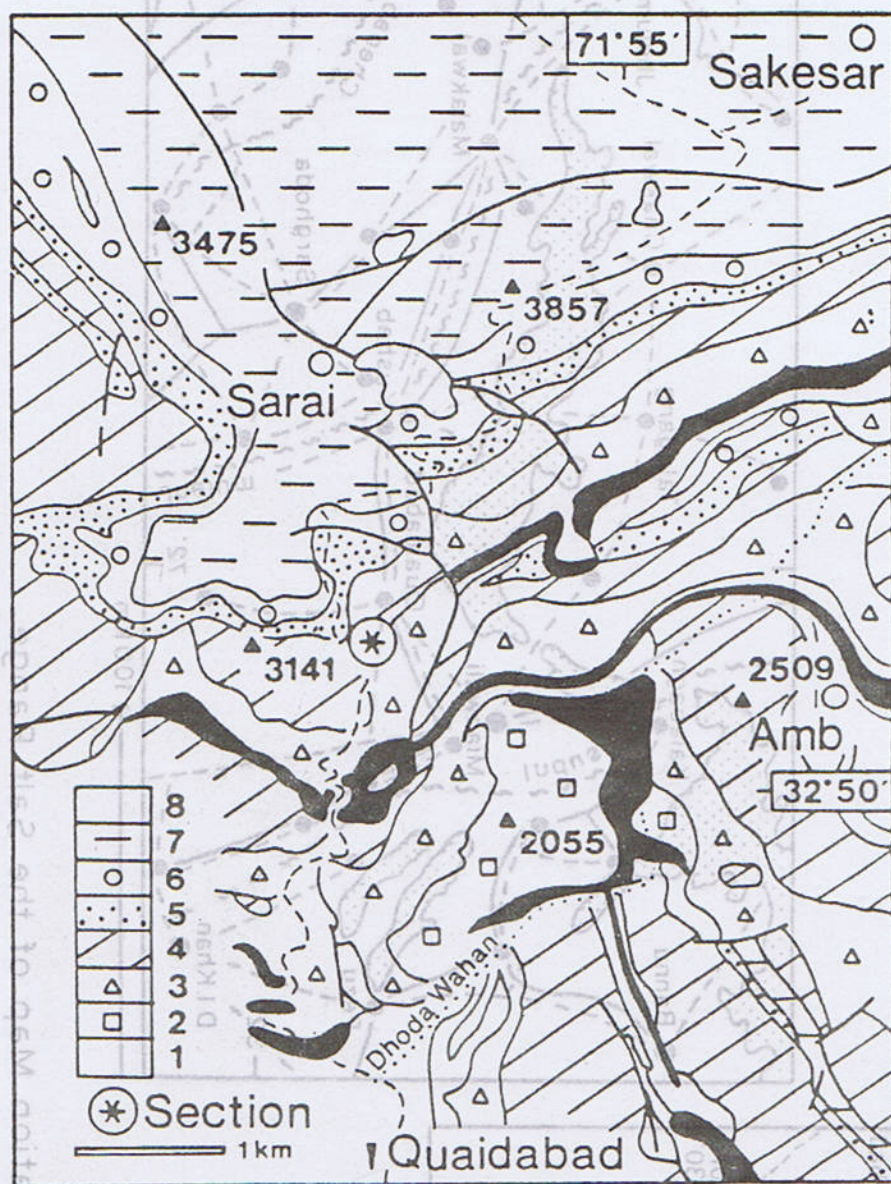


Fig. 2 Position of Sakesar Section northeast of the main road to Sakesar, about 1.9 km south of Sarai (drawn after Gee, 1980 ). Scale: 1 km.

- 1- Salt Range Formation, 2- Jhelum Group, 3- Nilawahan Group, 4 - Zaluch Group, 5- Musa Khel Group, 6- Baroch / Surghar Group, 7- Tertiary, 8- Quaternary.



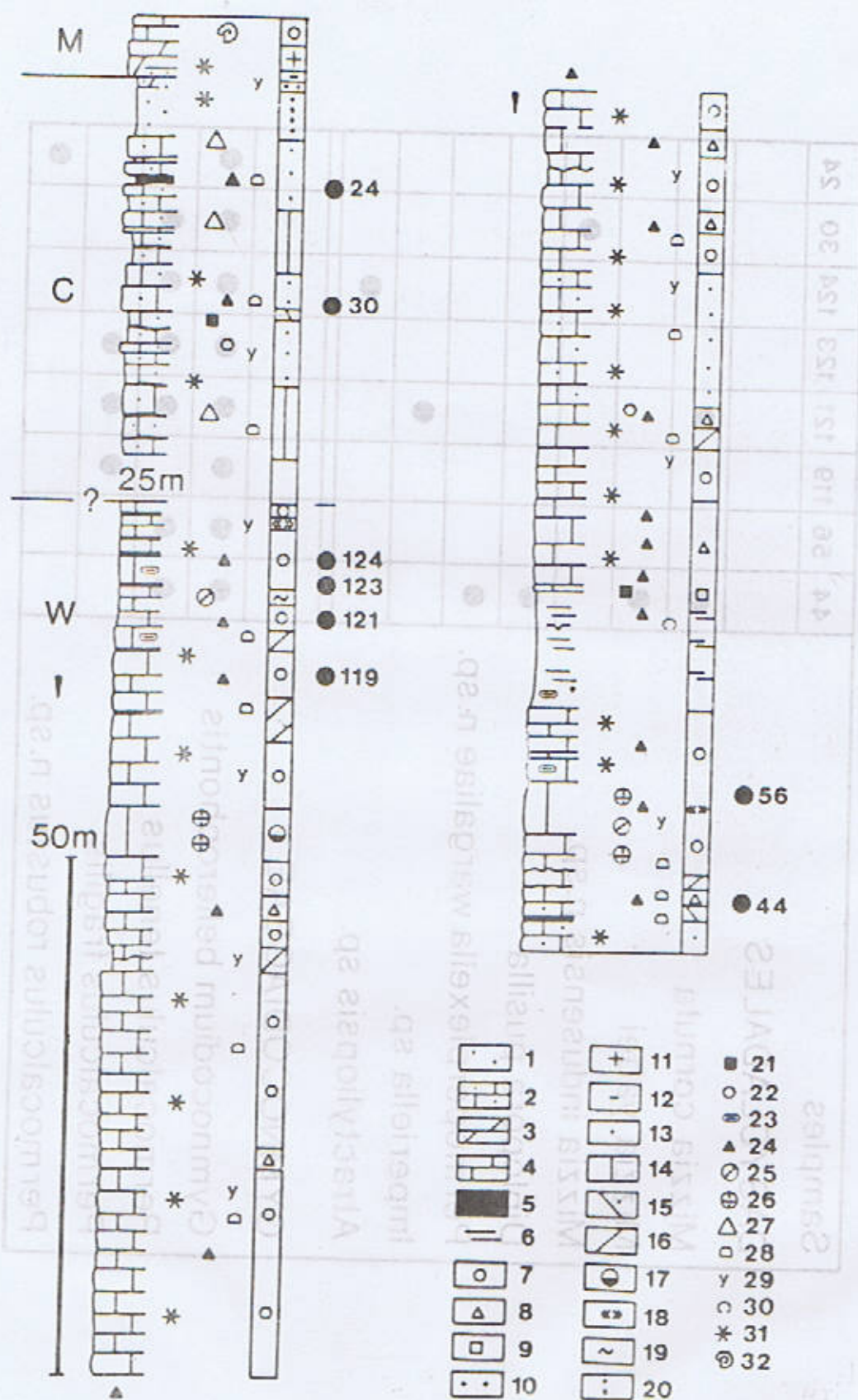


Fig. 3



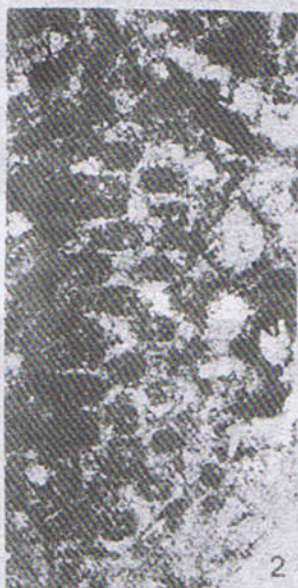
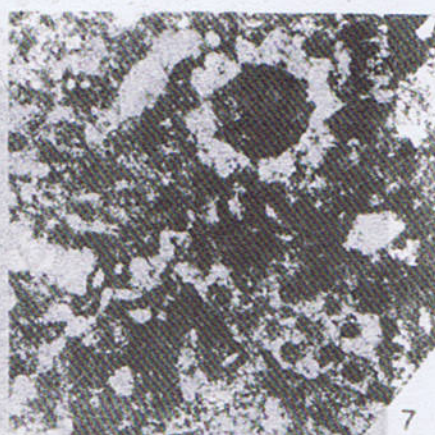
Samples	44	56	119	121	123	124	30	24
<b>DASYCLADALES</b>								
<i>Mizzia cornuta</i>	●		●					
<i>Mizzia yabei</i>	●							
<i>Mizzia indusensis</i> n.sp.								
<i>Diplopora pusilla</i>	●						●	
<i>Permoperplexella wargaliae</i> n.sp.	●							
<i>Imperiella</i> sp.			●					
<i>Atractyliopsis</i> sp.					●			
<b>GYMNOCODIACEAE</b>								
<i>Gymnocodium bellerophontis</i>	●	●	●	●	●	●	●	●
<i>Permocalculus tenellus</i>	●	●	●	●	●	●	●	
<i>Permocalculus fragilis</i>			●	●				
<i>Permocalculus robustus</i> n.sp.								●

Fig. 4 Distribution of dasycladacean and gymnocodiacean algae mentioned in Sakesar-Section, Salt Range.



x25

PLATE I





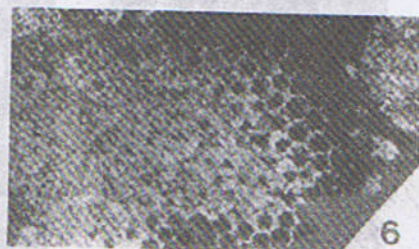
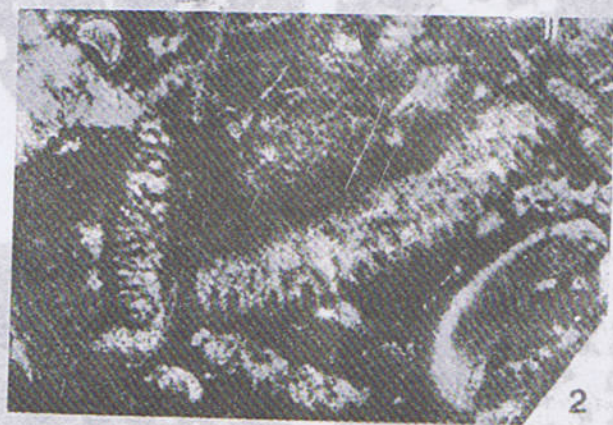




## PLATE 3





## REFERENCES

- Accordi, B., 1956. Calcareous algae from the Upper Permian of the Dolomites (Italy) with stratigraphy of the "Bellerophon Zone". *Journ. Pal. Soc. India*, 1, 75-84.
- Balme, B.E., 1970. Palynology of Permian and Triassic strata in the Salt Range and Surghar Range, West Pakistan. *Univ. Kansas, Spec. Publ.*, 4, 305-453.
- Dragastan, O., Mertmann, D. & Ahmed, S., 1989. Some algal species from the marine Permian deposits, Sakesar Section, Salt Range, Pakistan. *Rev. Paleobiol.*, (in press).
- Dunbar, C.O., 1933. Stratigraphic significance of the fusulinids of the Lower Productus Limestone of the Salt Range. *Rec. Geol. Surv. India*, 66, 405-413.
- Elliott, F.G., 1955. The Permian calcareous algae *Gymnocodium*. *Micropaleontology*, 1, 83-90.
- Elliott, F.G., 1968. Permian to Paleocene calcareous algae (Dasycladaceae) of the Middle East. *Bull. Brit. Mus. Nat. Hist. Geol., Suppl.* 4, 1-111.
- Elliott, F.J., 1970. New and little-known Permian and Cretaceous Codiaceae (calcareous algae) from the Middle East. *Paleontology*, 13, 327-333.
- Fatmi, A.N., 1974. Lithostratigraphic units of the Kohat-Potwar Province, Indus Basin, Pakistan. *Mem. Geol. Surv. Pakistan*, 10, 1-80.
- Flügel, E., 1966. Algen aus dem Perm der Karnischen Alpen. *Carinthia II, So.* 25, 1-76.
- Furnish, W.M. & Glenister, B.F., 1970. Permian ammonoid *Cyclolobus* from the Salt Range, West Pakistan. *Univ. Kansas Spec. Publ.*, 4, 155-175.
- Gee, E.R., 1947. Further note on the age of Saline of the Punjab and Kohat. *Proc. Nat. Acad. Sci. India*, 14, 95-154.
- Gee, E.R., 1980. Salt Range Maps. *Geol. Surv. Pakistan*.
- Gerth, H., 1950. Die Ammonoiten des Perm von Timor und ihre Bedeutung für die stratigraphische Gliederung der Perm-Formation. *N. Jb. Geol. Palaont. Abh.*, 91, 233-320.
- Grant, R.E., 1970. Brachiopods from Permian-Triassic Boundary Beds and age of Chhidru-Formation. *Univ. Kansas Spec. Publ.*, 4, 117-151.
- Haneef, M. et al., 1981. Sections of the Wargal Limestone, Western Salt Range, Pakistan. *Geol. Bull. Univ. Peshawar*, 14, 63-71.
- Kochansky, V. & Herak, M., 1960. On the Carboniferous and Permian Dasycladaceae of Yugoslavia. *Geoloski Vjesnik*, 13, 65-96.
- Kummel, B., 1970. Ammonoids from the Kathwai Member, Mianwali Formation, Salt Range, West Pakistan. *Univ. Kansas Spec. Publ.*, 4, 177-192.
- Kummel, B. & Teichert, C., 1966. Relations between the Permian and Triassic formations in the Salt Range and Trans Indus Ranges, West Pakistan. *N. Jb. Geol. Palaont. Abh.*, 125, 297-333.
- Kummel, B. & Teichert, C., 1970. Stratigraphy and paleontology of the Permian-Triassic Boundary Beds, Salt Range and Trans Indus Range, West Pakistan. *Univ. Kansas Spec. Publ.*, 4, 1-110.



- Middlemiss, C.S., 1891. Notes on the geology of the Salt Range with a re-considered origin and age of the Salt Marls. *Rec. Geol. Surv. India*, 24, 19-42.
- Noetling, F., 1894. On the Cambrian Formation of the Eastern Salt Range. *Rec. Geol. Surv. India*, 27, 71-86.
- Noetling, F., 1896. Beitrage zur Kenntniss der glacialen Schichten permischen Alters in der Salt Range, Punjab (India). *N. Jb. Miner. Geol. Palaont.*, 2, 61-68
- Noetling, F., 1900. Notes on the relationship between the Productus Limestone and the Ceratite Formation of the Salt Range. *Report Geol. Surv. India*, 1899/1900, 173-183.
- Okimura, Y., 1988. Primitive colaniellid foraminiferal assemblage from the Upper Permian Wargal Formation of the Salt Range. *J. Paleont.*, 62, 715-723.
- Okimura, Y. et al., 1985. Biostratigraphical significance and faunal provinces of Tethyan late Permian smaller foraminifera. *The Tethys*, 111-132.
- Pakistani-Japanese Research Group, 1985. Permian and Triassic Systems in the Salt Range and Surghar Range, Pakistan. *The Tethys*, 221-312.
- Reed, F.R.C., 1931. New fossils from the Productus Limestone of the Salt Range with notes on other species. *Pal. Indica*, N.S. 17, 1-56.
- Roux, A., 1985. Introduction a l'etude des algues fossiles paleozoiques (de la bacterie a la tectonique des plaques). *Bull. Centr. Rech. Explor. Prod. Elf-Aquitaine*, 9, 465-699.
- Roux, A., 1986. Microfiores algaires paleozoiques (tendances evolutives, repartitions) et tectonique globale. *Bull. Centr. Rech. Explor. Elf-Aquitaine*, 10, 555-563.
- Schindewolf, O.H., 1954. Uber die Faunenwende vom Palaozoikum zum Mesozikum. *Z. dt. geol. Ges.*, 105, 154-183.
- Sohn, I.B., 1970. Early Triassic marine ostracodes from the Salt Range and Surghar Range, West Pakistan. *Univ. Kansas Spec. Publ.*, 4, 193-206.
- Sweet, W.C., 1970. Uppermost Permian and Lower Triassic conodonts of the Salt Range and Trans Indus Ranges, West Pakistan. *Univ. Kansas Spec. Publ.*, 4, 207-275.
- Waagen, W., 1884. Salt Range Fossils IV, 1-Geological results. *Pal. Indica*, Ser. 13, IV, 1-242.
- Wittaker, E.J. et al., 1979. Further remarks on the micropaleontology of the late Permian of eastern Burma. *Notes Lab. Paleont. Univ. Geneve*, 5, 11-18.
- Wynne, A.B., 1875. The Trans Indus Salt Range in the Kohat District. *Mem. Geol. Surv. India*, 11, 101-330.
- Wynne, A.B., 1878. On the Geology of the Salt Range in the Punjab. *Mem. Geol. Surv. India*, 14, 1-309.
- Zaninetti, L. et al., 1978. Microfacies et microfaunes du Permien au Jurassique au Kuh-e-Gahkm, Sud-Zagros, Iran. *Riv. Ital. Paleont.*, 84, 865-896.
- Zaninetti, L. et al., 1981. Foraminiferes et biostratigraphie dans le Permien superieur du Taurus oriental, Turquie. *Notes Lab. Paleont. Univ. Geneve*, 7, 1-36.



## GEOTECHNICAL ASPECTS OF THE DHOK PATHAN FORMATION AT THE KALABAGH DAM SITE

BY

M.H. MALIK and SAEED FAROOQ

Institute of Geology, Punjab University, New Campus, Lahore-20, Pakistan

**Abstract :** The claystone/siltstone samples obtained from the Dhok Pathan Formation of the Siwalk Group at proposed Kalabagh Dam Site were thoroughly investigated to find out their index values. The concerned data have been collected from the previous studies through the boreholes, drillholes and trenches excavated for investigations. For frequency of jointing, the data were limited to outcrops and trenches only. The Dhok Pathan Formation (alternate sandstones and claystones) exposed in the area of study has been divided into different beds in their stratigraphic order. These are designated negative numbers for siltstone/claystone and positive numbers for alternate sandstone beds. The maximum exploration depth in the area is upto bed 9, while data upto bed-7 has been analysed and presented. The claystone/siltstone beds between two sandstone beds are given numbers by the reference sign as prefix. Beds 3 to 9 are exposed on the left bank, while beds 1 to 4 are exposed on the right bank of the Indus River. The graphical correlation and presentation of index values could be utilized for the quick assessment of the strength characteristics of the materials occurring at different horizons. The study also reveals that the angle of residual friction decreases with increase in clay fraction and claystones exhibit greater intensity or frequency of jointing with higher index values.

### INTRODUCTION

The Kalabagh Dam Site is located in the western extremity of the Salt Range about 20 km northeast of Kalabagh Town. For the proposed dam, this area has been under investigation for the last thirty years. The present study is concentrated at systematic evaluation of index properties and related to strength of fine grained materials occurring at different elevations. Data from various boreholes, drill-holes and trenches have been used to collect information regarding index properties and engineering behaviour of soil and rock strata. For study of intensity of jointing and shearing in claystone, data collected only from trenches and natural outcrops.

The sediments of the Dhok Pathan Forma-

tion (upper part of the middle Siwalik) cover the project area flanking the Indus River. These rocks are composed of alternate Sandstone and claystones/siltstones with lenses and layers of gravels. Beds have very low dip (3-5 degrees) towards north.

The geological sequence at the site is as under :

River Channel Deposits

Terrace Deposits

Dhok Pathan Formation

The channel and terrace deposits consist of fresh sand, gravels, cobbles and boulders of igneous, metamorphic and sedimentary origin with silty sand matrix.



The gravels mixed with silt, sand and clay overlying Dhok Pathan Formation at places are alluvial gravels which are reworked and derived from the pre-existing Siwaliks in the upper parts of the depositional basin (Taseer, 1979).

The sandstone beds of the Dhok Pathan Formations vary in thickness from a few feet to about 300 feet and are friable with occasional harder ribs, containing varying amounts of cementation material.

The claystones are over consolidated sediments with medium plasticity (plasticity index ranging from 8 to 30), while the siltstones have little plasticity. The presence of shear zones in the claystones render a great difference in the intact and residual strength parameters. The claystone/siltstones have varied clay fraction (.002) which can be related with the plasticity, angle of residual friction and intensity of fracturing within them (Figs. 4, 5 & 6).

An attempt has been made to collect bed-wise data in the stratigraphic order and to present a correlation between index values varying with depth. This bed-wise graphical correlation has been helpful in knowing not only the variation in index values but also gives a quick idea about the corresponding variation in strength characteristics.

The present study gives only the broad pattern about strength parameters or jointing. However, thorough and precise evaluation of these parameters, particularly, at the levels where these materials are going to serve as foundations, is inevitable for the design criterion.

## INDEX PROPERTIES

The particle size distribution and Atterberg Limits were plotted for each claystone/siltstone bed, and an attempt was made to correlate these index values with the strength parameters.

The variation of index properties with depth in the stratigraphic column at regular intervals (about 1 foot) is presented in the form of graphs for an ease in correlation and interpretation (Fig. 2 & 3). Only the data regarding the weak bed rock strata (claystones/siltstones) are correlated and presented because of their significance to serve as foundation materials. The sandstone beds were simply considered for their particle size distribution by virtue of their non plastic nature.

For grain size analysis in claystones/siltstones, only the percentage of clay and silt passing sieve 200 is plotted, whereas the percentage of less than 0.002 mm size is considered as clay fraction.

The Atterberg Limits of claystone/siltstone beds and their corresponding clay fraction are very well correlated, indicating the well known relationship of grain size with the limits (Fig. 2-3). However, the sudden decrease noticed in clay fraction and the corresponding limits in some places within the claystone/siltstone beds, is attributed to the presence of small sandy patches and lenses (Fig. 3a & b).

A number of samples taken from trenches were tested for residual strength which was then plotted against clay fraction (Fig. 6). As can be seen from this figure, there is a gradual decrease in angle of residual friction ( $\phi_{rf}$ ) with increase in clay fraction. Another attempt was made to find out any relation of frequency of jointing and clay fraction in the claystone/siltstone beds. The study carried out in trenches etc. reveals this relation as given in figure 4. Since the data is restricted to only six beds, the relationship is not very pronounced, although, there is a general tendency of an increase in joint frequency with the increase in clay fraction.



Figure 5 shows relation of average values of clay fraction and average plasticity index of various beds. Invariable in all cases there exists a linear relationship between these two i.e. plasticity index increases with increase in clay fraction.

For correlation purposes, data from a number of boreholes and trenches encountering different beds were cumulatively plotted (Fig. 2 & 3). The variation of index properties in different beds is given as under :

**BED-1.** Fines passing 200 sieve range from 77% to about 93% and clay fraction is 5 to 35%. The corresponding values of liquid limit, plastic limit and plasticity index are 33 to 41, 23 to 28 and 10 to 17 respectively. At the bottom of bed-1, lower values of limits indicate the transitional contact with sandstone.

**BED-2.** Fines vary from 58 to 92% with a sandy patch in the middle of the bed. The clay fraction varies from 18 to 53% while L.L., P.O. and P.I. are of the order of 35 to 40, 20 to 30 and 10 to 15 respectively.

**BED-3a.** In the centre of the bed, low index values indicate a lens of sandstone while fines in the rest of the bed fluctuate from 73 to 99%. The value of clay fraction is 23 to 53% whereas L.L., P.L. and P.I. vary 33 to 51, 20 to 38 and 12 to 21 respectively.

**BED-3b.** The percentage of fines throughout the bed range from 88 to 94 and maximum values are found in centre while decrease on either side. The value of clay fraction is from 23 to 46, liquid limit 32 to 46, plastic limit 26 to 30 and plasticity index is 12 to 20.

**BED-4a.** This is a very thin bed and lower part consists of fairly large amount of sand which is about 24 to 48%. In the lower part of the bed, the percentage of fines is something like 59 to 76 whereas clay fraction is 22 to 33%.

The values of limits are as follows : liquid limit 18 to 23, plastic limit 21 to 32 and plasticity index 12 to 20.

**BED-4b.** Test results indicate the higher percentage of silt and clay in the middle of the bed, 62 to 100, with clay fraction 7 to 41% and decreases on either side. The range of liquid limit, plastic limit and plasticity index is 25 to 44, 19 to 34 and 16 to 22 respectively.

**BED-5.** From the test data it is evident that fines are maximum in the middle and lower percentage is found towards upper and lower contact. The fines and clay fraction vary from 72 to 78% and 28 to 40% respectively in the central portion whereas, near the top and bottom material is non-plastic. The Atterberg limits range as : L.L. 31 to 52, P.L. 23 to 32 and P.I. 12 to 20.

**BED-6.** It is quite clear from the test results that low index values indicate three sandstone lenses in the upper part of the bed and lower part consists of large amount of sand as well. The fines in the upper portion excluding sandstone lenses are very high, i.e. 80 to 100% with clay fraction 23 to 52%. The corresponding values of L.L. ; P.L. and P.I. vary from 43 to 63, 28 to 32 and 15 to 29 respectively.

## CONCLUSION

The correlation and interpretation of data from different claystone/siltstone beds at different depths reveals the significance of index properties in assessment of strength parameters. As the Atterberg Limits and grain size affect these parameters, the claystone beds with higher values of clay fraction and the Limits, will need thorough investigations. The study of joints and shear zones in claystone/siltstones (in trenches only) indicates that the beds with higher index values have greater intensity of jointing and shearing.



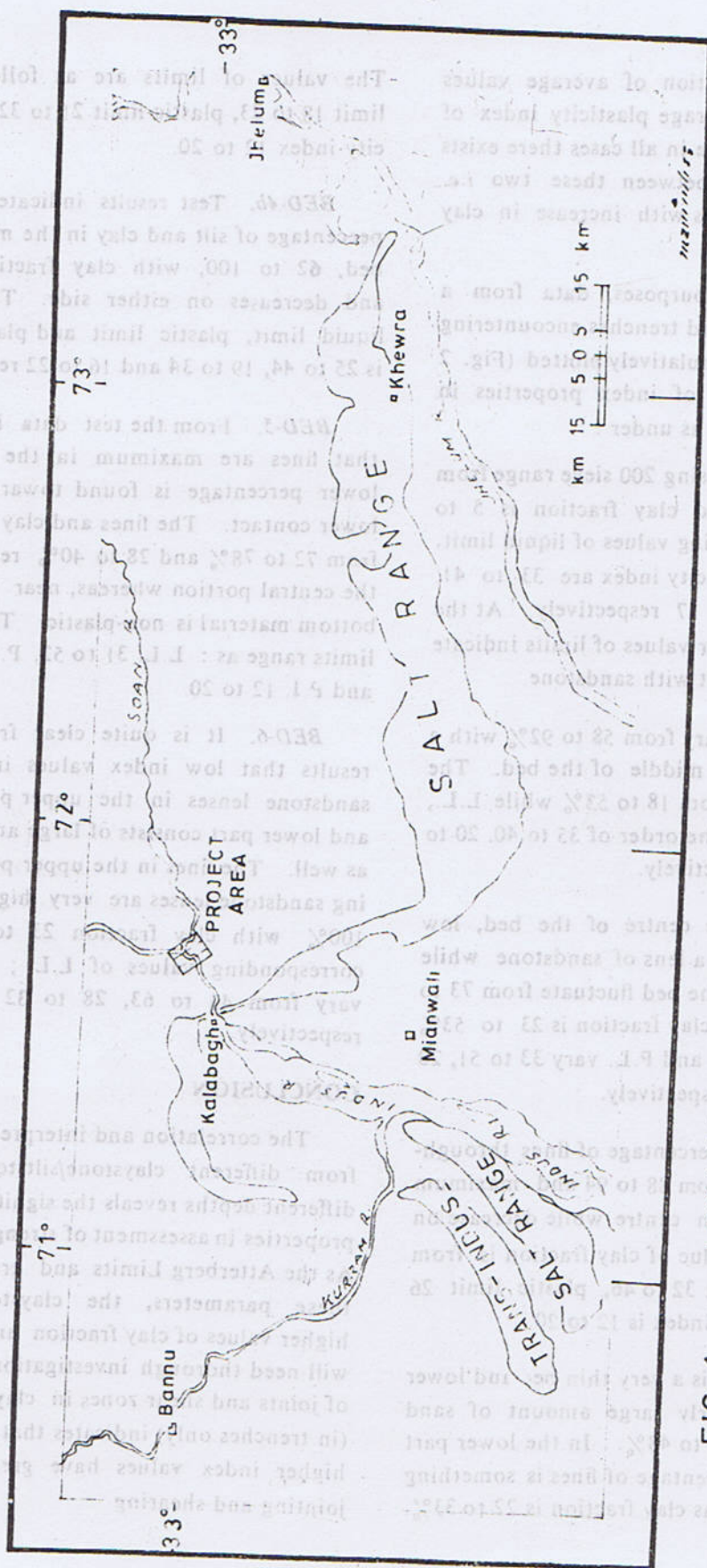
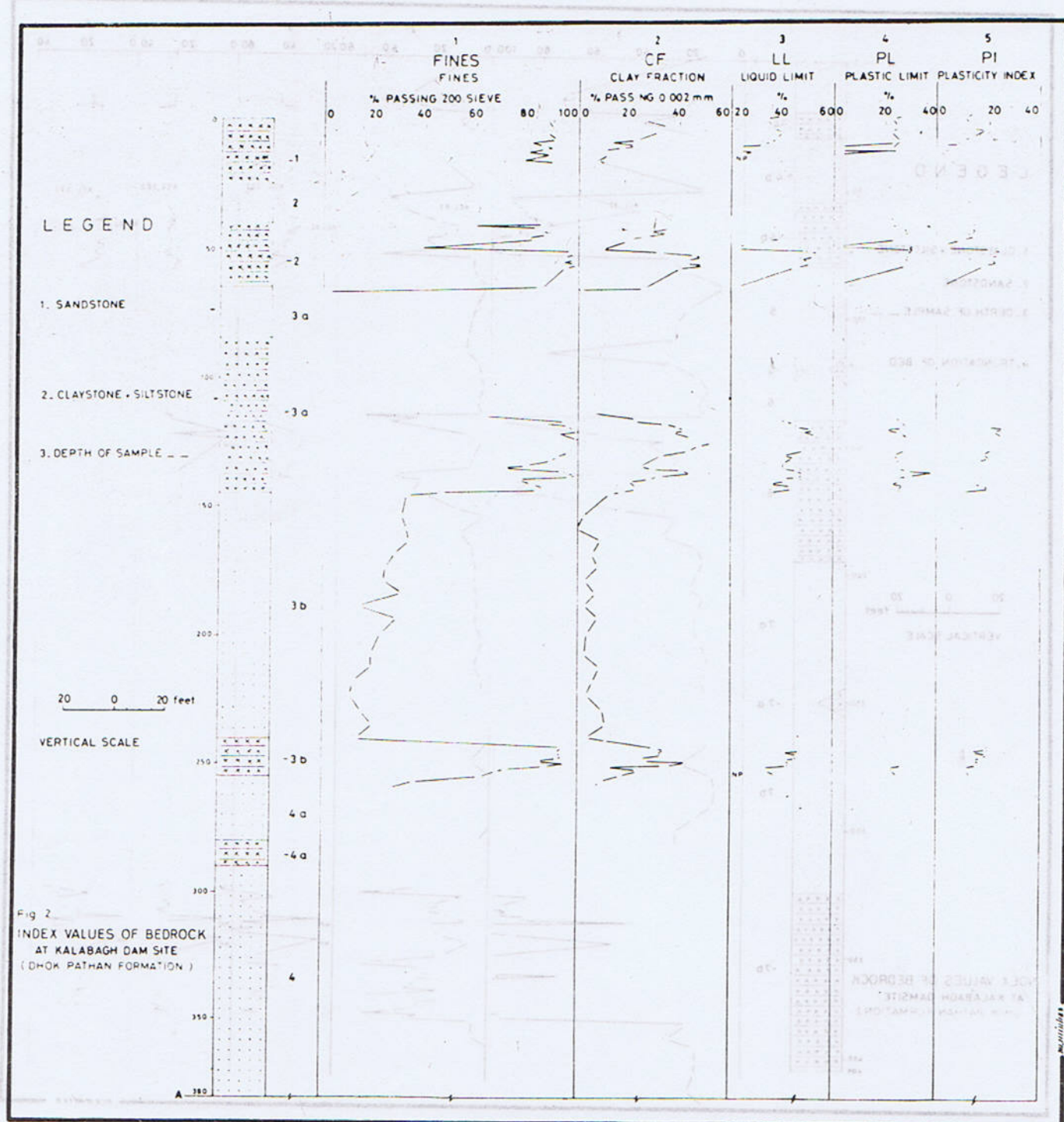
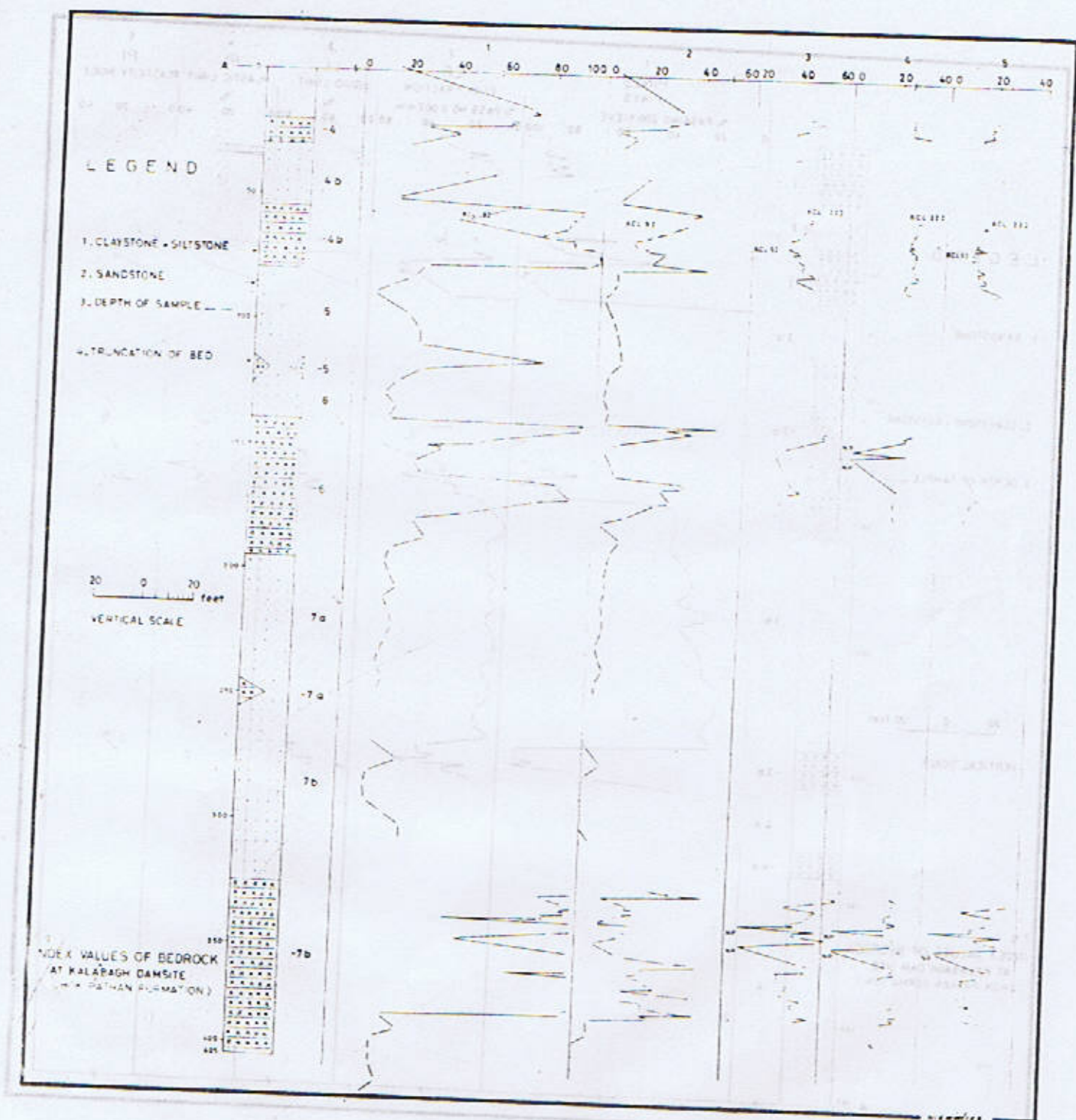


FIG. 1. LOCATION MAP OF PROJECT AREA











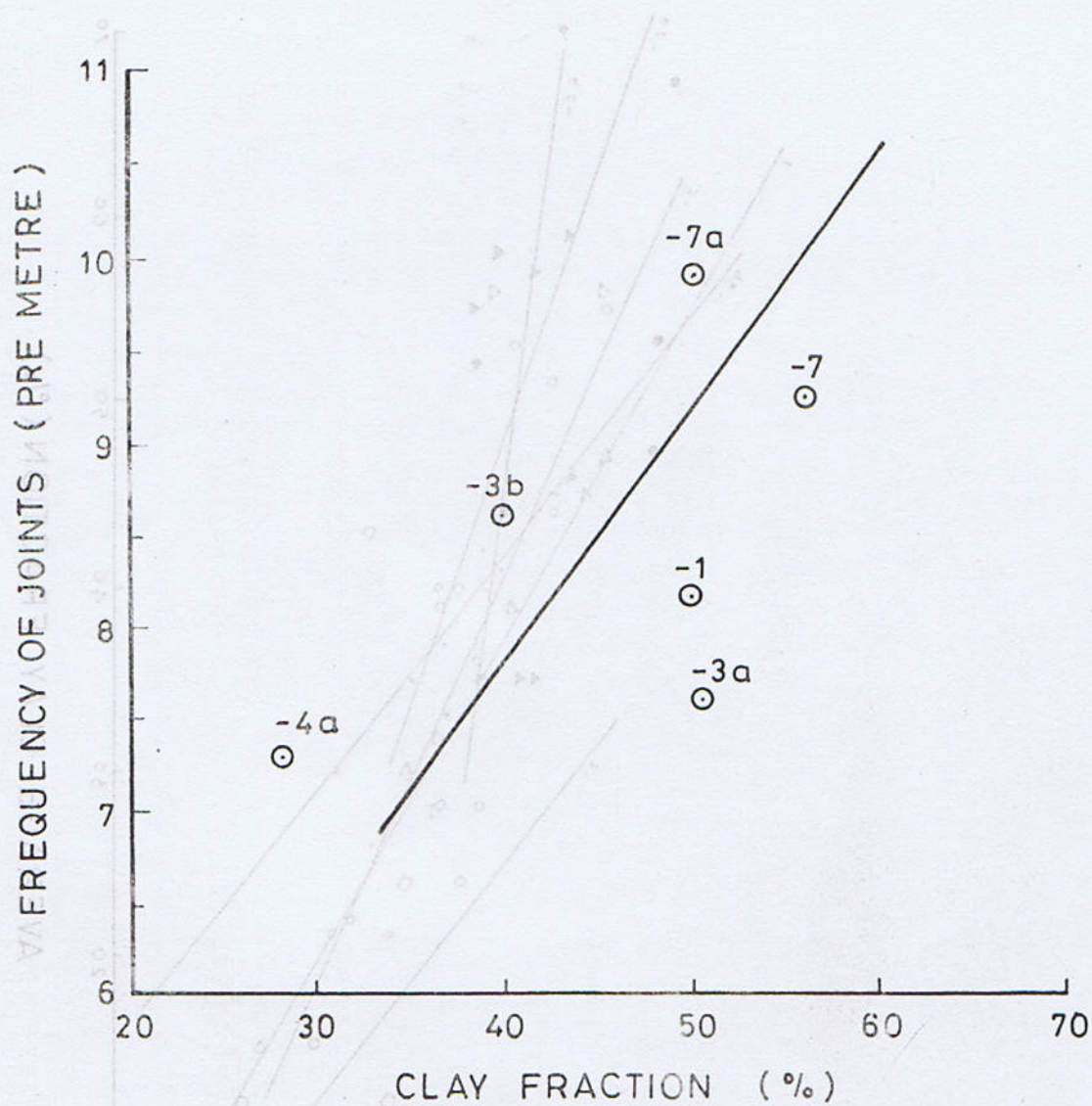
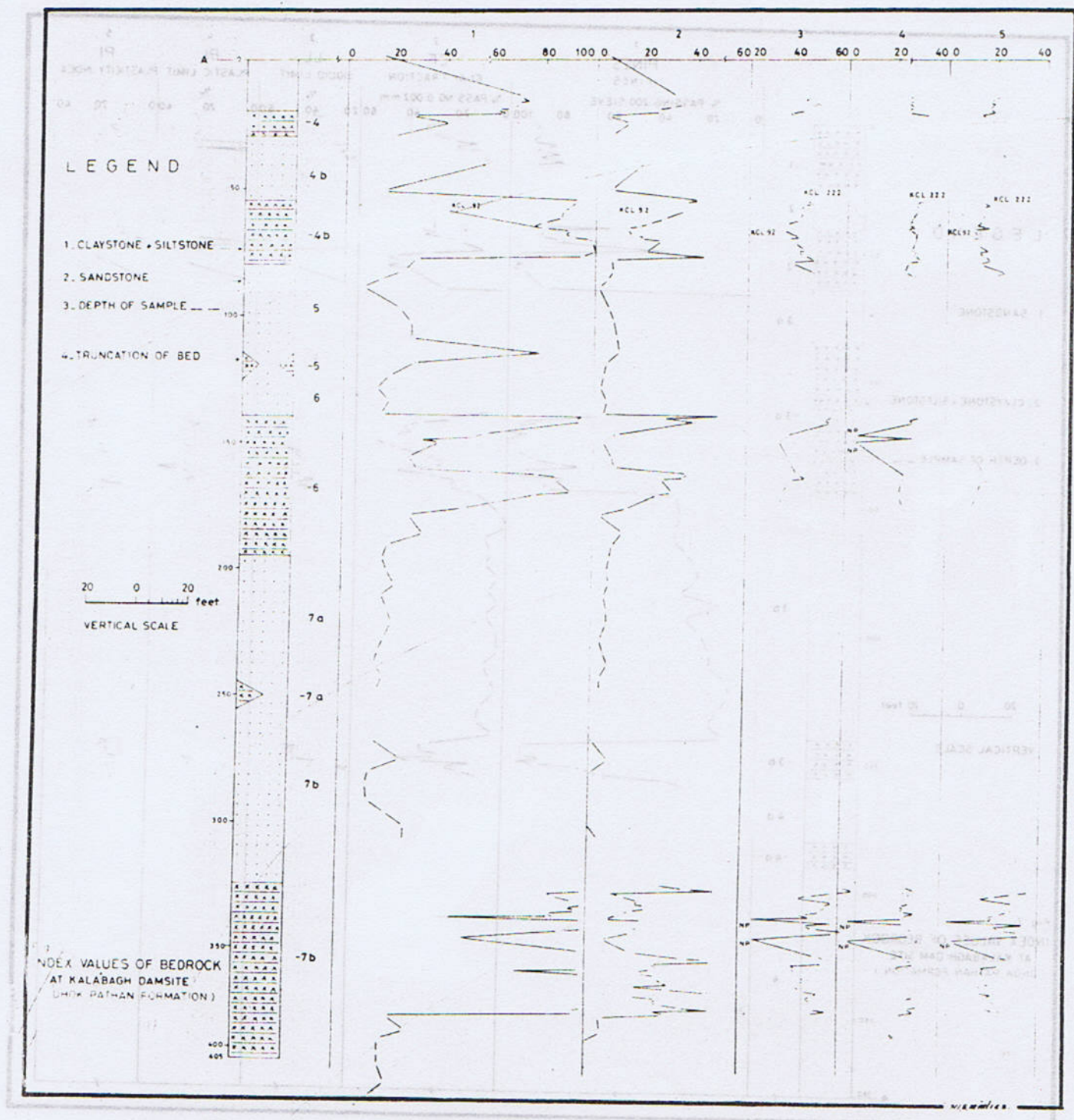


FIG. 4. RELATIONSHIP BETWEEN C.F. AND JOINT FREQUENCY IN CLAYSTONE BEDS.







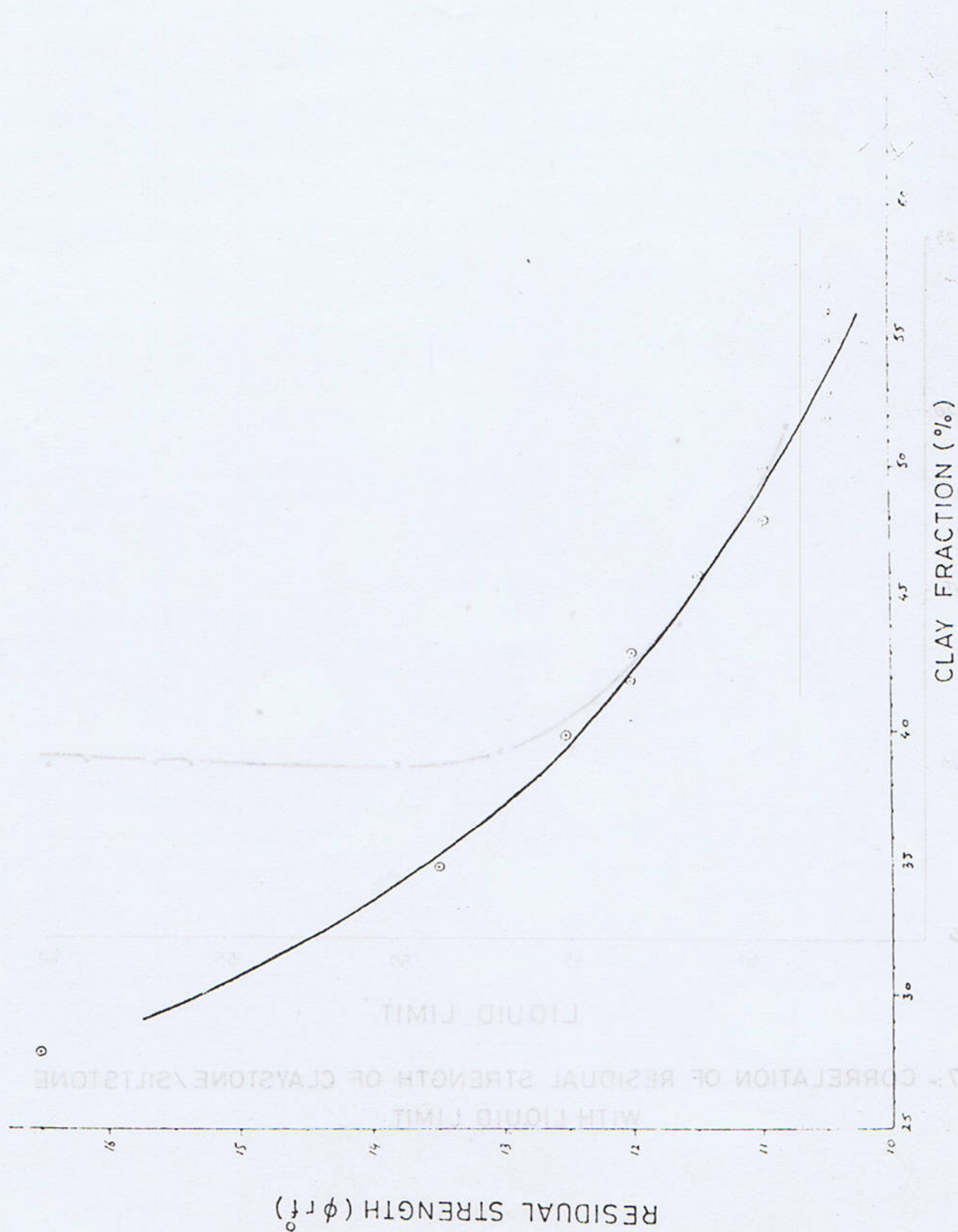


Fig. 6:- RELATIONSHIP BETWEEN CLAY FRACTION AND  $\phi_{rf}$  IN CLAYSTONE BEDS



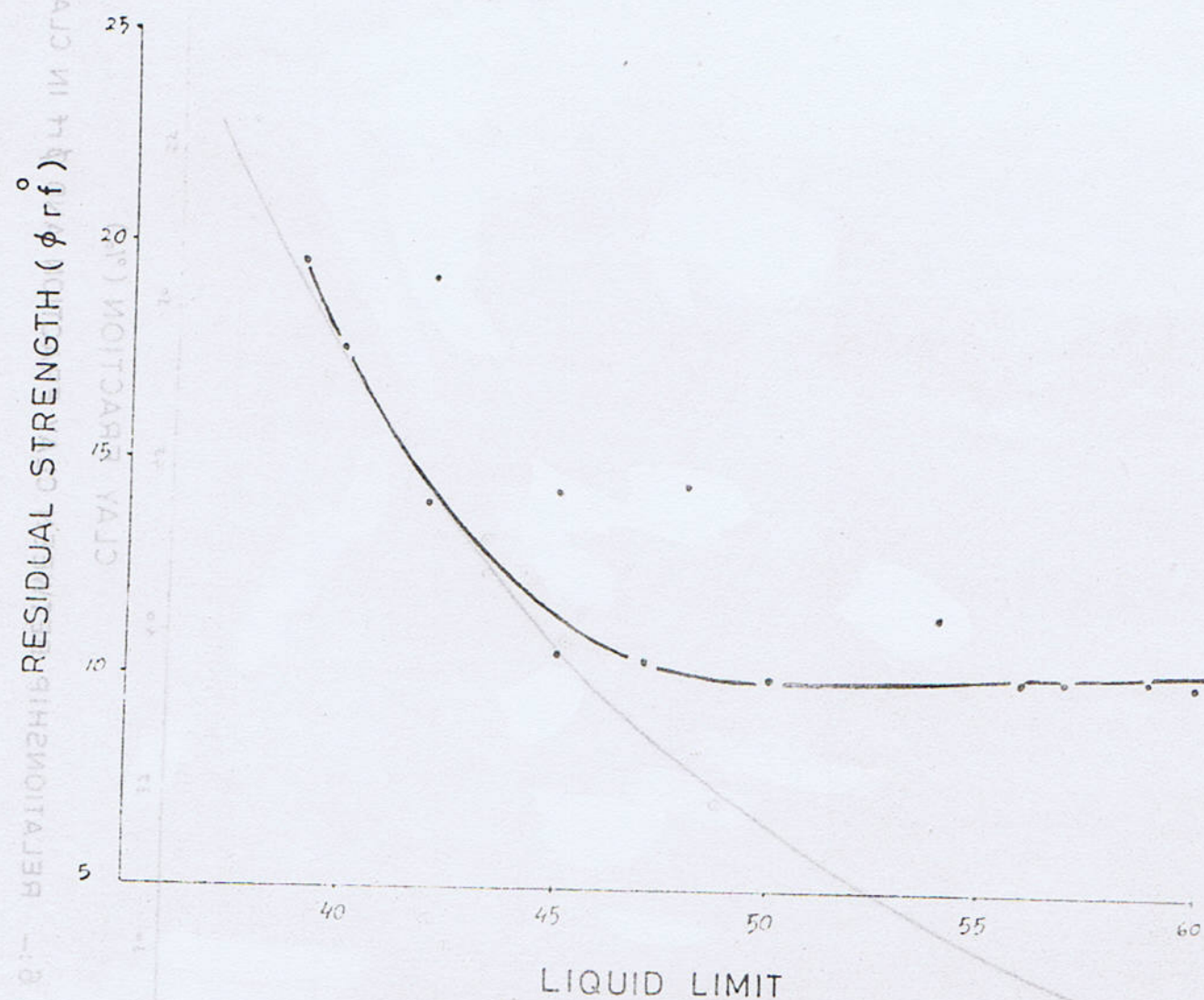


Fig.7:- CORRELATION OF RESIDUAL STRENGTH OF CLAYSTONE/SILTSTONE WITH LIQUID LIMIT



## REFERENCES

Geology and Geo-Technical Assessment at Kalabagh Dam Project 1983. Kalabagh Consultants. Report unpublished.

Taseer, S.H., Morthe, J., Shah, S.M.I., West, R.M., and Lukacs, J. R., 1989. Neogene stratigraphy and Fossil Vertebrates of the Daud Khel Area, Mianwali District, Pakistan. *Mem. Geol. Surv. Pakistan*. 13, 1-27.

F. A. SHAMS

Institute of Geology, Punjab University, Lahore-20, Pakistan.

**Abstract:** The surface texture study of feldspar grains of Soan Formation of Pleistocene age from Potwar Plateau, Pakistan under scanning electron microscope revealed that most of the surface features were developed by glaciation, which were later on attacked by chemical etching during transportation or deposition.

## INTRODUCTION

Surface features of two feldspar grains of Soan Formation of Pleistocene age from Sukho section of Jhelum district (Potwar Plateau), Punjab, Pakistan were studied on scanning electron microscope (SEM) and black and white polaroid pictures with magnification of 200X, 300X and 1500X, prepared at Kyoto University, Mineralogy Laboratory, Kyoto, Japan.

## Laboratory Procedures

For the study of surface features of feldspar grains under scanning electron microscope, the grains were separated from the disaggregated sand of the Soan Formation, with the help of a wet tiny brush and needle, under the binocular microscope. After the separation, the grains were washed with water and mounted on the surface of small metallic disc with the help of double sided adhesive plastic tape.

Before study under SEM, gold-coating of grains was necessary to make them good conductors of electricity. For this purpose the mounted grains were placed in the gold-coating

machine. Purplish red colour in the bell-jar of the machine showed that coating was proceeding. The coating was continued for about 4 minutes, under conditions of 1200 V and 5-10 mA.

## Scanning Electron Microscopy

The scanning electron microscope (SEM) has been recently used to study a wide variety of objects (e.g., Smith and Catley, 1953; Thornton, 1963; Hay and Sandburg, 1967, 1968; Krineley and Margolis, 1969). Its wide range of magnification (about 15x to 50,000x), the ability to examine entire specimens rather than restricted portions of objects, such as sand grains, and great depth of field make it an extremely valuable tool for studying surface textures. Additionally, it is not necessary to construct a replica (The preparation of replicas has been described in detail by Rochow and Others, 1960; Haine, 1961; and Key, 1961). Surface can be examined directly, thus saving a great deal of time, and simplifying interpretation. The construction of a sand grain replica is a time consuming, rather complicated



# STUDY OF SURFACE FEATURES OF FELDSPAR GRAINS OF PLEISTOCENE SANDSTONES FROM POTWAR, PAKISTAN

BY

M. SALEEM BAJWA

Geological Survey of Pakistan, Quetta Pakistan.

and

F. A. SHAMS

Institute of Geology, Punjab University, Lahore-20, Pakistan.

**Abstract :** *The surface texture study of feldspar grains of Soan Formation of Pleistocene age from Potwar Plateau, Pakistan under scanning electron microscope revealed that most of the surface features were developed by glaciation, which were later on attacked by chemical etching during transportation or deposition.*

## INTRODUCTION

Surface features of two feldspar grains of Soan Formation of Pleistocene age from Sukho section of Jhelum district (Potwar Plateau), Punjab, Pakistan were studied on scanning electron microscope (SEM) and black and white polaroid pictures with magnification of 200X, 300X and 1500X, prepared at Kyoto University, Mineralogy Laboratory, Kyoto, Japan.

## Laboratory Procedures

For the study of surface features of feldspar grains under scanning electron microscope, the grains were separated from the disaggregated sand of the Soan Formation, with the help of a wet tiny brush and needle, under the binocular microscope. After the separation, the grains were washed with water and mounted on the surface of small metallic disc with the help of double sided adhesive plastic tape.

Before study under SEM, gold-coating of grains was necessary to make them good conductors of electricity. For this purpose the mounted grains were placed in the gold-coating

machine. Purplish red colour in the bell-jar of the machine showed that coating was proceeding. The coating was continued for about 4 minutes, under conditions of 1200 V and 5-10 mA.

## Scanning Electron Microscopy

The scanning electron microscope (SEM) has been recently used to study a wide variety of objects (e.g., Smith and Catley, 1955; Thornton, 1965; Hay and Sandburg, 1967, 1968; Krineley and Margolis, 1969). Its wide range of magnification (about  $15\times$  to  $50,000\times$ ), the ability to examine entire specimens rather than restricted portions of objects, such as sand grains, and great depth of field make it an extremely valuable tool for studying surface textures. Additionally, it is not necessary to construct a replica (The preparation of replicas has been described in detail by Rochow and Others, 1960; Haine, 1961; and Key, 1961). Surface can be examined directly, thus saving a great deal of time, and simplifying interpretation. The construction of a sand grain replica is a time consuming, rather complicated



process, thus precluding the possibility of examining large number of grains, many introduce artifacts and distortion, and may not reproduce all of the original detail on the specimen. Replicas are notoriously fragile; 30 to 40% of specimens prepared may be unusable. It is usually difficult to determine, what portion of the grain is being observed with the transmission electron microscope (TEM), for low power magnification, about 200X, may not enable observation of the entire grain. Only half the grain is commonly replicated, and about 40% of that surface is supported on grid bars, where it cannot be observed. Only one or two grain surfaces can be mounted on one specimen grid and observed at a given time (Krinseley and Margolis, 1969).

These problems can be eliminated with the scanning electron microscope (SEM). Grains are observed directly without the need for replication, thus avoiding most artifacts and distortion. Much more detail can be seen with SEM, indicating that many small features are not observed, or are somewhat distorted with the replica method, e.g. V-shaped dents seem something elevated instead of depression in the TEM picture (Pl. 1, 2). A number of grains can be directly observed at one time with the SEM, permitting selection of a particular grain to be zoomed at, and photographed at high magnification. Finally, depth of focus and certain other SEM features give a simulated three-dimensional photograph that simplifies interpretation.

## EXPLANATION OF SEM PICTURES

### PLATE 1

1-A (500 X). Feldspar grains, from Soan sandstone of Sukho section (106S-3). Note the angular corners of the grains. Some corners have become rounded

due to diagenetic processes. Twinning of feldspar is also visible. The surface shows marks of glaciation and chemical etching.

1-B (1500 X). Enlarged view of the same grain. Note many pits and flower type structures, formed due to glaciation and chemical etching.

1-C (1500 X). Enlarged view of a different portion of the same grain. Surface shows effects of glaciation and chemical etching, represented by many pits and flower type structures. Parallel lines of twinning are also visible.

### PLATE 2

2-A (200 X). Picture includes two grains, very angular, the right one feldspar and the left one quartz, of Soan sandstone, from Sukho section (106S-3). Note the very angular edges of the grains. Some corners have been rounded off by diagenetic processes, during transportation of the grains.

2-B (1500 X). Enlarged view of the right hand feldspar grain. Note the effects of chemical etching on the left side of the picture. The right side of the picture exhibits a freshly broken surface, may be due to diagenesis. The feldspar twinning is clearly visible.



Study of surface textures of two feldspar grains of Soan Formation of Pleistocene age, from Sukho section of Jhelum district revealed that most of the features were developed by glaciation which were later on attacked by chemical etching during transportation or deposition. Surface features included pits, lines and flower type structures (Pls. 1, 2, 1-A-C, 2A-B). Pits and lines were developed by glaciation, whereas flower type structures by chemical etching. Lines of twinning are also visible in the pictures. The grains had angular edges, some of which were rounded off by

diagenetic processes, during transportation by stream.

Some early workers, e.g. Porter (1962); Krinsley (1962b, 1968b, c); Krinsley and Takashashi (1962a, b, c; 1964); Krinsley and Newman (1965); Harvey (1966); Margolis (1966a, b; 1968, 1970); Hay and Sandberg (1967); Sautendam (1967); Krinsley and Donahue (1968a, b, c); Hideo Mii (1972a, b); Setlow and Karpovich (1972); Blackwelder and Pilkey (1972); Read (1973); R.S. Chaudhri (1986) and Bajwa, Shams, Shik and Kamiya (1989a) also observed similar surface textures during their studies (Tab. 1, Figs. 1, 2).

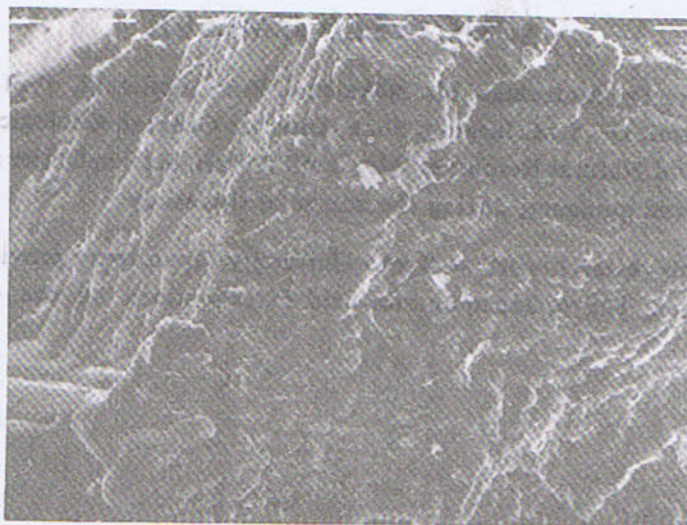
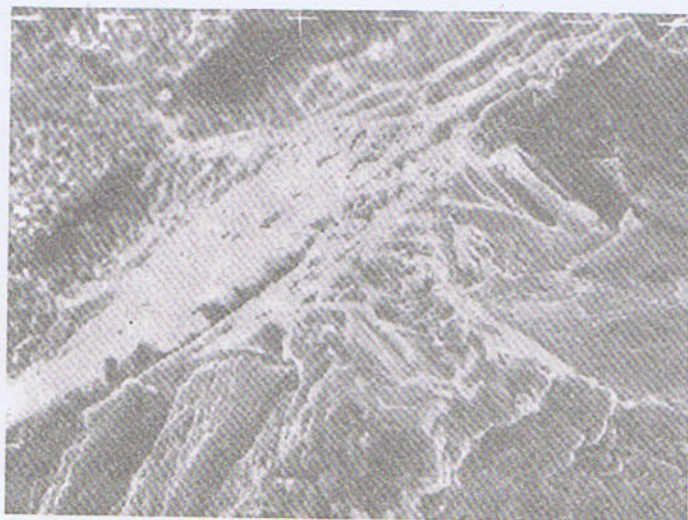
### ACKNOWLEDGEMENTS

Thanks are due to Dr. Matsumae, Mr. Nakajema, Prof. Fujimaki, Prof. T. Shiki, Prof. H. Kamiya, Dr. A. N. Fatmi, Dr. S.M. Ibrahim Shah, Director General, Geological Survey of Pakistan, Secretary, Petroleum and Natural Resources, Mr. Jamil Ansari, Section Officer and Dr. M. Nawaz Ch. for their co-operation and guidance, during the course of this study.

The funds for this research work at Kyoto University Japan, were provided by the Matsumae International Foundation, Tokyo, Japan and for field investigations by the Geological Survey of Pakistan.

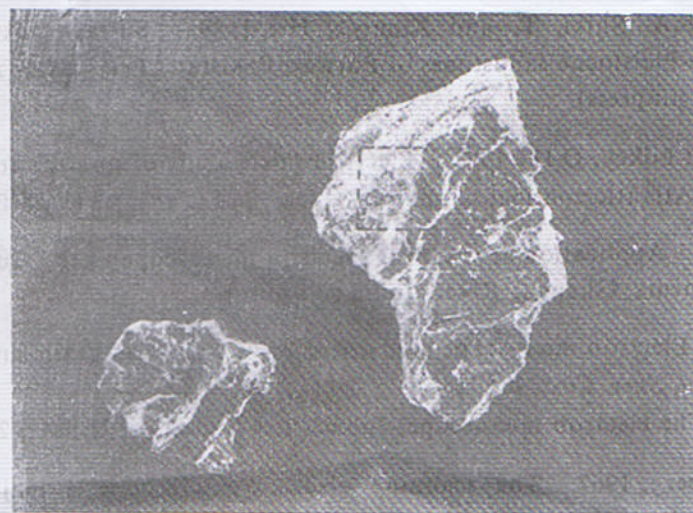
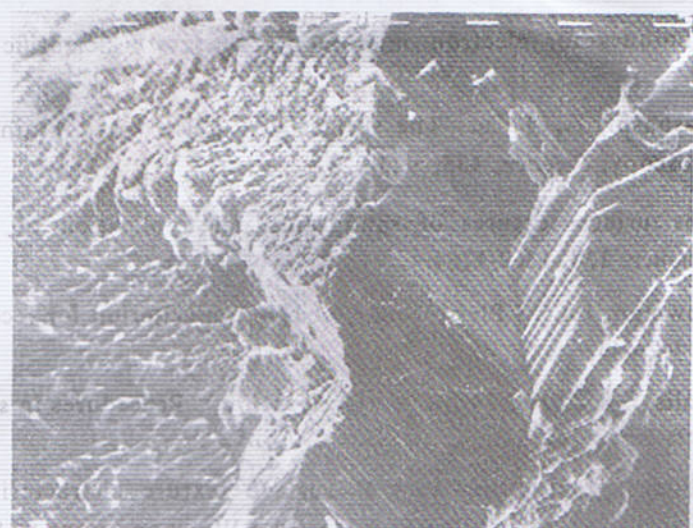
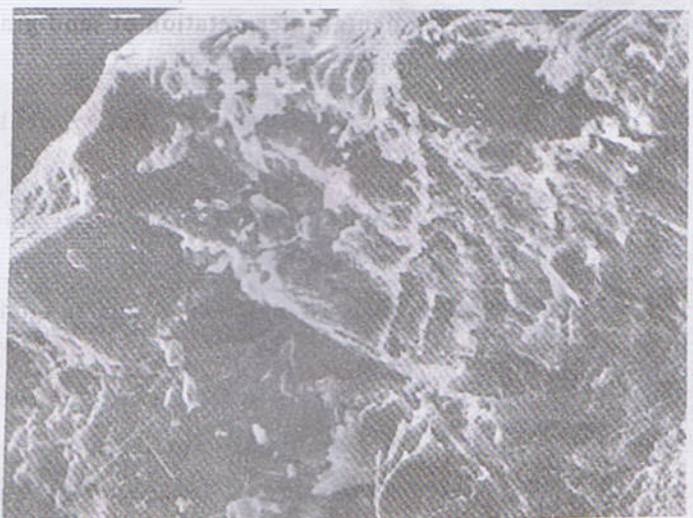


## PLATE 1

SEM 1-A  
(500 X)SEM 1-B  
(1500 X)SEM 1-C  
(1500 X)



## PLATE 2

SEM 2-A  
(200 X)SEM 2-B  
(1500 X)SEM 2-C  
(1500 X)



## REFERENCES

- Bajwa, M.S., Shams, F.A., Shiki, T. and Kamiya, H., 1989a. Surface texture study of quartz grains of Plio-Pleistocene sandstones of Potwar, Pakistan. *Fell. Res. Rep. Mat., Int. Found., Tokyo, Japan* (in press).
- Blackwelder, P.L. and Pilkey, O.H., 1972. Electron microscopy of quartz grain surface textures, U.S. Eastern Atlantic continental margin. *Jour. Sed. Pet.*, 42 (3), 520-526.
- Chaudhri, R.S., 1986. Application of scanning electron microscope in the study of surface textures of river sediments, Ghaggar River, India (un-pub.).
- Harvey, R.D., 1966. Electron microscope study of microtexture and grain surfaces in limestones, Illinois. *Geol. Surv. Circ.* 404, 18.
- Haine, H.E., 1961. The electron microscope, John Wiley and Sons, U.S.A., 282.
- Hay, W. and P. Sandberg, 1967. The scanning electron microscope a major breakthrough for micropaleontology. *Micropal.*, 13, 407-418.
- Key, D., 1961. Techniques for electron microscopy, Blackwell Scientific Publishers Oxford, England, 331.
- Krinsley, D. and Takashashi, T., 1962a. The surface textures of sandgrains, an application of electron microscopy, *Science*, 135, 923-925.
- , 1962. The surface textures of sandgrains, an application of electron microscopy, glaciation, *Science*, 138, 1262-1264.
- and W. Newman, 1965. Pleistocene glaciation, a criterion for recognition of its onset. *Science*, 149, 442-443.
- and Margolis, S.V., 1969. Grain surface texture : Procedures in sedimentary petrology (Editor Carver, R.E.) John Wiley and Sons, U.S.A.
- and Donahue, J., 1968. Summary of surface texture characteristics : Procedures in sedimentary petrology (editor Carver, R.E.) John Wiley and Sons, U.S.A.
- and Donhue, J., 1968a. Environmental interpretation of sand grain surface textures by electron microscopy. *Bull. Geol. Soc. Am.*, 79, 743-748.
- 1968c. Some methods to study surface texture of sand grains, a discussion, *Sedimentology*, 10, 217-221.
- Margolis, S., 1966a. Electron microscopy of modern and ancient quartz sandgrains, M.S. thesis, Florida State Univ., (un-pub.) manuscript.
- , 1966b. Electron micrography of modern and ancient quartz sand grains, *Coastal Res. Notes* 2, 7-8.
- Margolis, S., 1968. Electron microscopy of chemical solution and mechanical abrasion features on quartz sand grains. *Sed. Geol.*, 2, 243-256.
- Mii, H., 1972. Surface structures on quartz sand grains. *Assoc. Geol. Collab., Japan*, 58.



- , 1972. Selected papers of late Dr. Hideo Mii. *Assoc. Geol. Collab., Japan*, (in Japanese), 56-57.
- Porter, J.J., 1962. Electron microscopy of sand surface textures *Jour. Sed. Pet.*, 32, 124-135.
- Reed, S.J.B., 1973. Electron microscope analysis, Cambridge Univ. Press, London, England, 1-168.
- Rochow, T.G.A.M. Thomas and M. C. Botty, 1960. Electron microscopy, *Analytical chem.* 32, 92-103.
- Sandberg, P.A. and W.W. Hay, 1968. Application of scanning electron microscopy in paleontology, Proc Symp. Scanning Electron Microscope—The Instrument and its Application, *I.I.T. Inst. Chicago, Illinois*, 29-350.
- Setlow L. W. and Karpovich, R.P., 1972. Glacial micro-textures on quartz and heavy mineral sand grains from the littoral environment. *Jour. Sed. Pet.*, 42 (4), 864-875.
- Smith and C. Oatley, 1955. The Scanning electron microscope and its field of application. *Brit. Jour. Appl. Phys.*, 6, 391-399.
- Southendam, C.J.A., 1967. Some methods to study surface textures of sand grains. *Sedimentology*, 8, 281-290.
- Thornton, P., 1965. The Scanning electron microscope *Jour. Sci.* 1, 66-71.